EXPERIMENTAL SETUPS FOR DIFFRACTION

ASPECTS AFFECTING DIFFRACTION EXPERIMENTS

COLLECTION GEOMETRIES

RELATED TO DIFFRACTOMETERS, I.E. INSTRUMENT'S SETUP

RECORDING ARCHITECTURES

RELATED TO DETECTORS

RADIATION SOURCES

CONVENTIONAL SOURCES *versus* LARGE SCALE FACILITIES (synchrotron & neutrons)

FUNDAMENTAL PHOTON-EMISSION QUANTITIES

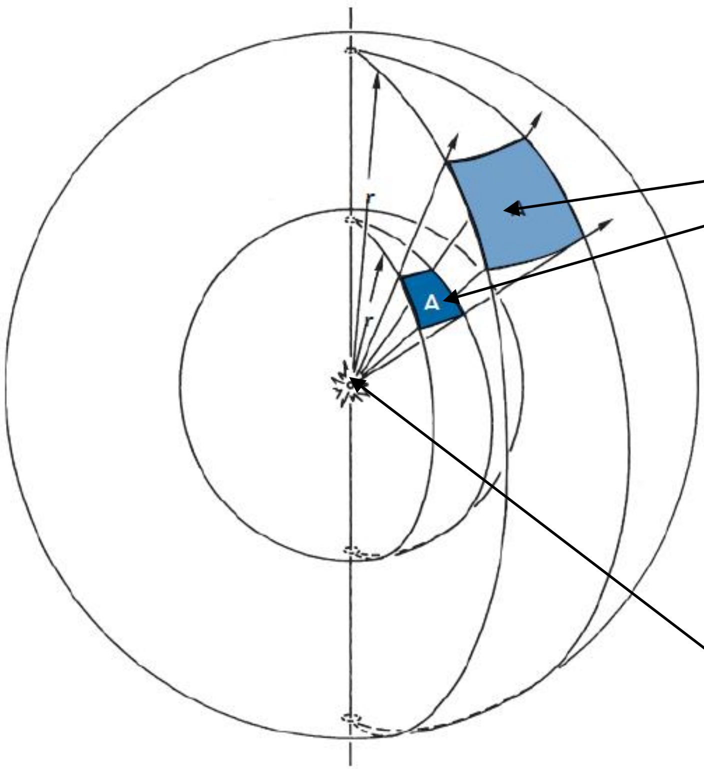

PHOTON IRRADIANCE=
(dN/dt)*1/Area

PHOTON FLUX=
dN/dt

WHAT IS A DETECTOR?
Some detector features/parameters

Sensitivity=efficacy to convert radiation into pulse

X-Ray

PHYSICAL RECORDING OF THE RADIATION: GENERATION OF CHARGE CARRIERS

$\Delta V = I \times R$

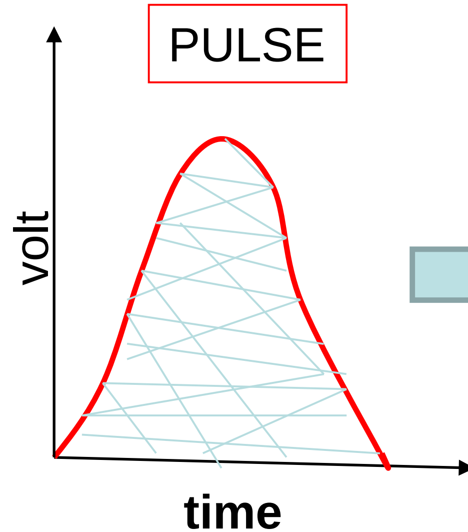

RECORDING ELECTRONICS: ANALOG TO DIGITAL SIGNAL TO COUNT PHOTONS

Response time

Readout=time to acquire countings and have the counting chain ready again

Dead time=time interval between two events during which a detector is not able to work

Response function=realtionship between counted photons and output signal intensity. For instance: linear response

Some detector parameters

Energy resolution=ΔE,$\Delta E/E$; Capacity to discriminate between photons with a ΔE difference

Total Efficiency

- **Intrinsic efficiency** $\varepsilon_{int\ eff}$=N(photons recorded)/N(photons on detector)
- **Geometrical acceptance** ε_{geom}

ε_{total}= N(photons recorded)/N(photons produced)=$\varepsilon_{int\ eff} * \varepsilon_{geom}$

doi:http://dx.doi.org/10.21013/jas.v10.n3.p2

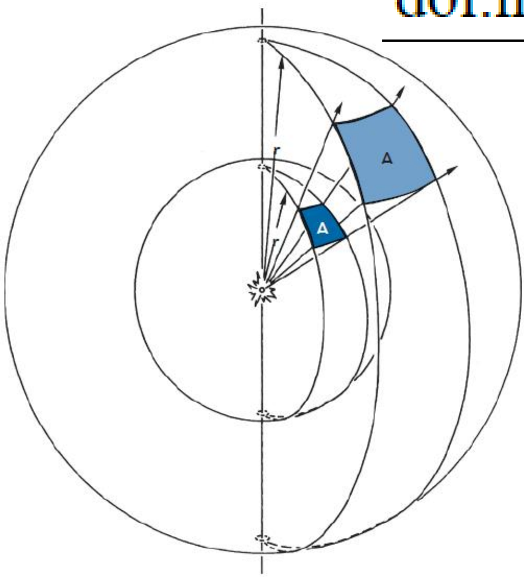

Total efficiency

DOI: 10.12693/APhysPolA.128.B-332

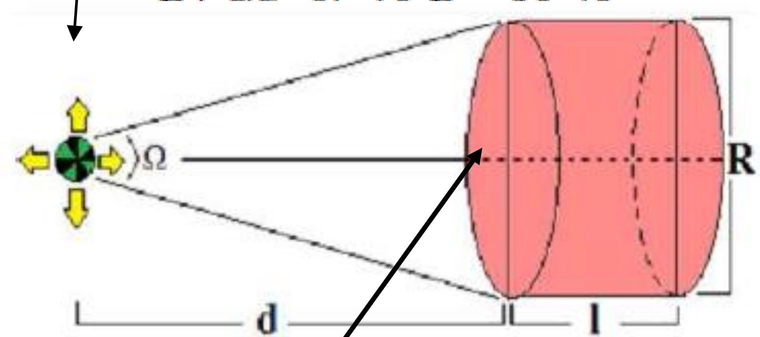

Geometrical acceptance

SENSITIVE AREA
EFFECTIVE SENSITIVE AREA, I.E. HOMOGENEOUS RESPONSIVITY

Intrinsic efficiency=it is related to the incident phtons' energy and detecting mechanism

AN EXAMPLE (a)

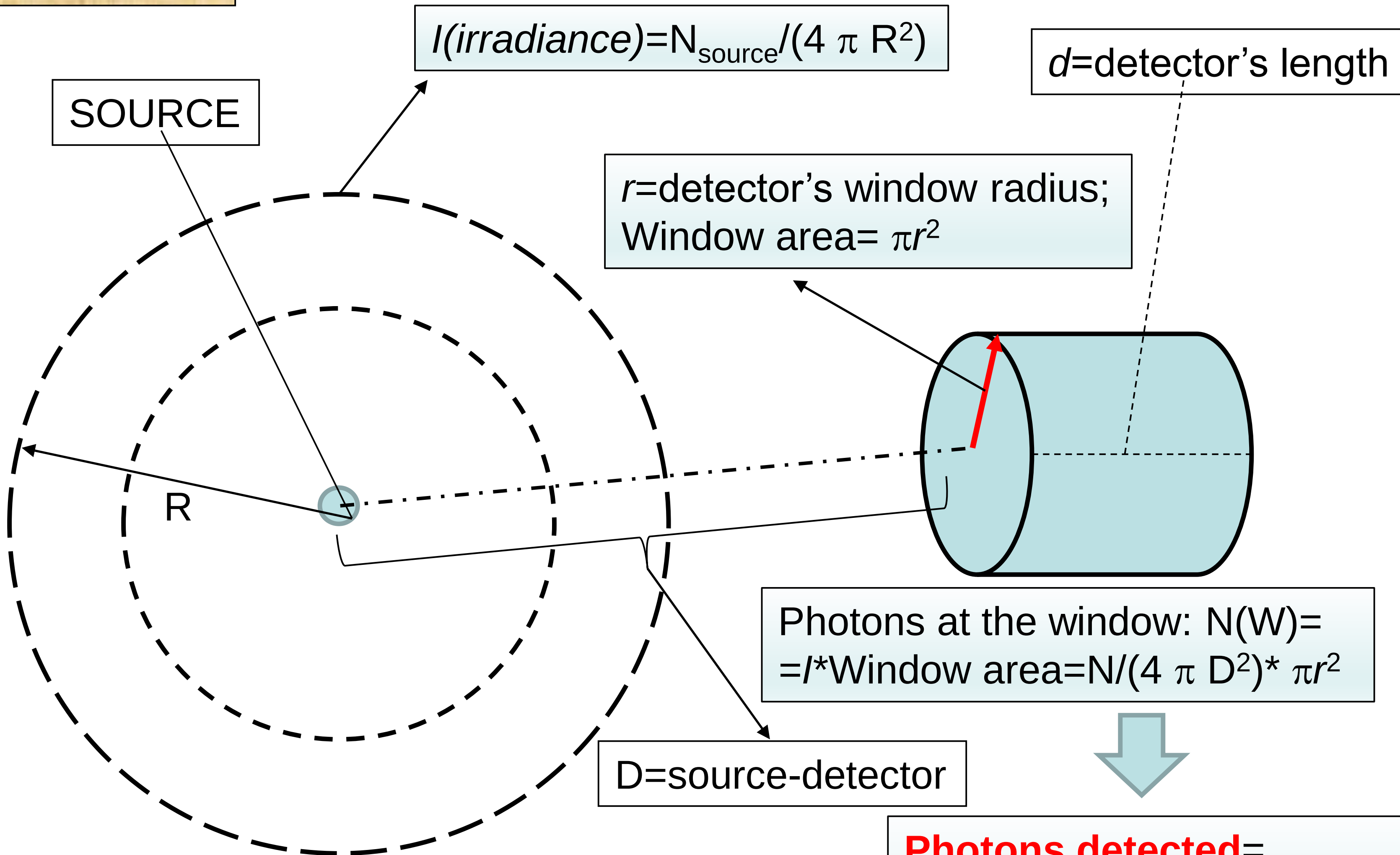

Photons detected=
N(W)*prob.being.recorded=
N/(4 π D^2)* πr^2*[1-exp(-μd)]

$\mu(\lambda)$

Total efficiency=
Photons detected/
Photons of source

Total efficiency~
(1/4 r^2/D^2) $\times$ [1-exp(-
μd)]

AN EXAMPLE (b)

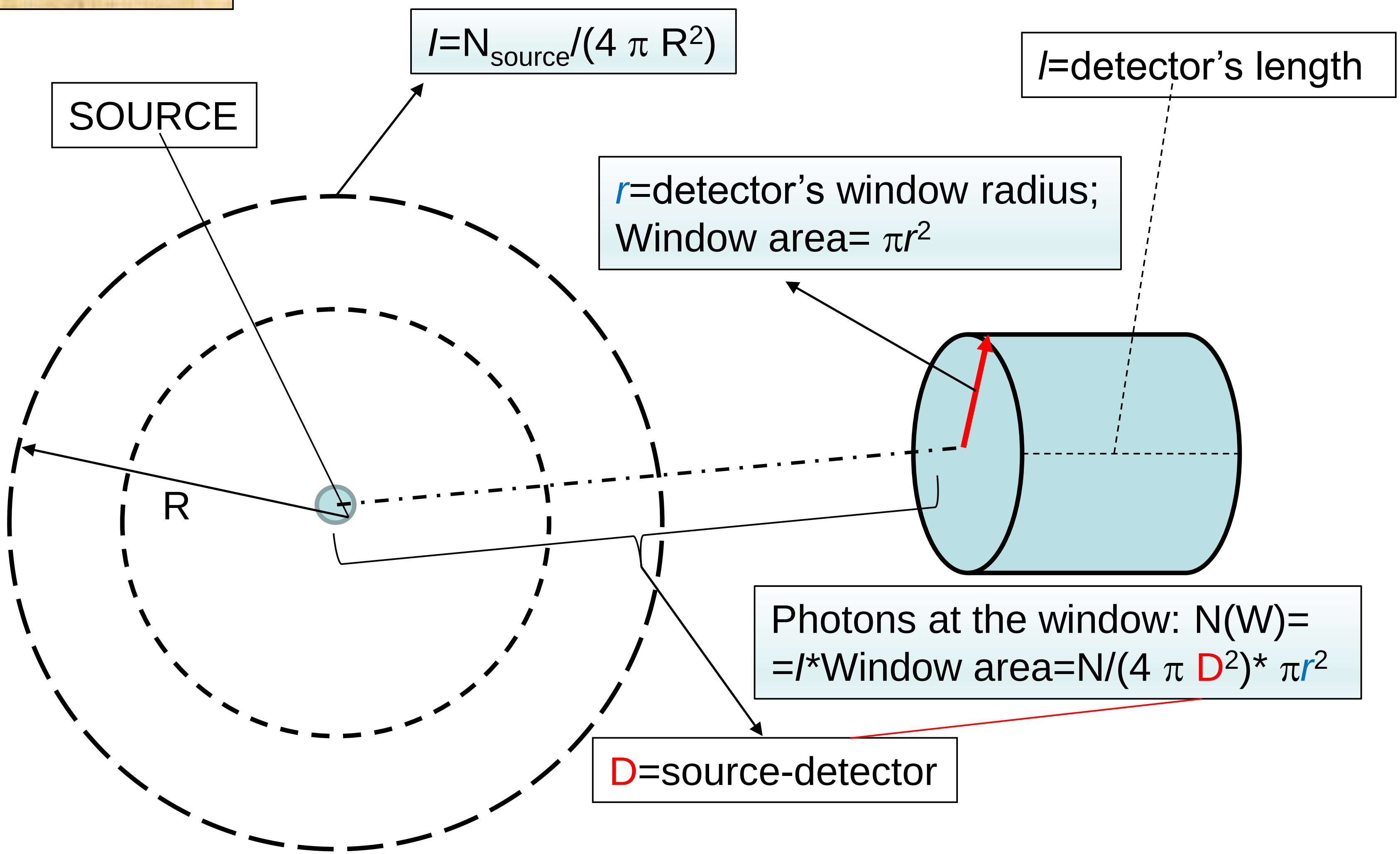

Geometrical acceptance= $\pi r^2/(4\pi D^2)$

Intrinsic efficiency~
1-exp(-μl)=probability that a photon is absorbed

Total efficiency~ (1/4 r^2/D^2) $\times$ [1-exp(-μl)]

$\mu(\lambda)$

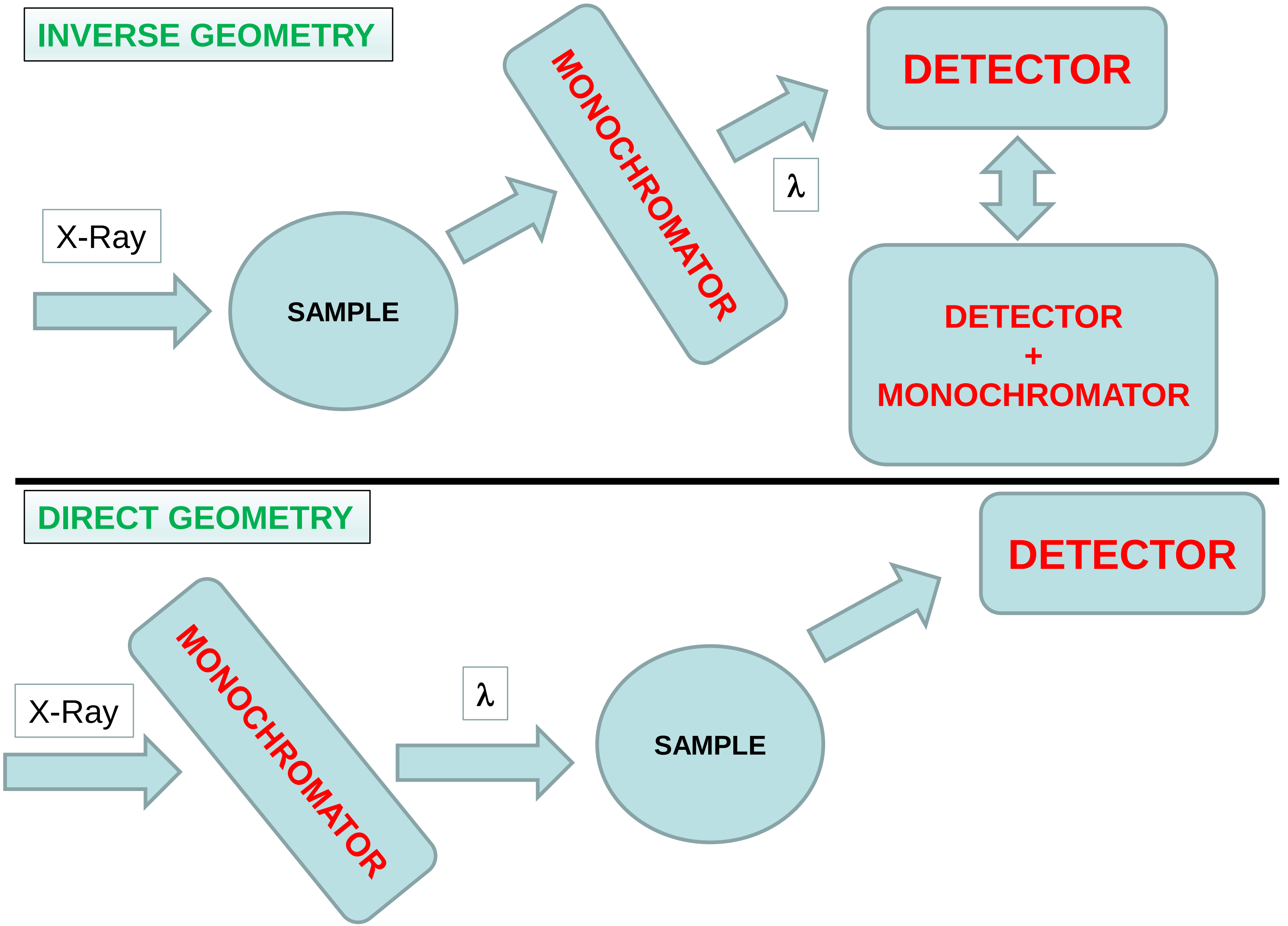
INVERSE GEOMETRY
X-Ray
SAMPLE
MONOCHROMATOR
λ
DETECTOR
DETECTOR
+
MONOCHROMATOR
DIRECT GEOMETRY
X-Ray
MONOCHROMATOR
λ
SAMPLE
DETECTOR

MONOCHROMATOR

CRYSTAL DISCRIMINATOR

ELECTRONIC DISCRIMINATION

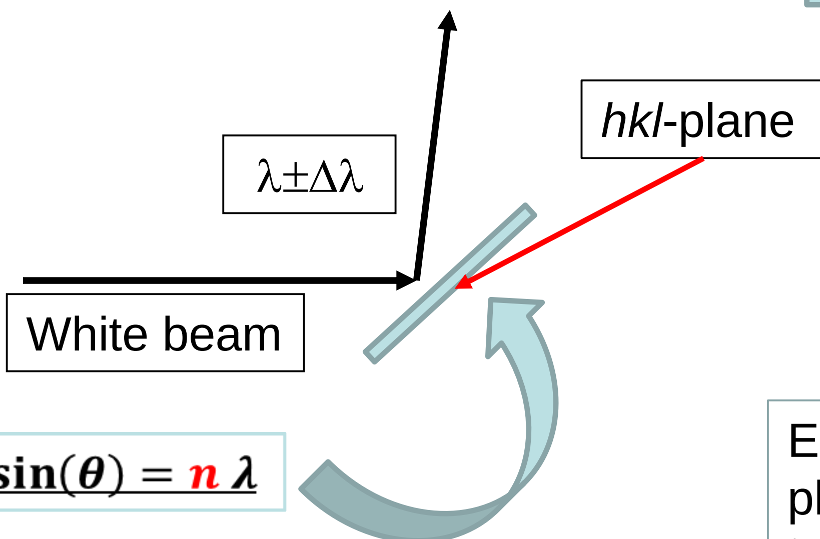

$$\underline{2\, d \sin(\theta) = n\, \lambda}$$

(constructive inteference between waves)

Electronics to discriminate between photons and select those having λ Around a given value

SINGLE CRYSTAL DIFFRACTION

RADIATION COLLECTION ARCHITECTURES
SINGLE CRYSTAL

OLD APPROACH: POINT DETECTORS

ONE DIFFRACTED BEAM AT A TIME

NOWADAYS: POSITION SENSITIVE/AREA DETECTORS

MANY DIFFRACTED BEAMS AT A TIME

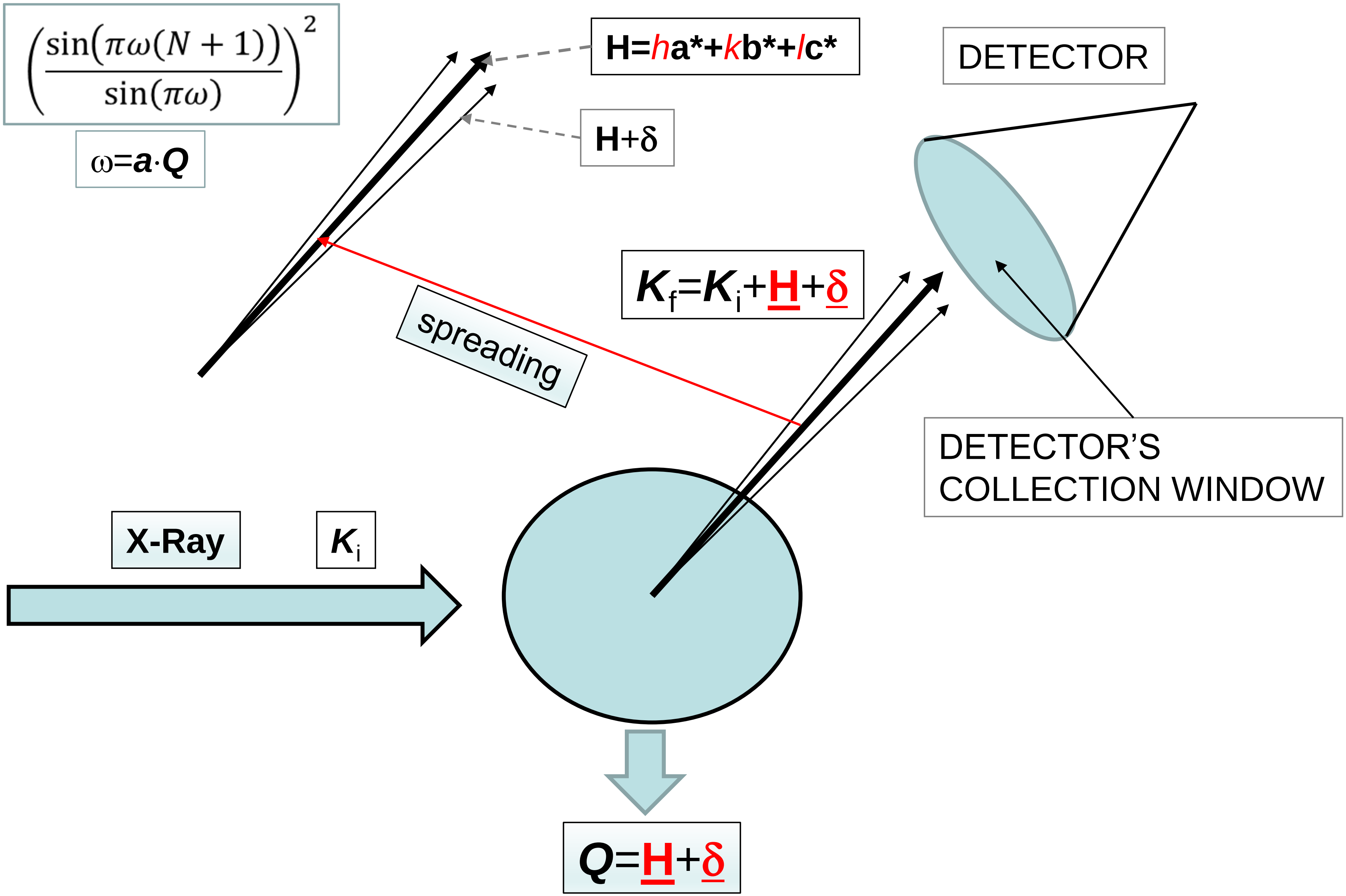

X-RAY SINGLE CRYSTAL EXPERIMENTAL PHENOMENOLOGY

BRAGG DIFFUSION & *hkl*-PLANES

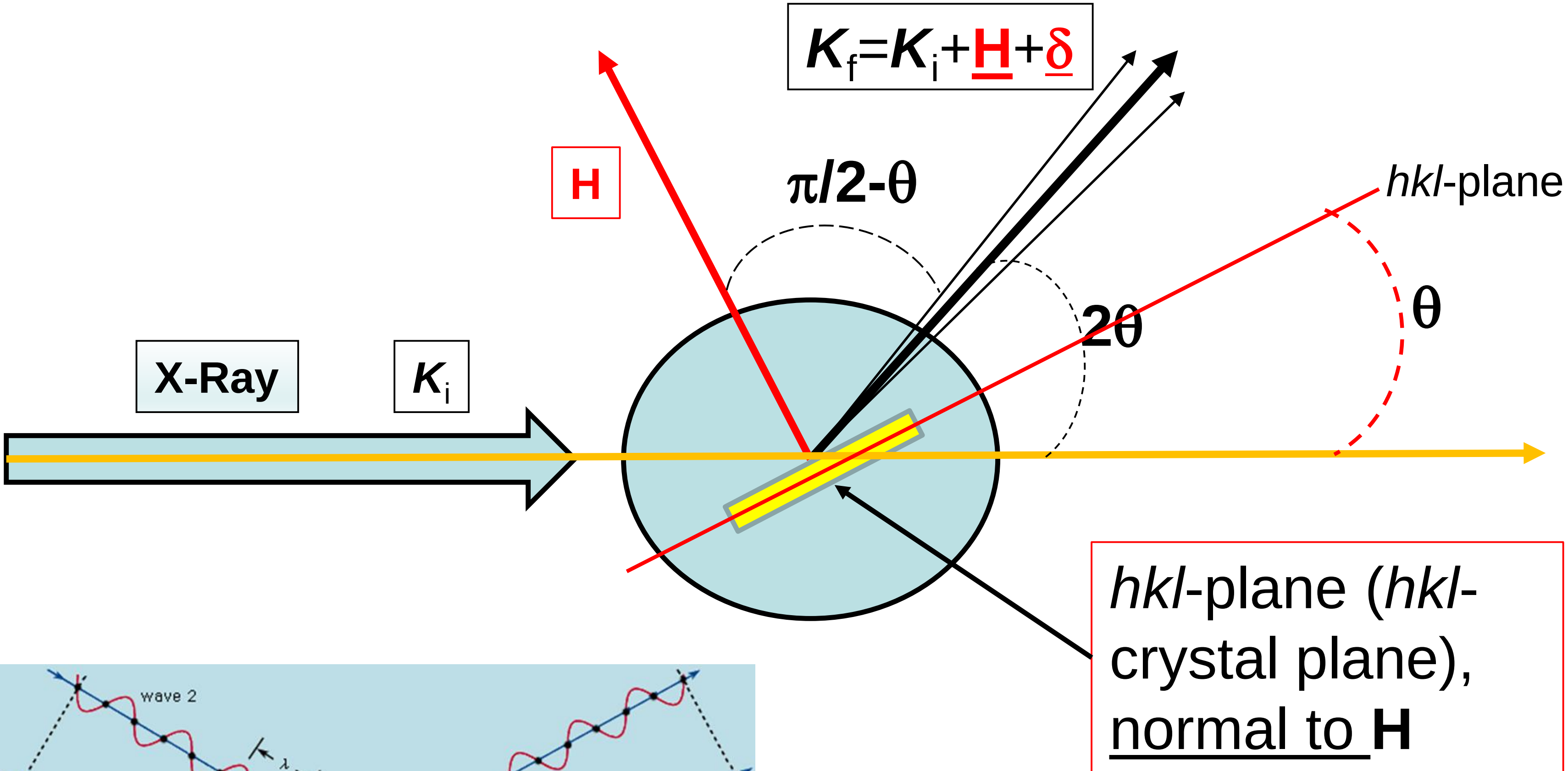

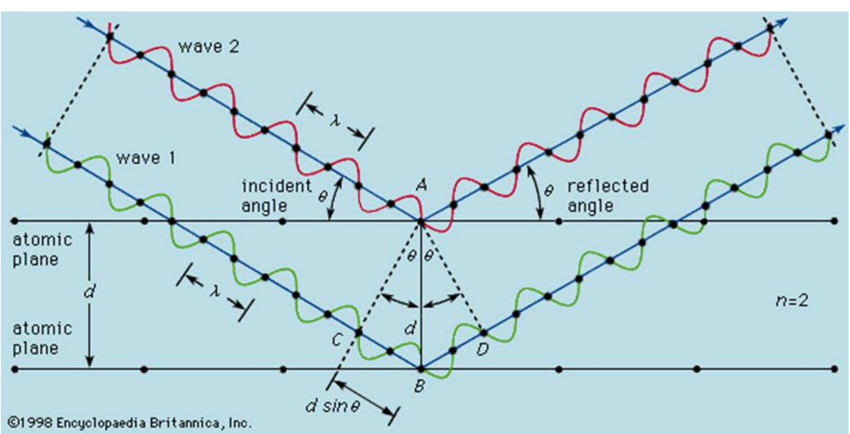

CONSTRUCTIVE INTEFERENCE CONDITIONS

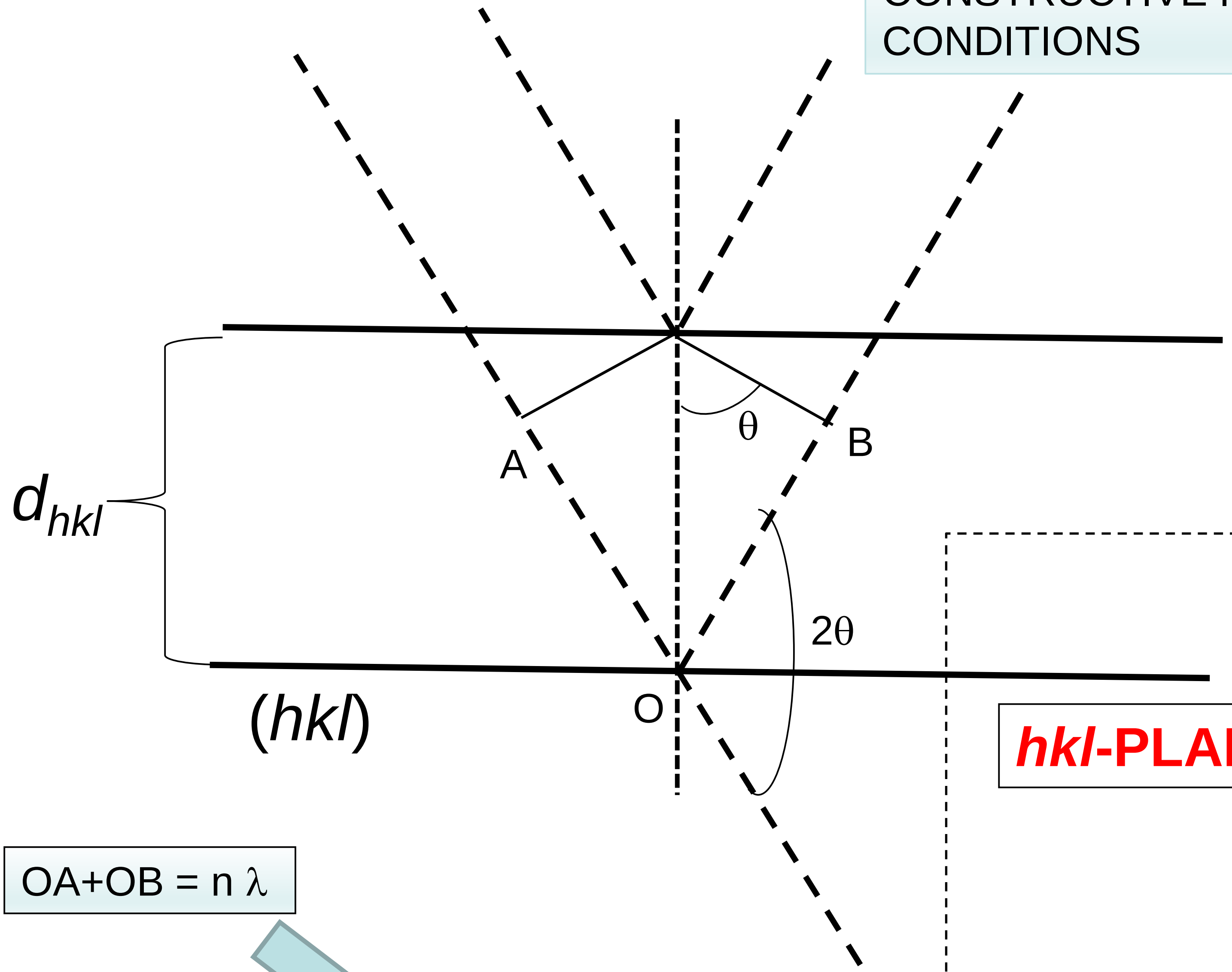

***hkl*-PLANE FAMILY**

OA+OB = n λ

$$2\ d_{hkl} \sin(\theta) = \lambda$$

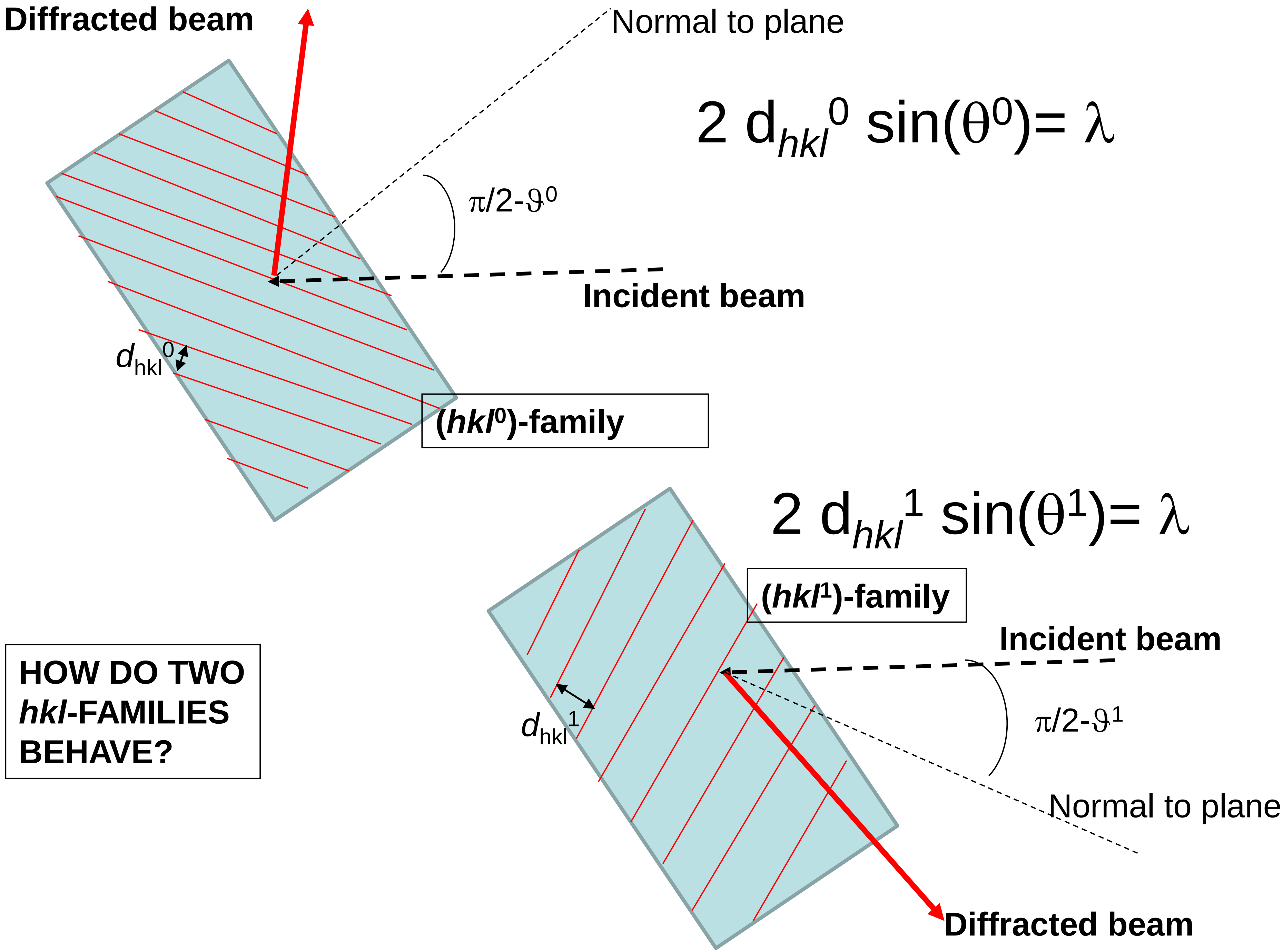

Diffracted beam
Normal to plane
$2\ d_{hkl}^{0}\ \sin(\theta^{0}) = \lambda$
$\pi/2-\vartheta^{0}$
Incident beam
d_{hkl}^{0}
(hkl^0)-family
$2\ d_{hkl}^{1}\ \sin(\theta^{1}) = \lambda$
(hkl^1)-family
Incident beam
d_{hkl}^{1}
$\pi/2-\vartheta^{1}$
Normal to plane
Diffracted beam
HOW DO TWO *hkl*-FAMILIES BEHAVE?

SINGLE CRYSTAL DIFFRACTION

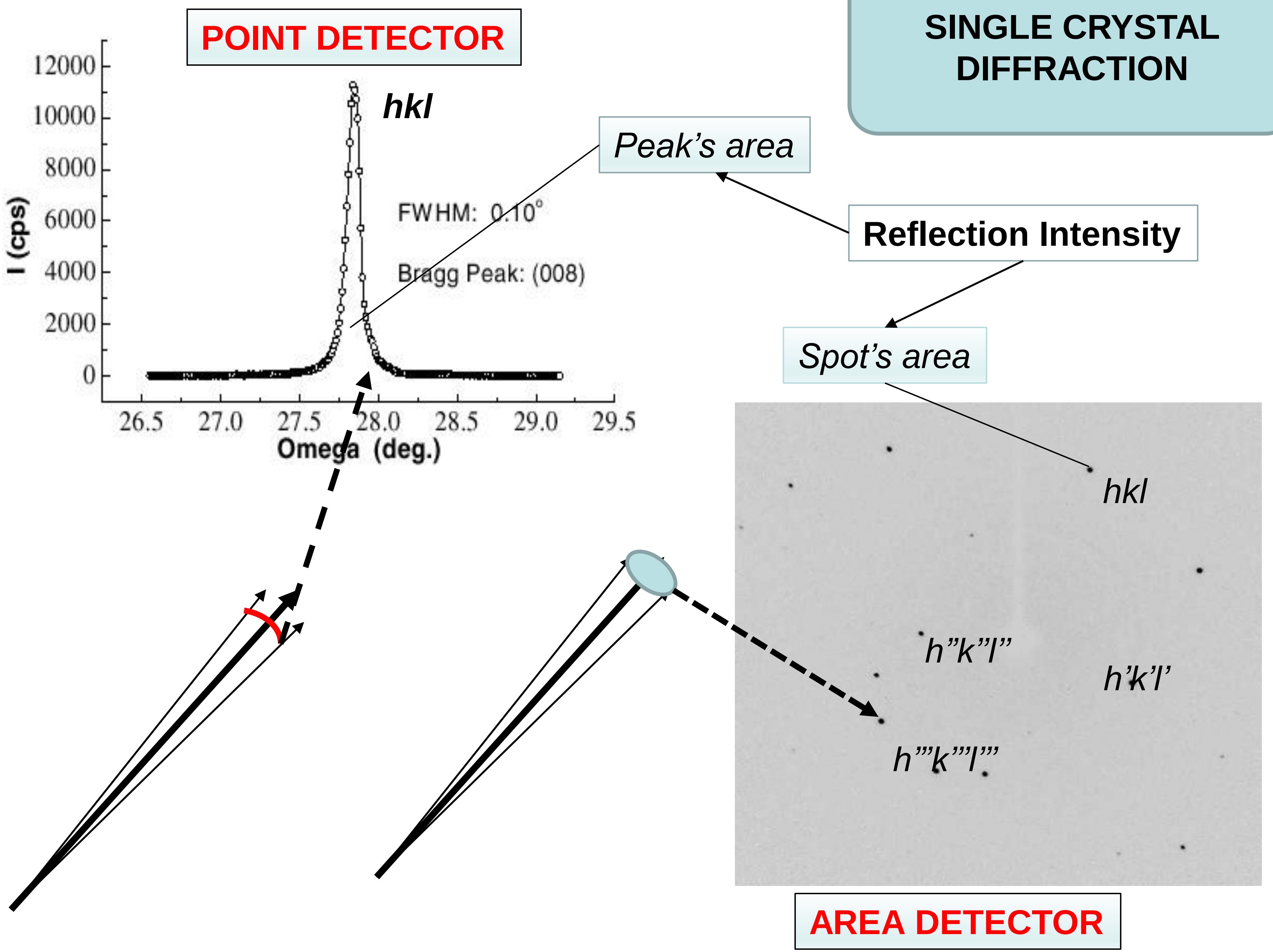

SINGLE CRYSTAL DIFFRACTION

Area detector

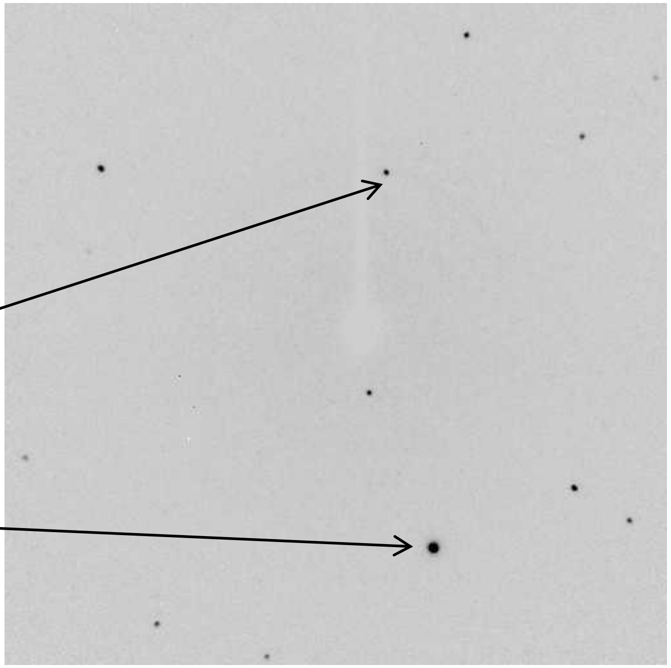

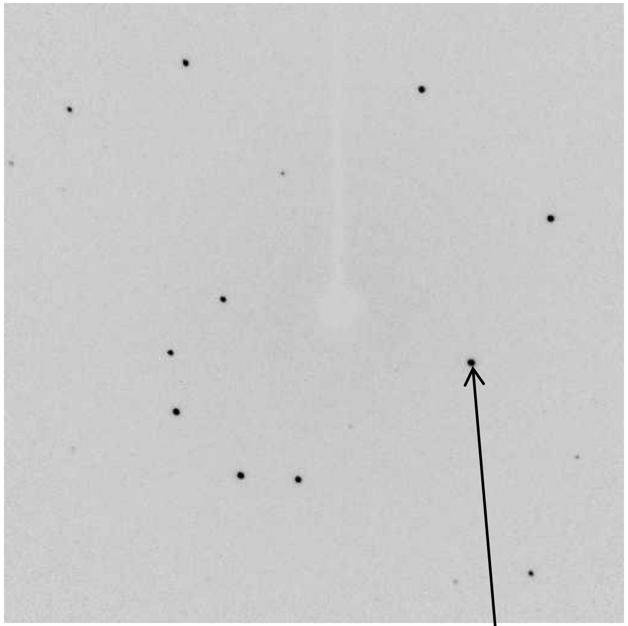

h'k'l'

hkl

h"k"l"

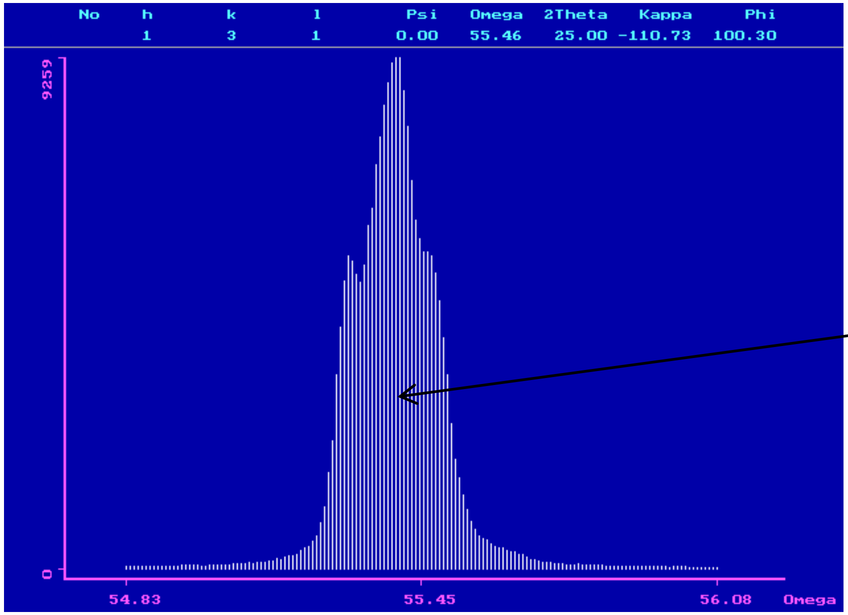

hkl

Point detector

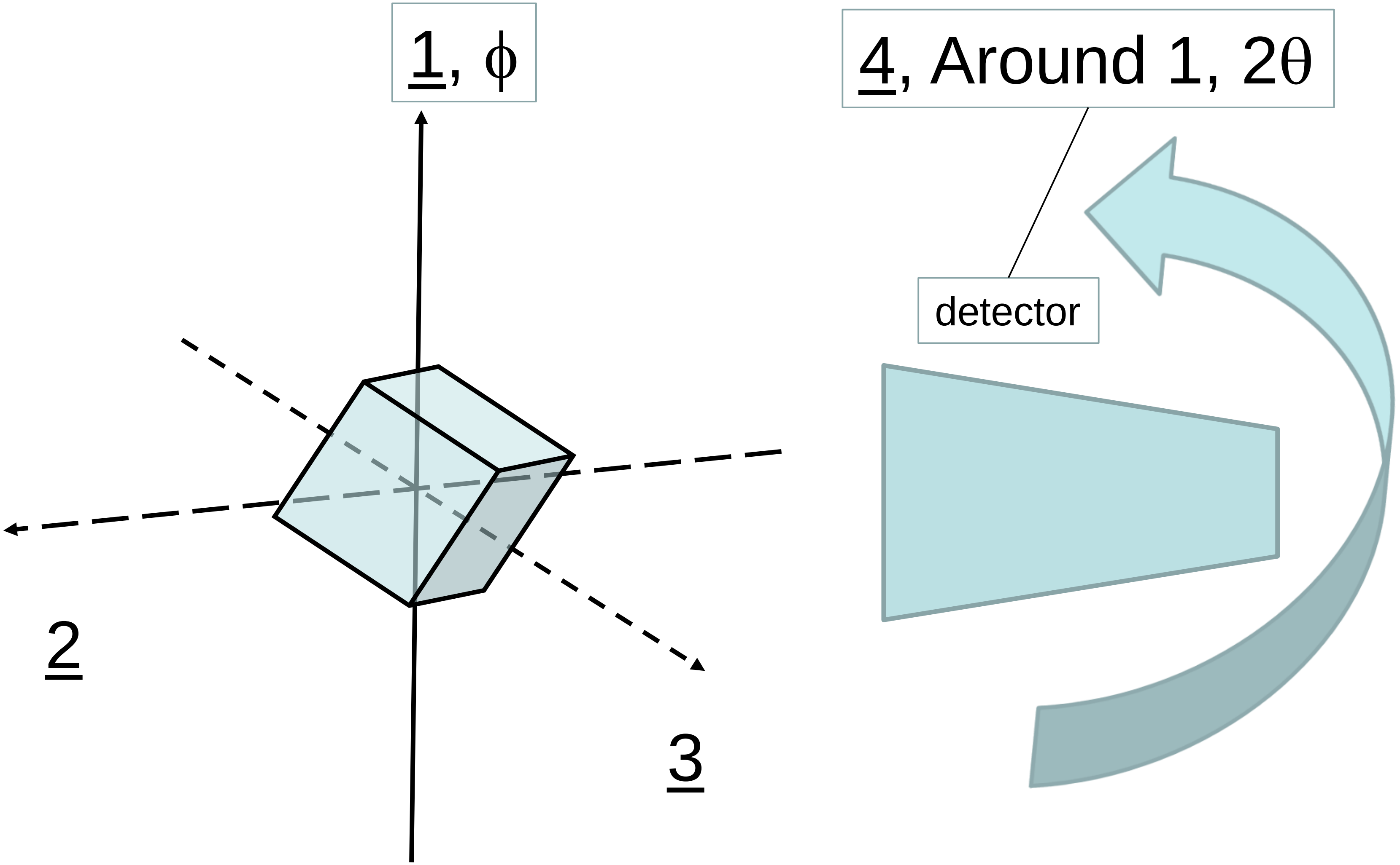

FOUR AXES PRINCIPLE FOR SINGLE CRYSTAL DIFFRACTION

SINGLE CRYSTAL DIFFRACTOMETER

4 ROTATION AXES THAT ALLOW ONE TO ORIENT A CRYSTAL IN ANY POSSIBLE WAY WITH RESPECT TO A DETECTOR

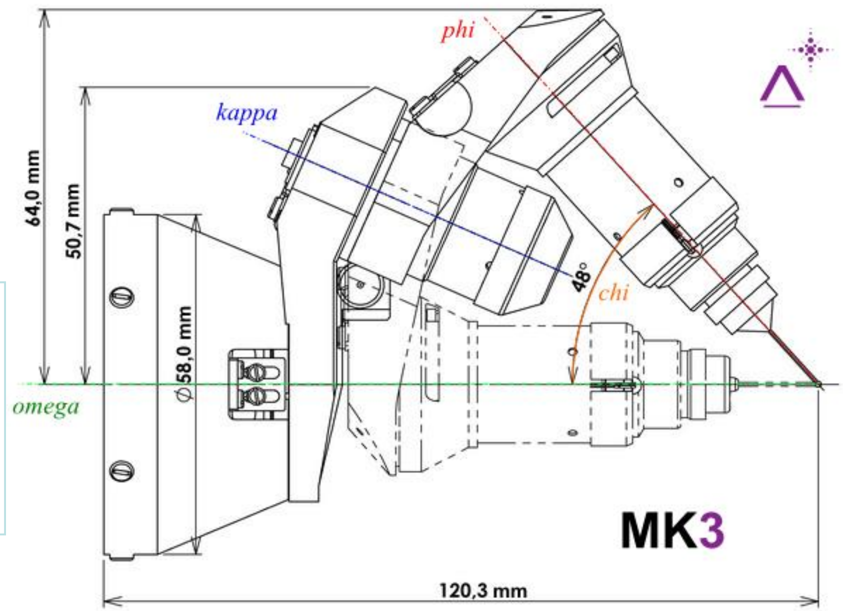

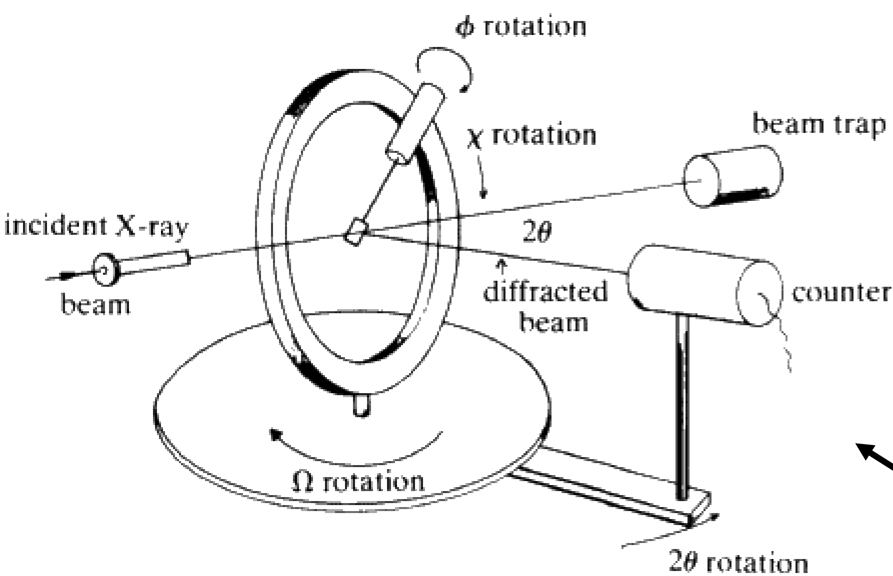

K-GEOMETRY

EULERIAN GEOMETRY

SINGLE CRYSTAL X-RAY DIFFRACTOMETERS

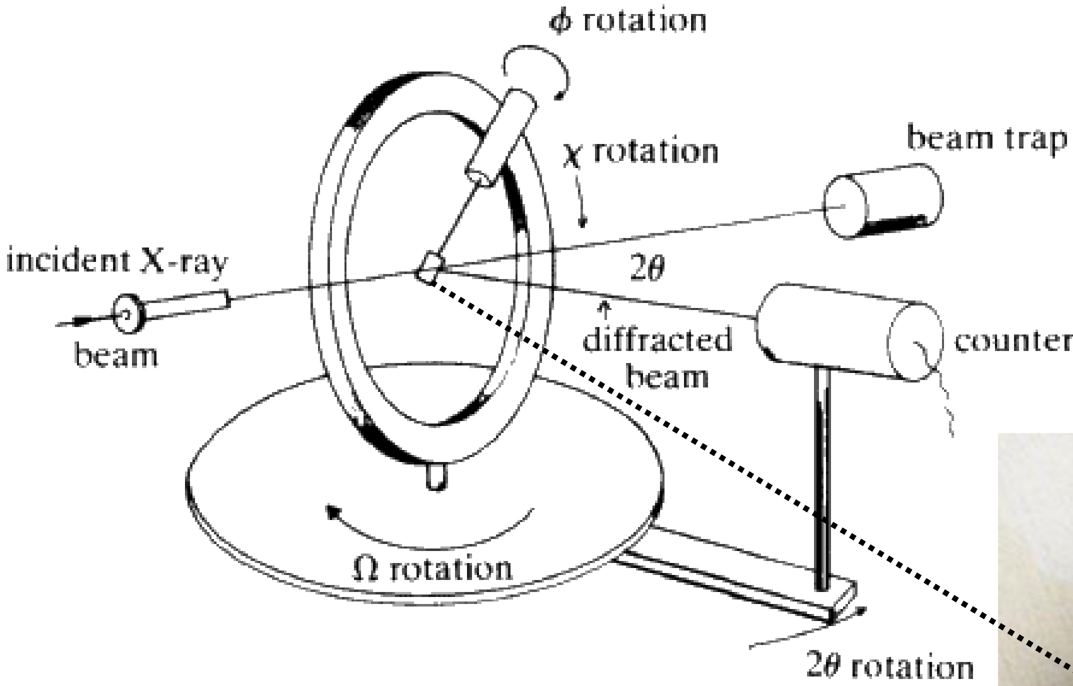

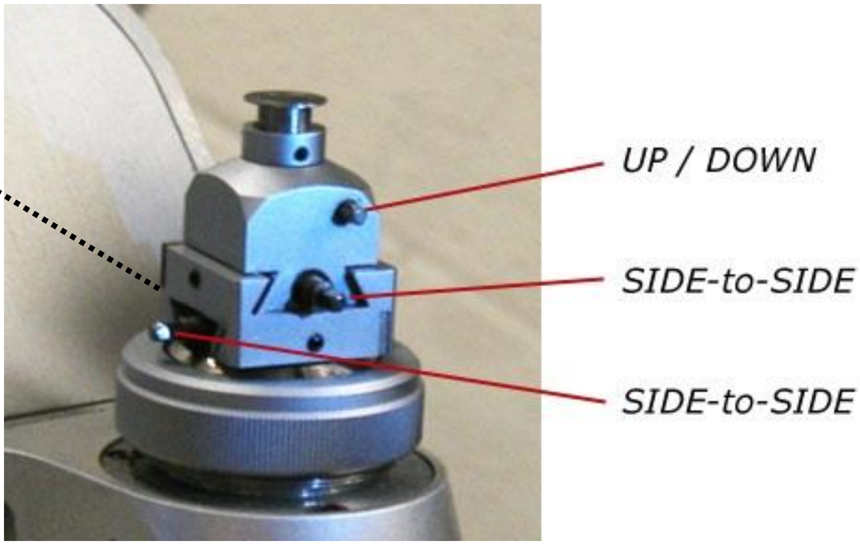

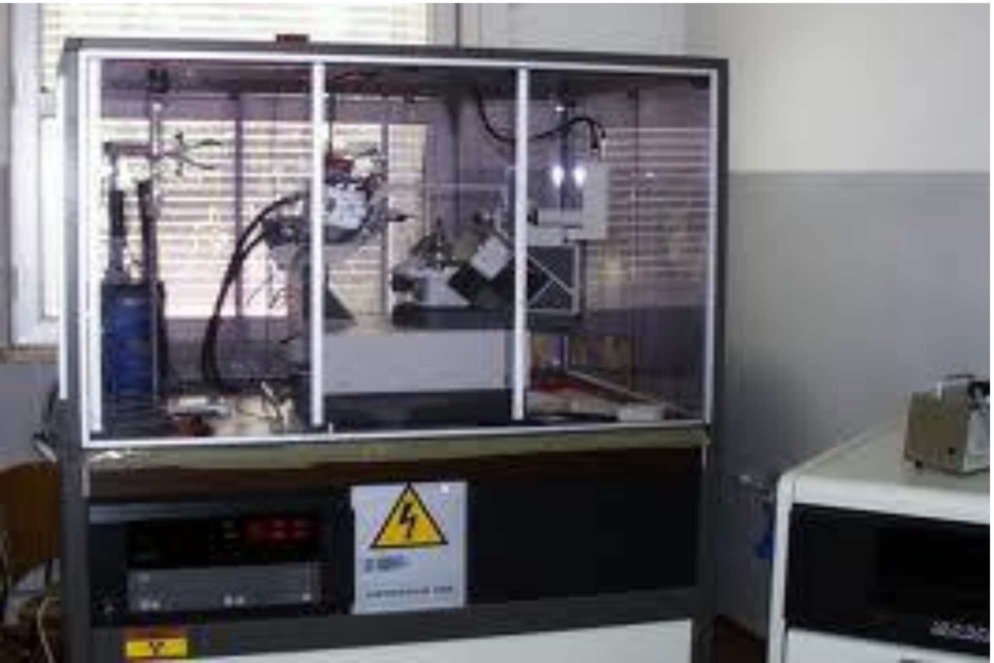

K-GEOMETRY

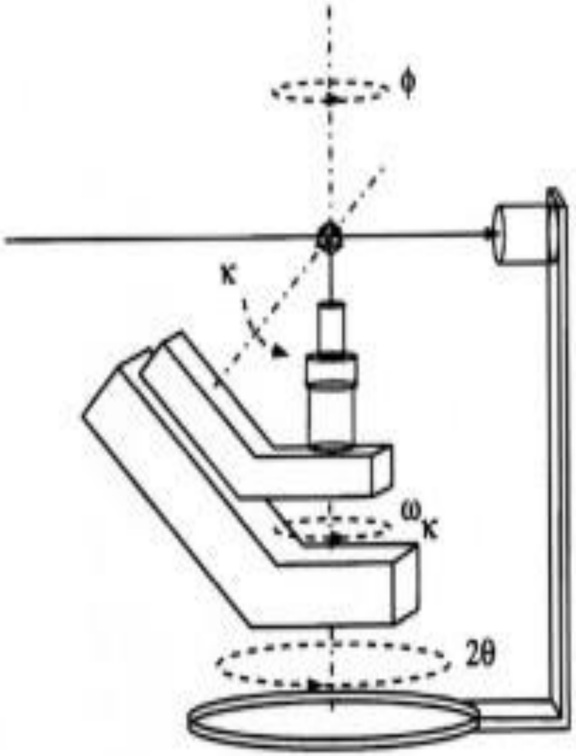

POSITION SENSITIVE/AREA DETECTOR, CHARGE COUPLED DEVICE (CCD)

2D-DETECTOR

POWDER DIFFRACTION

POWDER DIFFRACTION

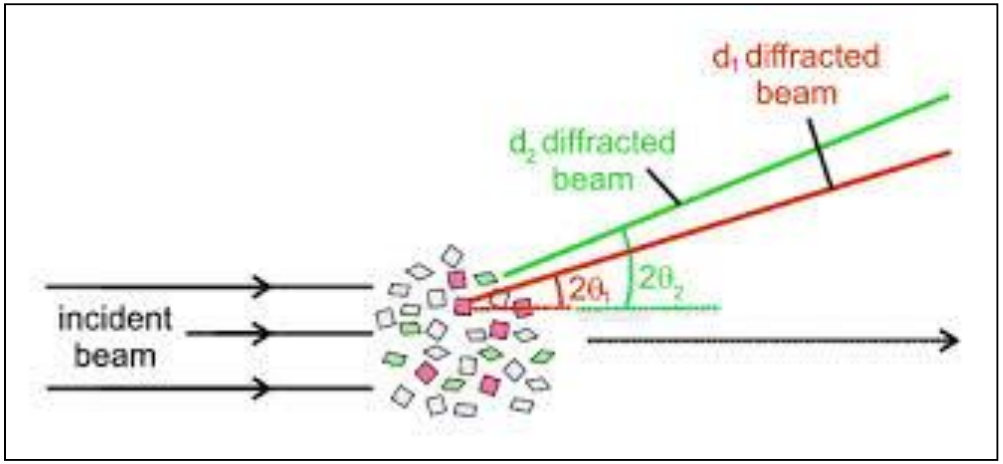

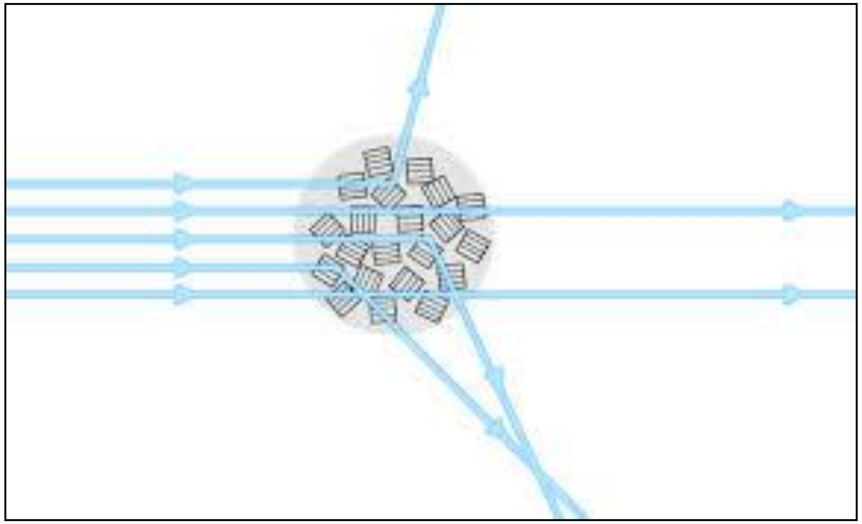

EXPERIMENTAL GEOMETRIES FOR POWDER DIFFRACTION

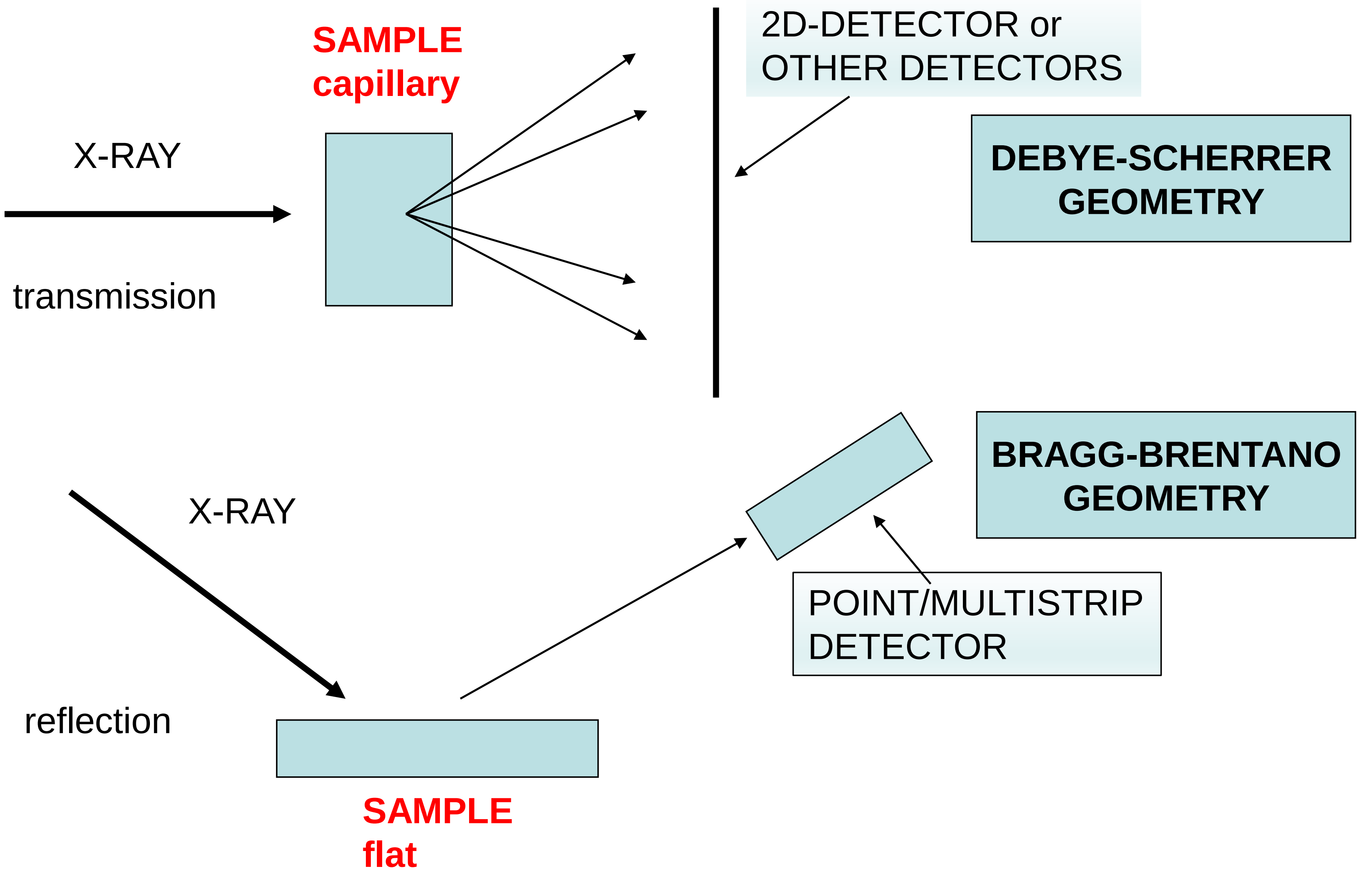

DEBYE-SCHERRER

POWDER DIFFRACTION INTENSITY DISTRIBUTION

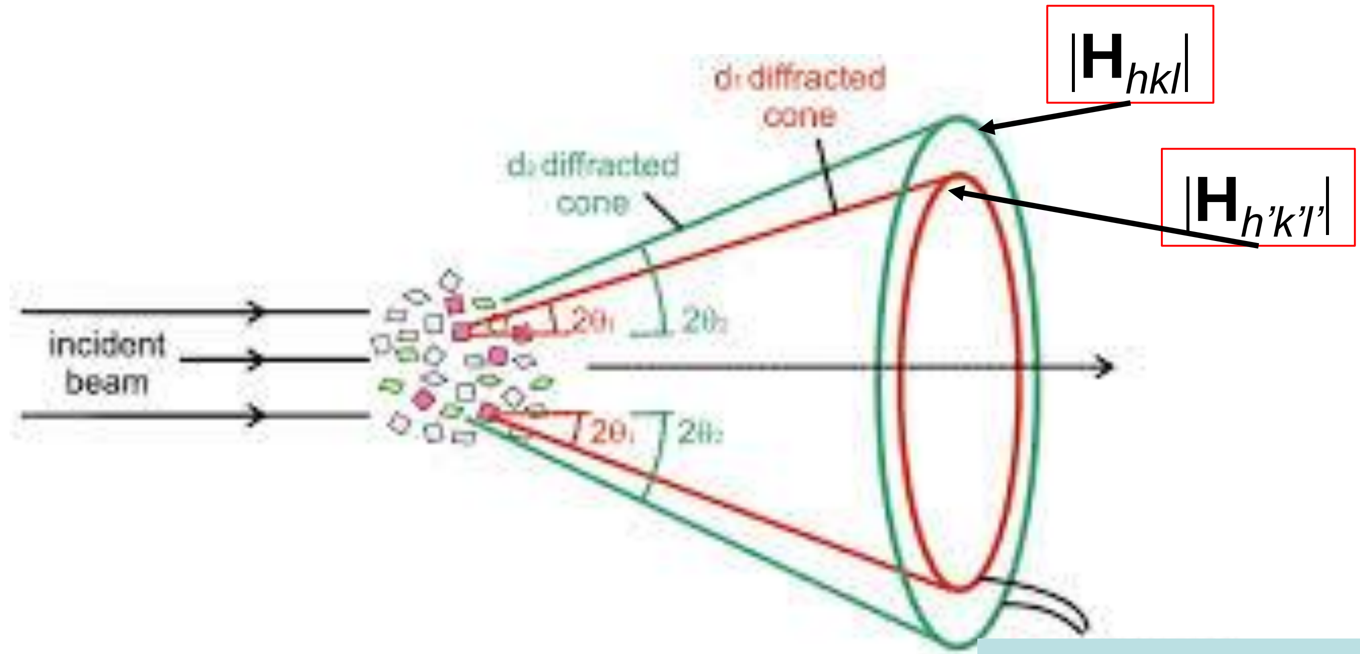

DIFFRACTION CONES & RINGS

ON EACH CONE SURFACE LIE THE DIFFRACTED BEAMS CHARACTERISED BY THE SAME $|\mathbf{H}|$, I.E. SUCH AS TO FULFIL THE BRAGG LAW AT THE SAME 2ϑ ANGLE

$$\frac{2}{|\mathbf{H}|} sin(\theta_{hkl}) = \lambda$$

POWDER DIFFRACTION

DEBYE-SCHERRER

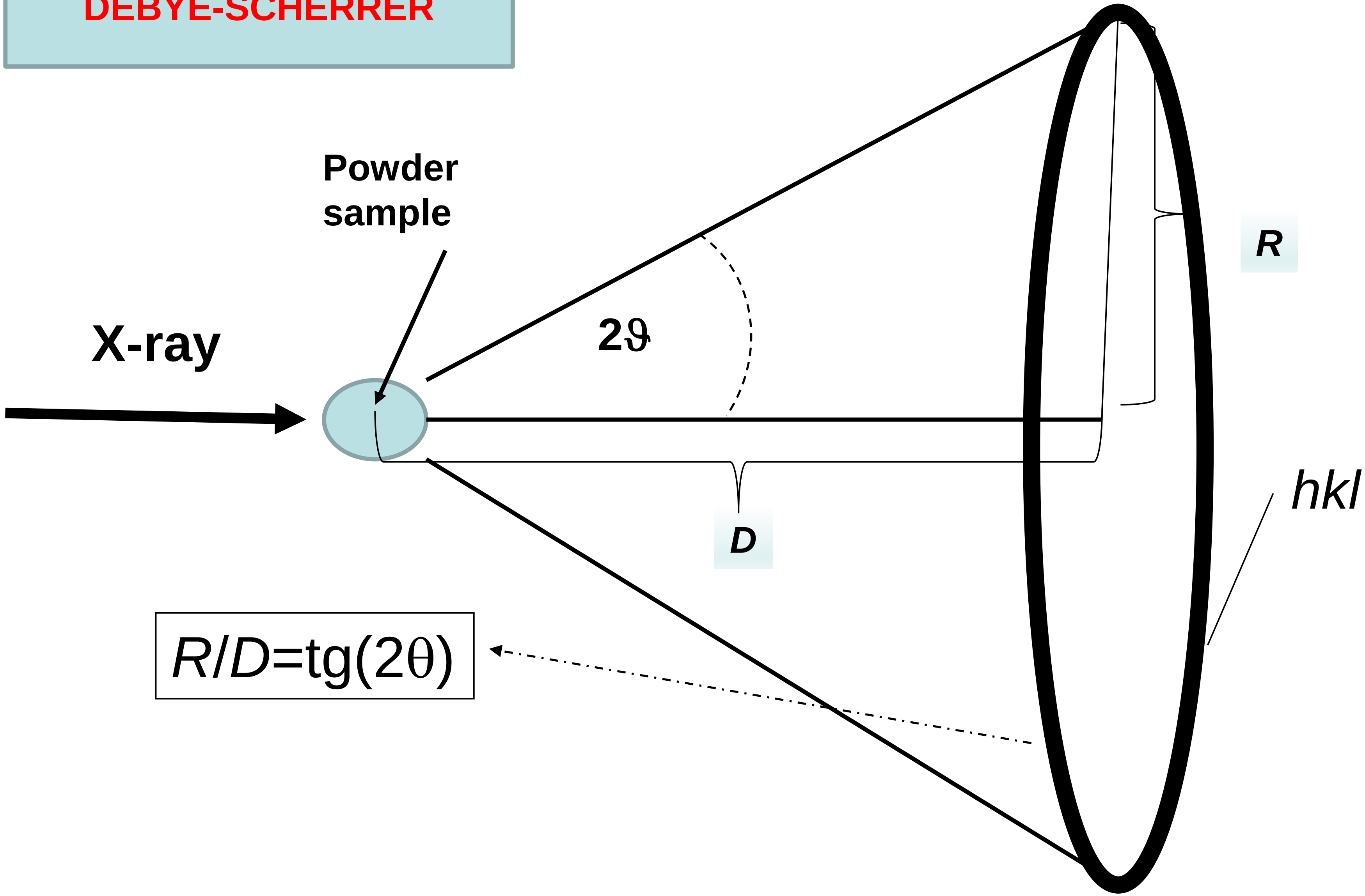

THE RESULTING PATTERN DEPENDS ON HOW A DETECTOR INTERSECTS THE DIFFRACTION CONES

POWDER DIFFRACTION-POSITION SENSITIVE/AREA DETECTORS

Resulting profile

A

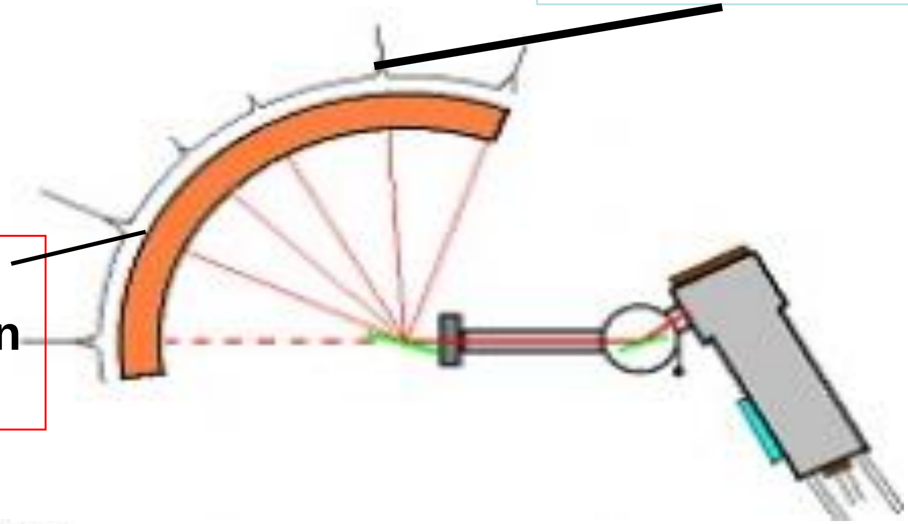

INEL-geometry
Multi-channel design
«position sensitive»

X-ray tube

B

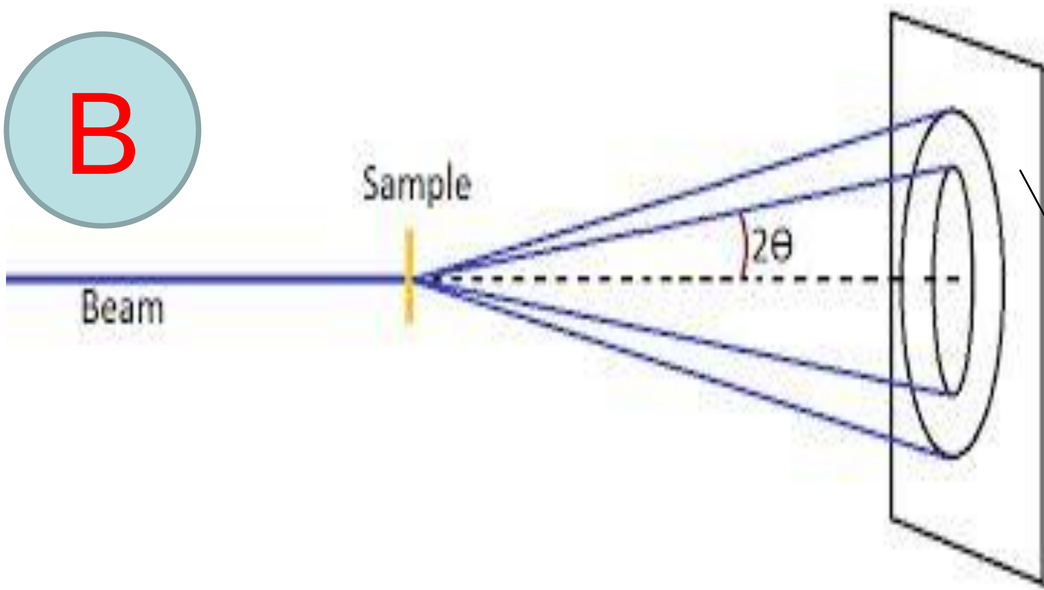

2D-detector

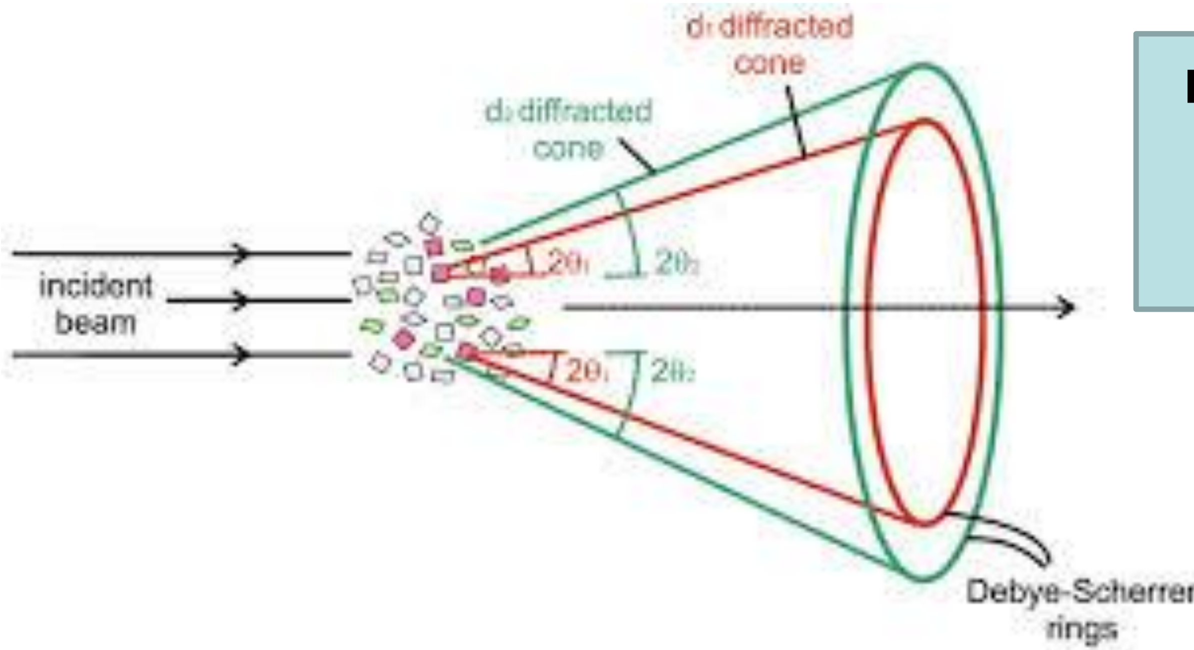

POWDER DIFFRACTION
DEBYE-SCHERRER
&
2D-DETECTOR

OUTPUT

DIFFRACTION RINGS

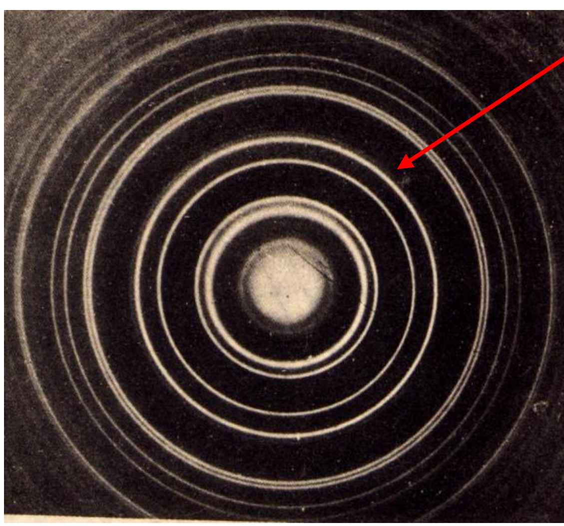

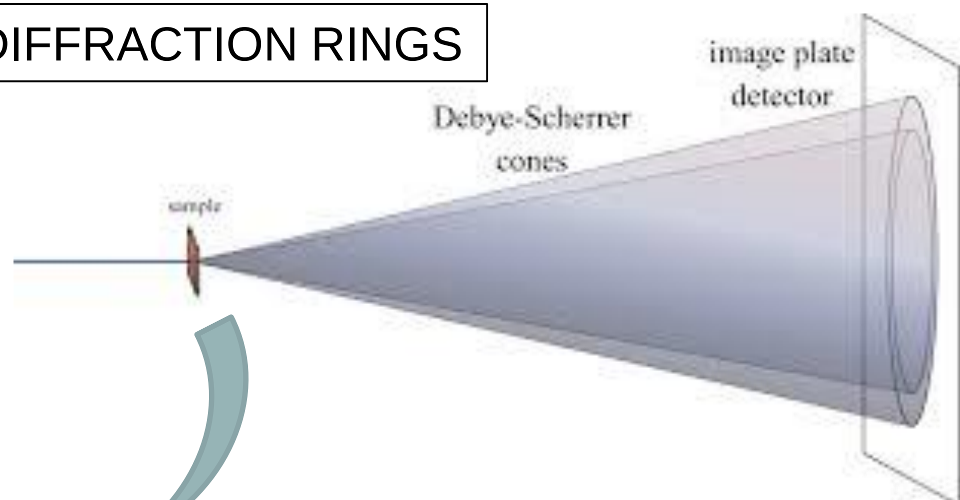

OLIVINE POWDER DIFFRACTION PATTERN COLLECTED BY A **DEBYE GEOMERTY**

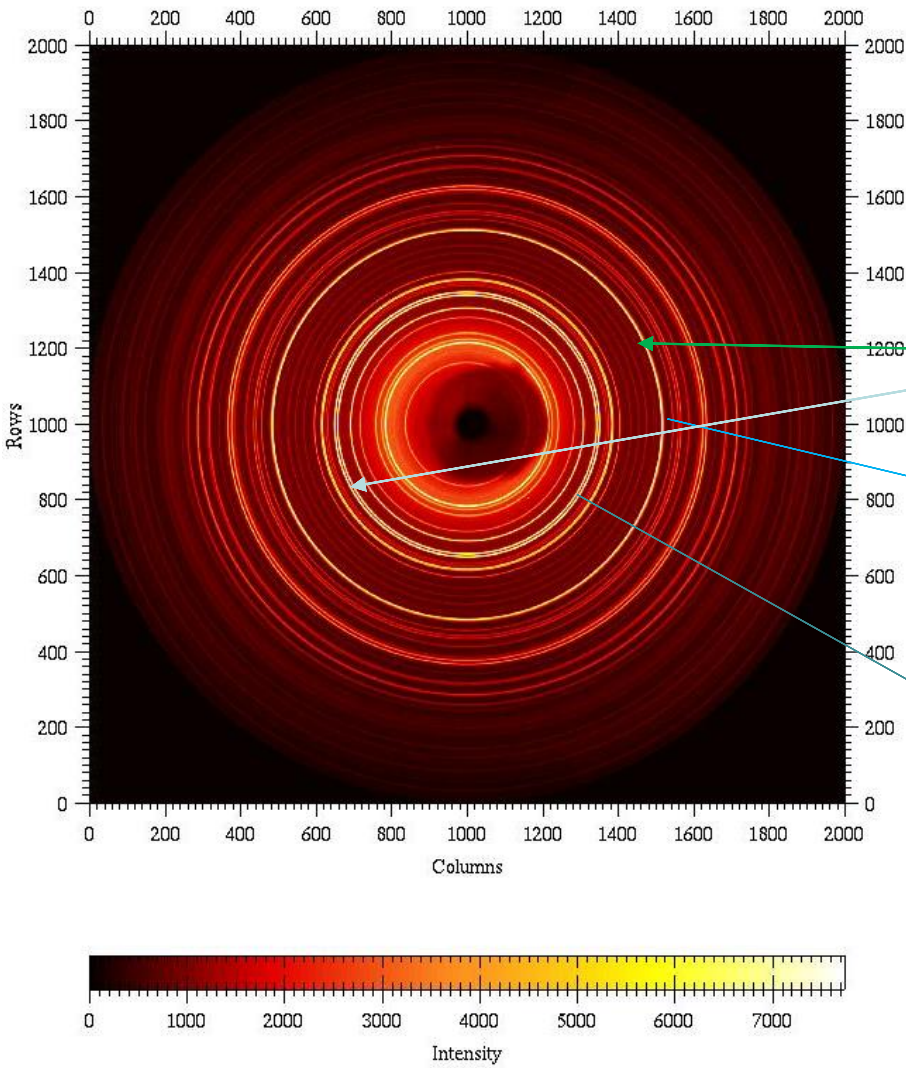

DIFFRACTION RINGS

$2\,d'\sin(\theta')=\lambda$

$2\,d''\sin(\theta'')=\lambda$

BRAGG-BRENTANO

BRAGG-BRENTANO GEOMETRY

A

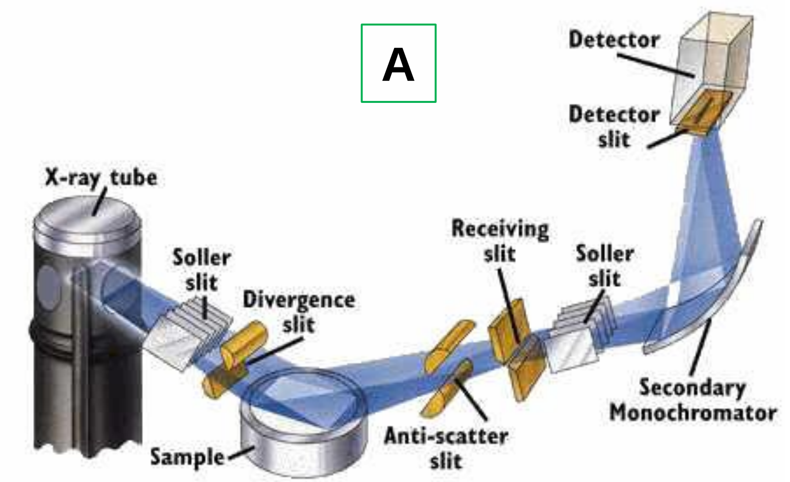

D

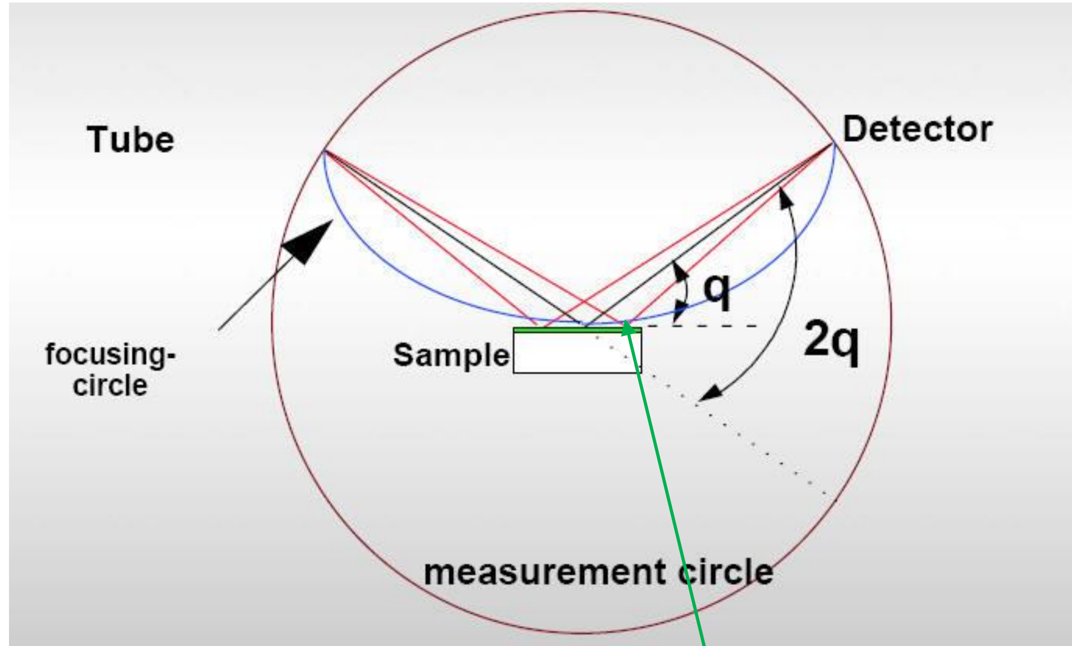

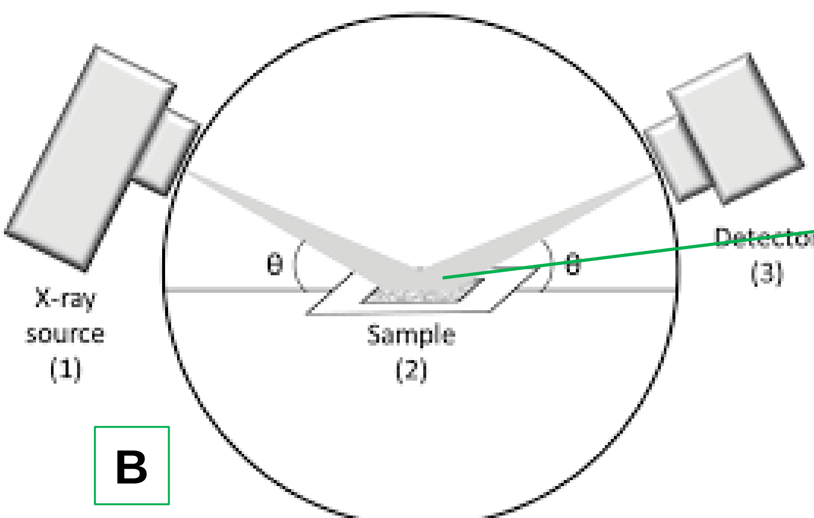

B

C

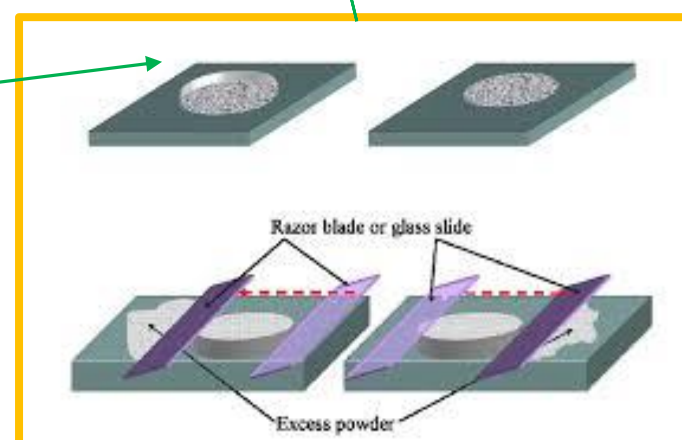

BRAGG-BRENTANO GEOMETRY (PARAFOCUSING GEOMETRY)

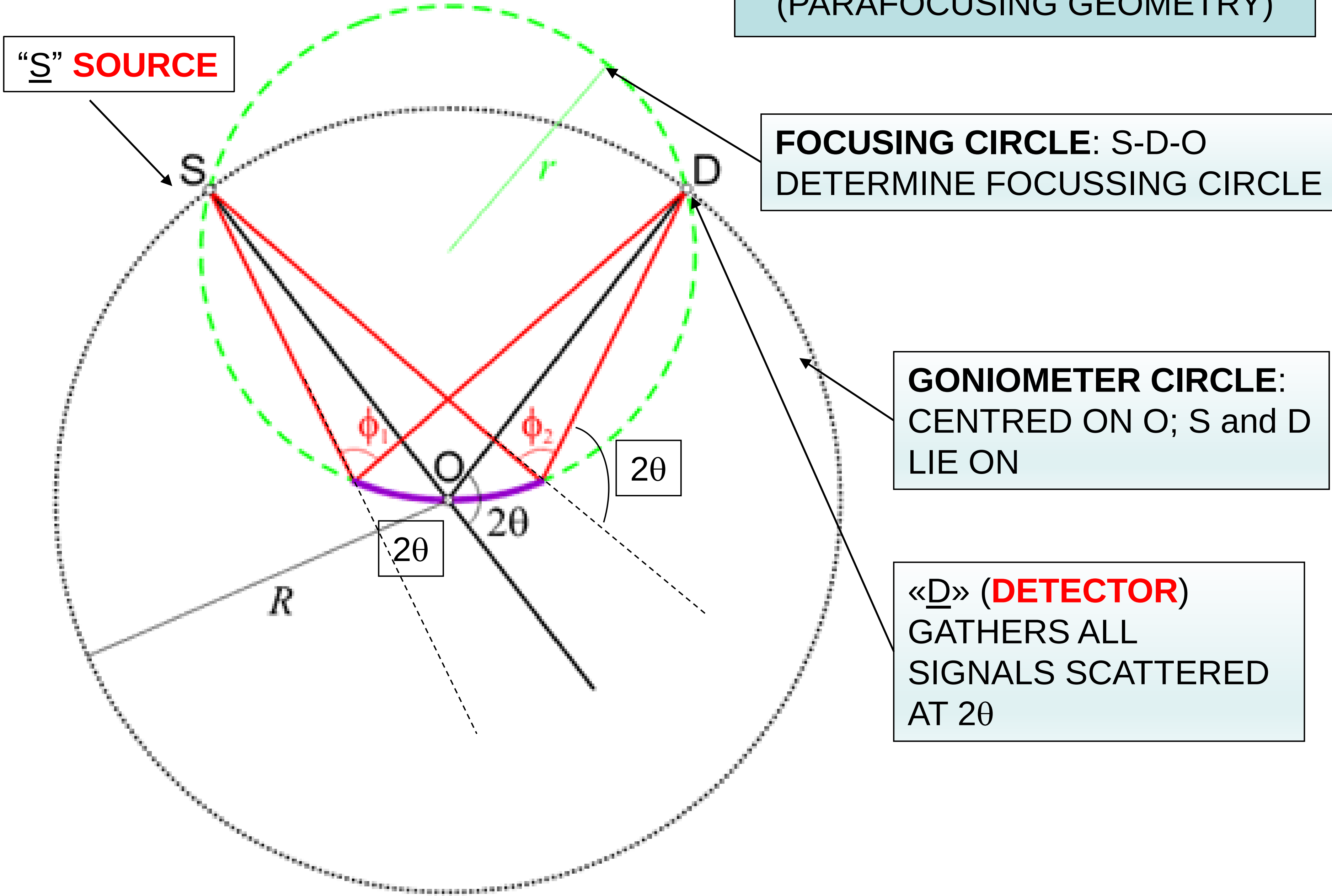

POWDER DIFFRACTION-<u>POINT</u> DETECTOR *versus* <u>MULTI-STRIP</u> DETECTORS

BRAGG-BRENTANO GEOMETRY

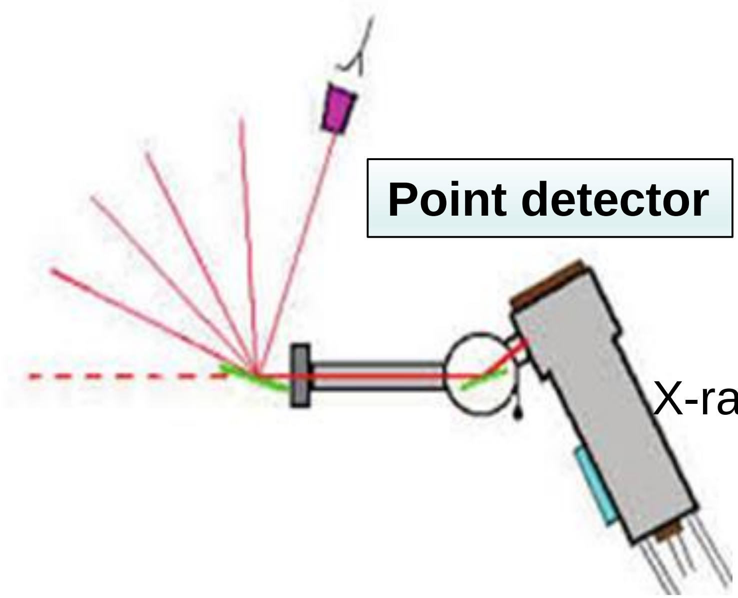

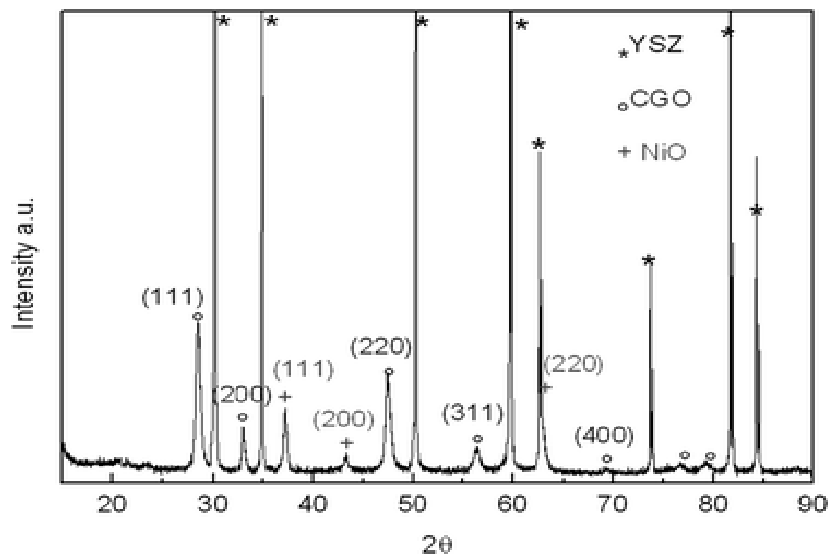

Each strip acts as an individual detector

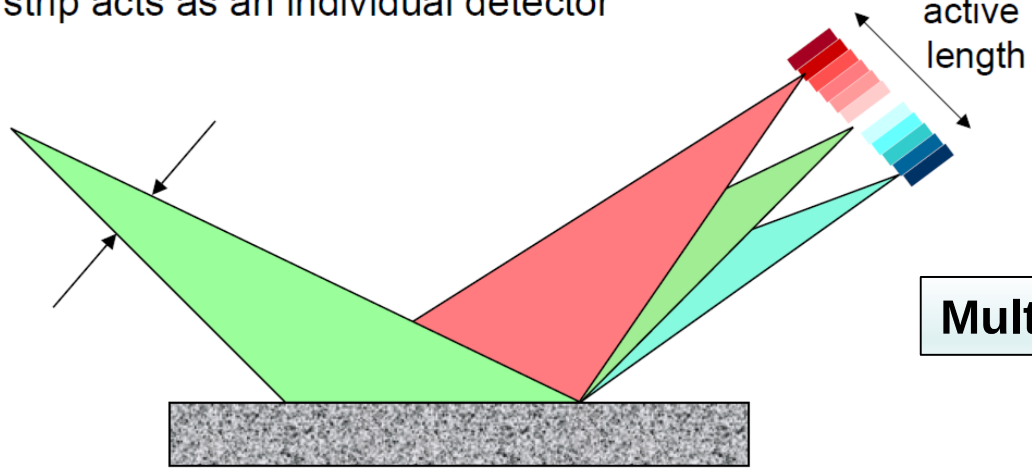

Multi-strip detector

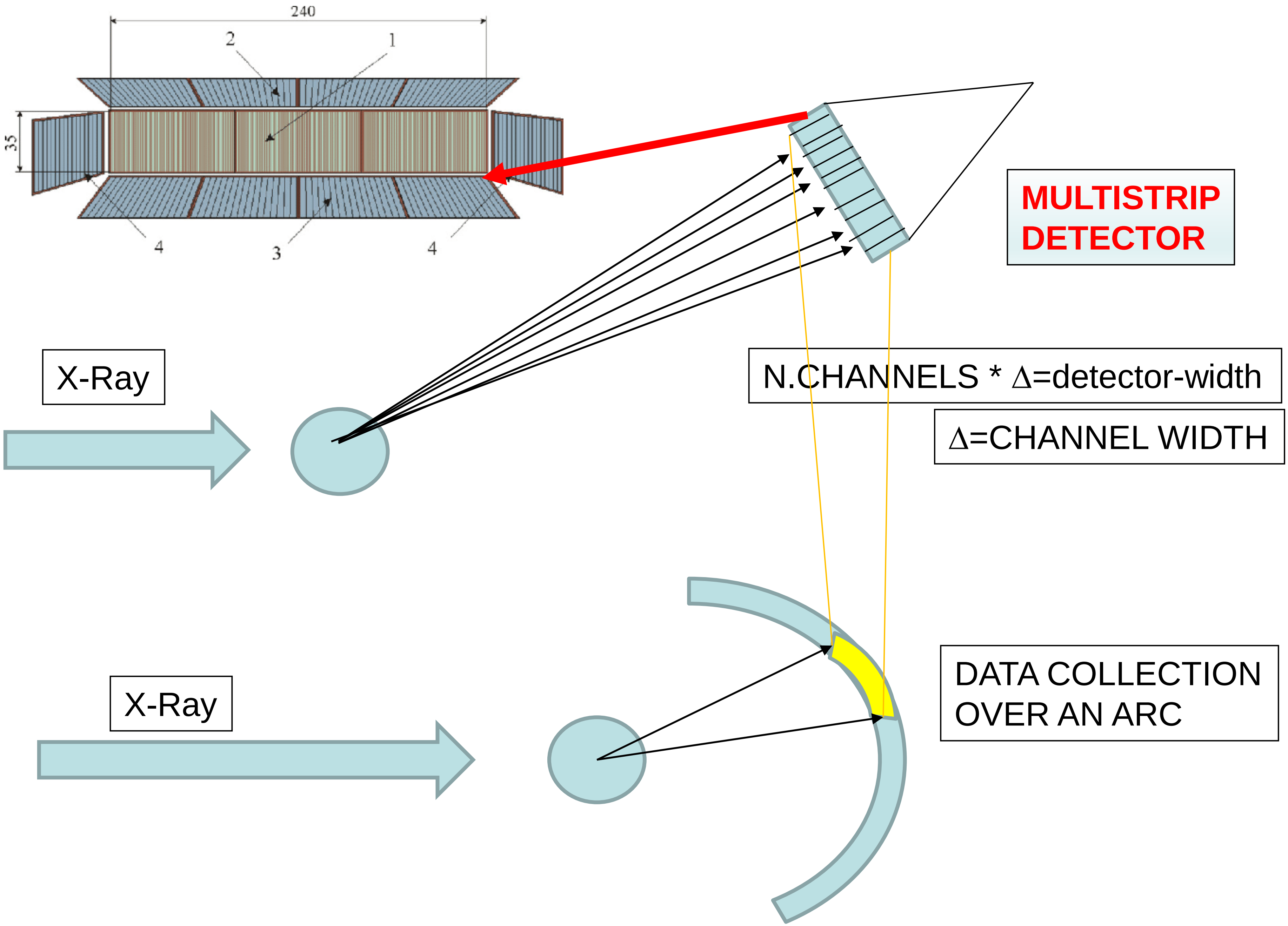

240
2
1
35
4
3
4
MULTISTRIP DETECTOR
X-Ray
N.CHANNELS * Δ=detector-width
Δ=CHANNEL WIDTH
X-Ray
DATA COLLECTION OVER AN ARC

DIFFRACTION PATTERN COLLECTED BY A **BRAGG-BRENTANO** GEOMETRY

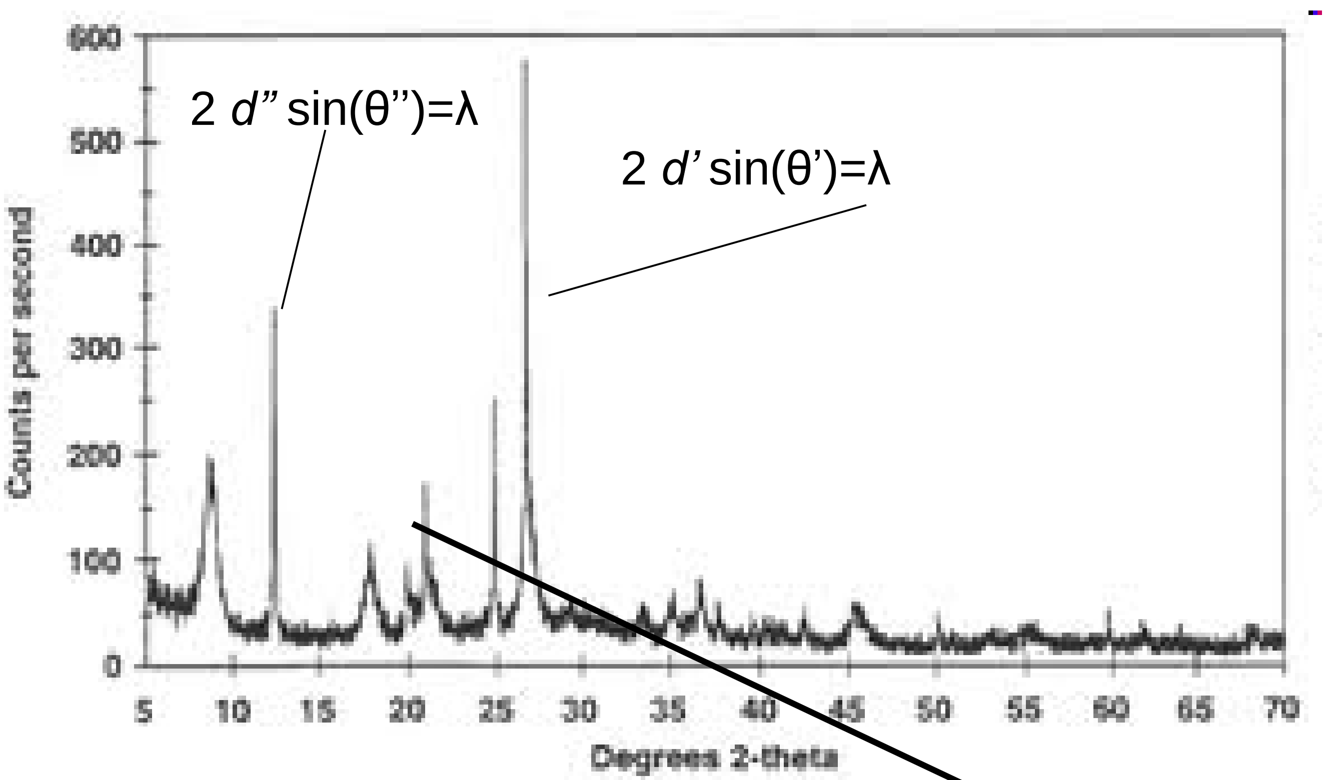

$$2\, d_{hkl} \sin(\theta) = \lambda$$

DIFFRACTION RINGS CAN BE TURNED INTO STANDARD BRAGG-BRENTANO PROFILE

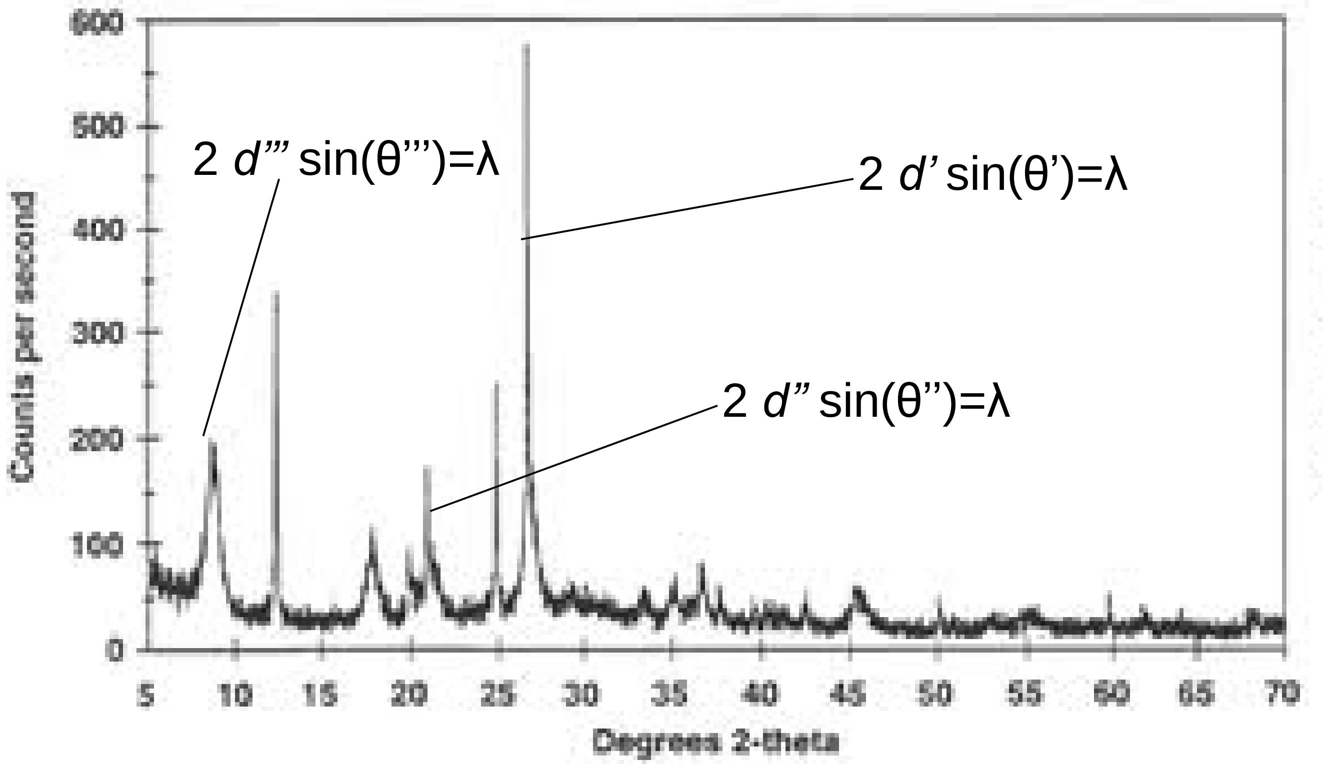

Every phase has its own diffraction pattern. In a mixture, the diffraction patterns of the occurring phases sum up, proportionally to the amount of each phase

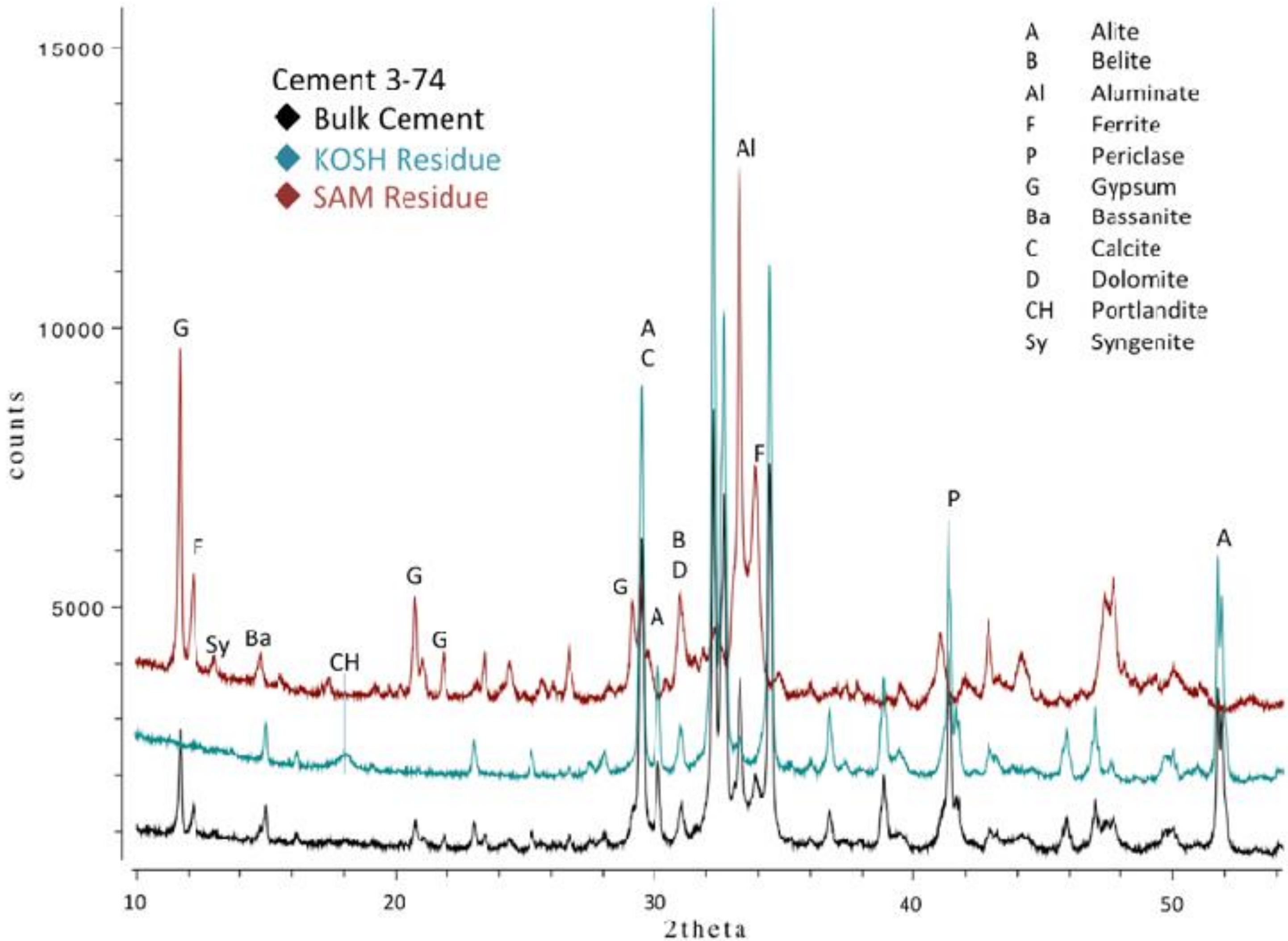

DIFFERENCES BETWEEN POWDER DIFFRACTION PATTERNS

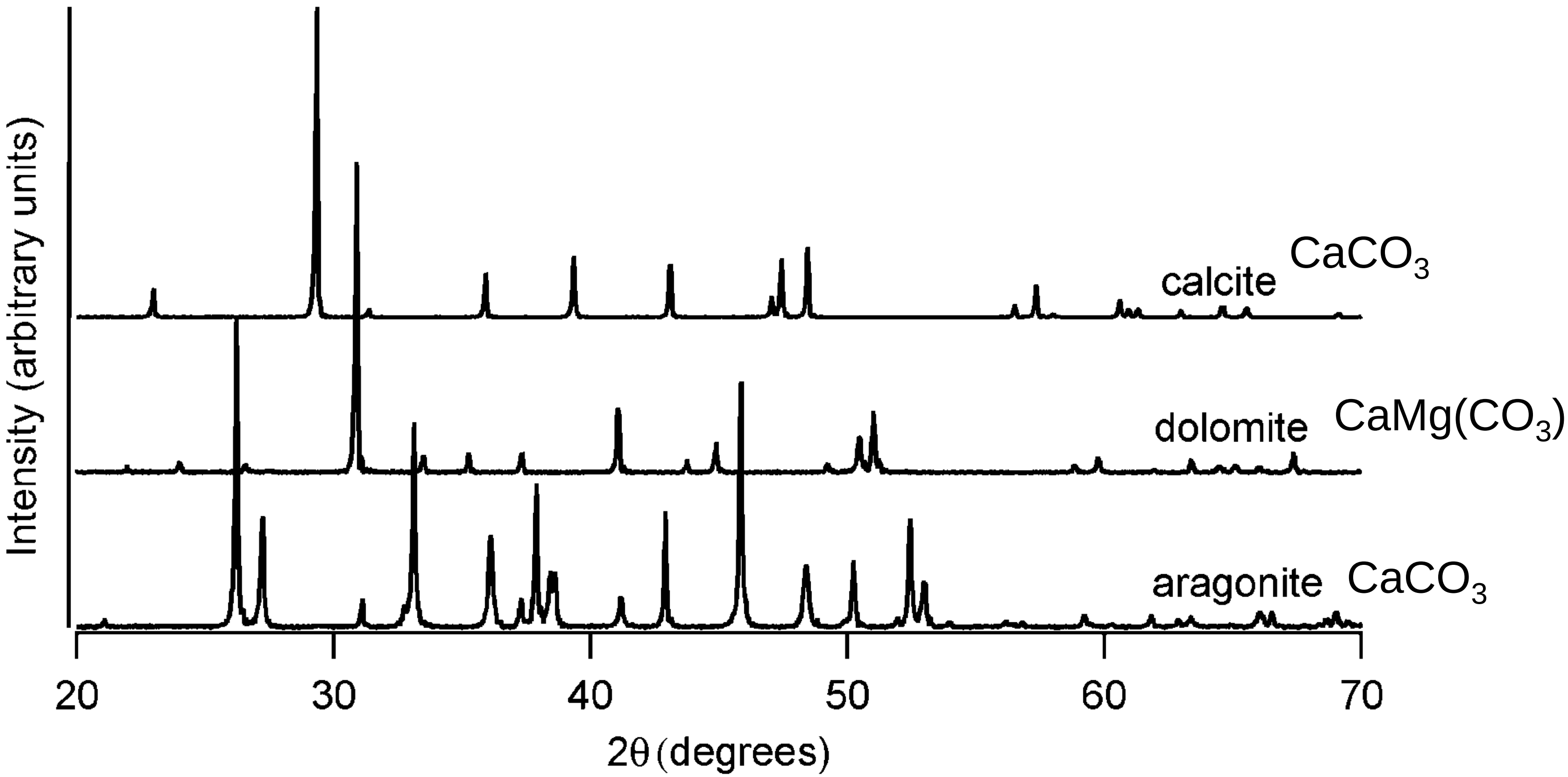

DEBYE-SCHERRER → **BRAGG-BRENTANO**

THE DEBYE-SCHERRER-LIKE OUTPUT (**DIFFRACTION RINGS**) CAN BE TURNED INTO BRAGG-BRENTANO LIKE OUTPUT (**PROFILE PATTERN**)

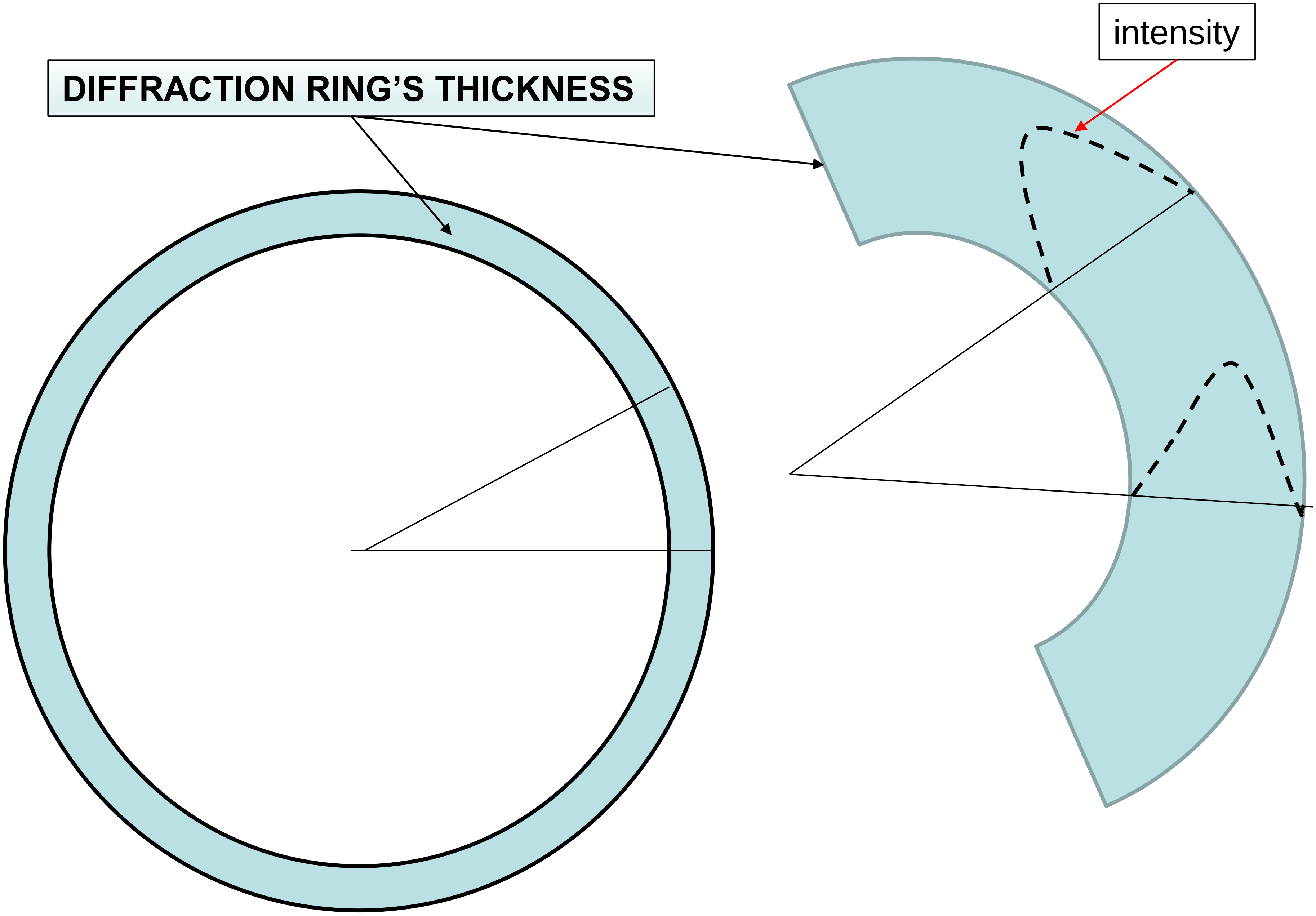
DIFFRACTION RING'S THICKNESS
intensity

DIFFRACTION RING'S THICKNESS

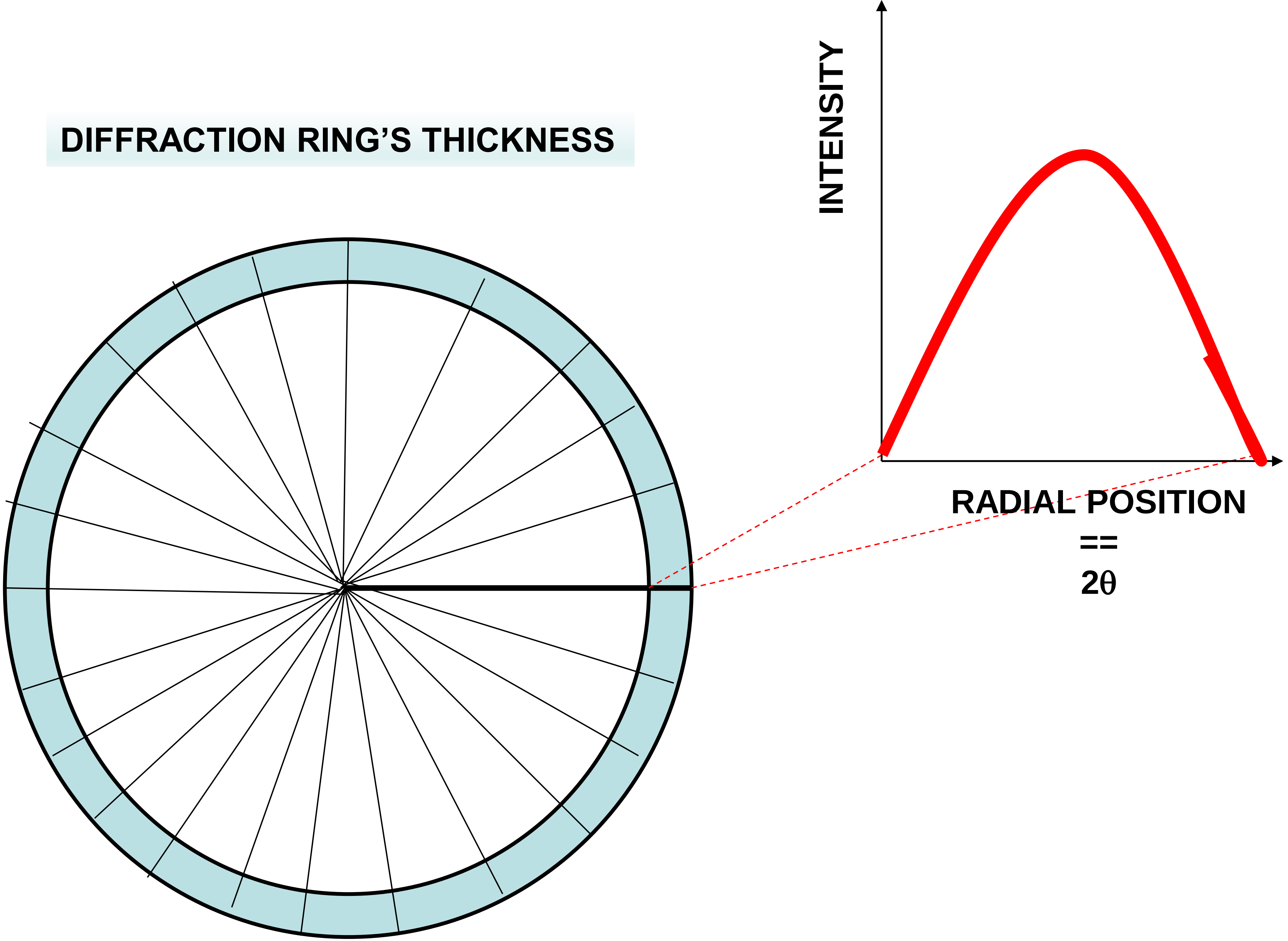

$$Profile(I,\ 2\theta) = \sum_{j=1,N} RADIAL\ PROFILE_J$$

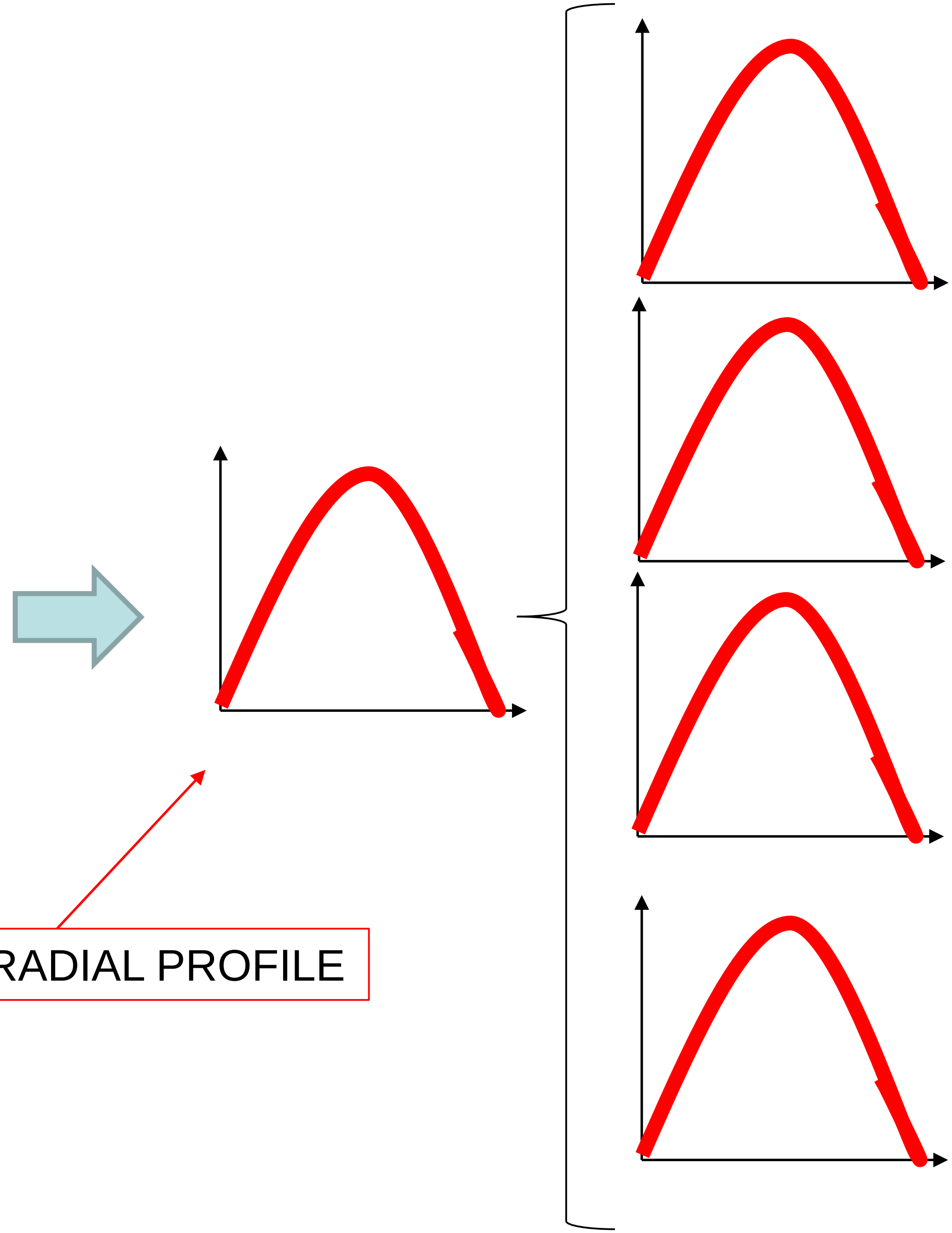

AVERAGE RADIAL PROFILE

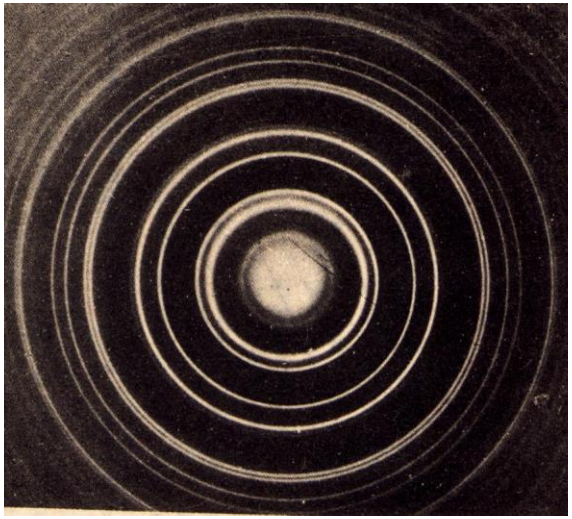

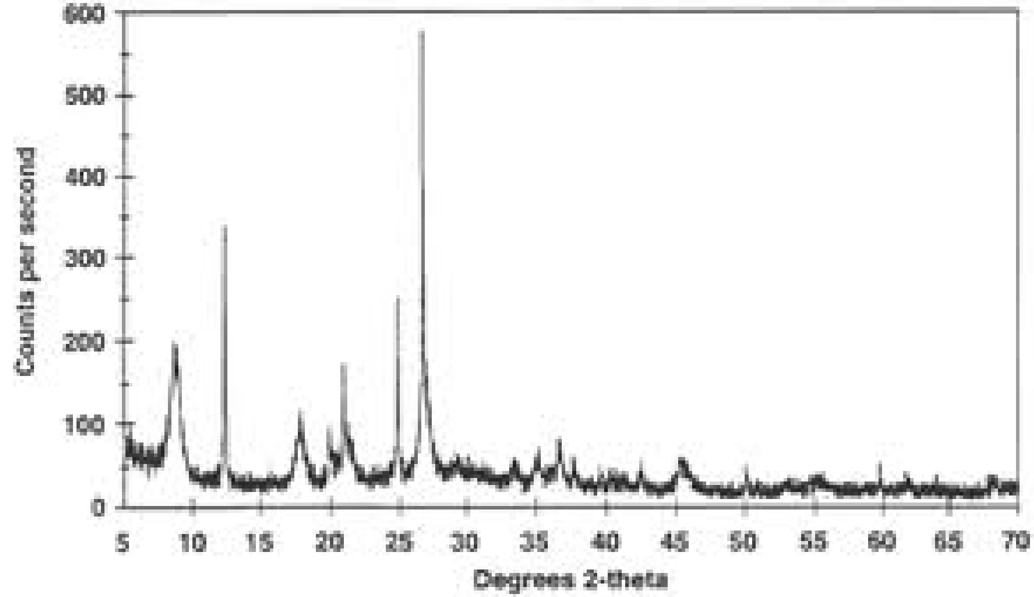

CONVERSION FROM DIFFRACTION RINGS TO 2θ-*I* PATTERN

PHYSICAL MEANING OF BRAGG PEAK IN POWDER DIFFRACTION

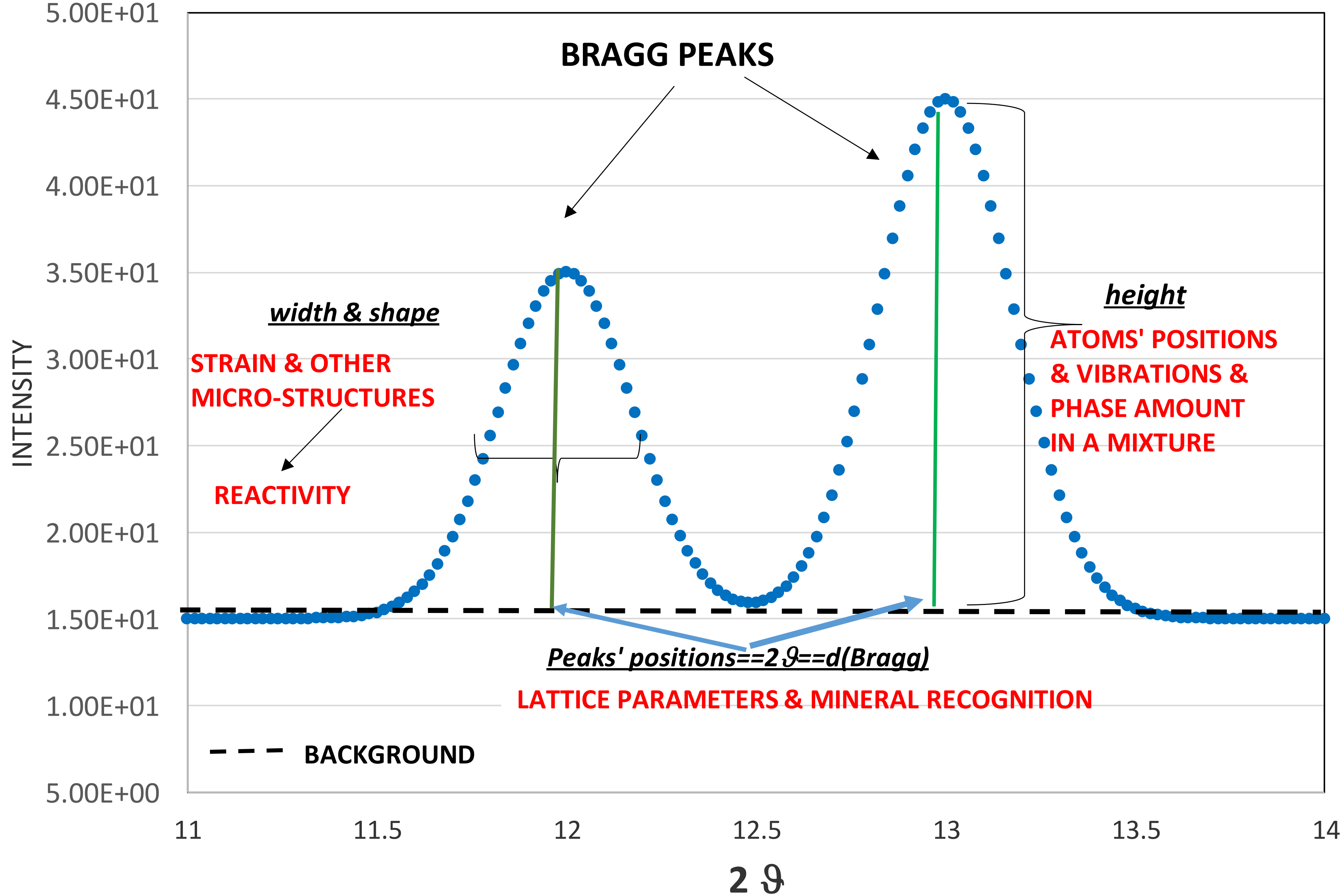

BRAGG PEAKS
width & shape
STRAIN & OTHER MICRO-STRUCTURES
REACTIVITY
height
ATOMS' POSITIONS & VIBRATIONS & PHASE AMOUNT IN A MIXTURE
Peaks' positions==2ϑ==d(Bragg)
LATTICE PARAMETERS & MINERAL RECOGNITION
BACKGROUND
INTENSITY
5.00E+01
4.50E+01
4.00E+01
3.50E+01
3.00E+01
2.50E+01
2.00E+01
1.50E+01
1.00E+01
5.00E+00
11
11.5
12
12.5
13
13.5
14
2 ϑ

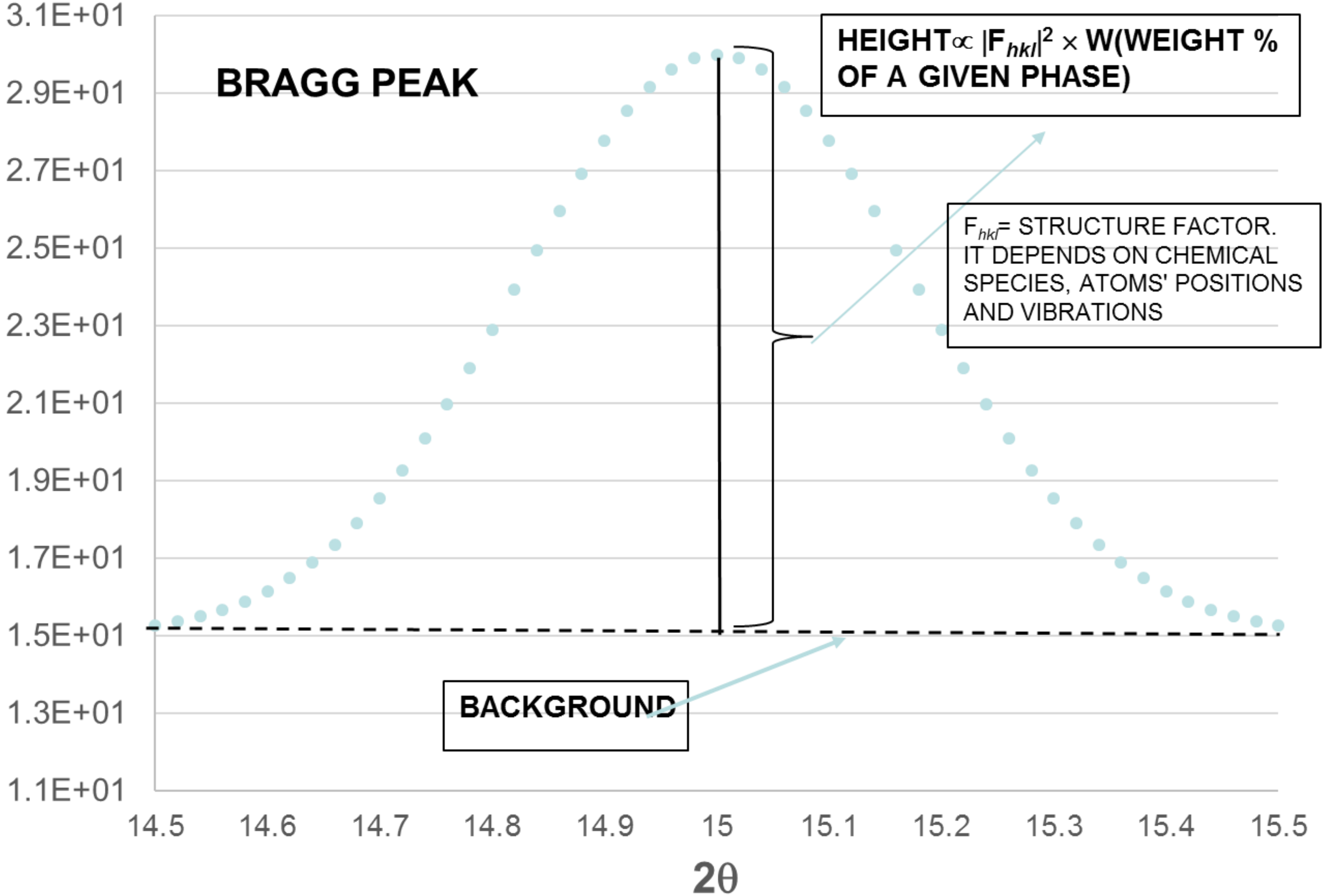
BRAGG PEAK
HEIGHT∝ |F_hkl|² × W(WEIGHT % OF A GIVEN PHASE)
F_hkl= STRUCTURE FACTOR. IT DEPENDS ON CHEMICAL SPECIES, ATOMS' POSITIONS AND VIBRATIONS
BACKGROUND
3.1E+01
2.9E+01
2.7E+01
2.5E+01
2.3E+01
2.1E+01
1.9E+01
1.7E+01
1.5E+01
1.3E+01
1.1E+01
14.5
14.6
14.7
14.8
14.9
15
15.1
15.2
15.3
15.4
15.5
2θ

RESOLUTION

ANGULAR RESOLUTION

$a_{1,2}$= physical distance of observation of the two peaks on detector
$\Rightarrow$ ANGULAR RESOLUTION

X-Ray

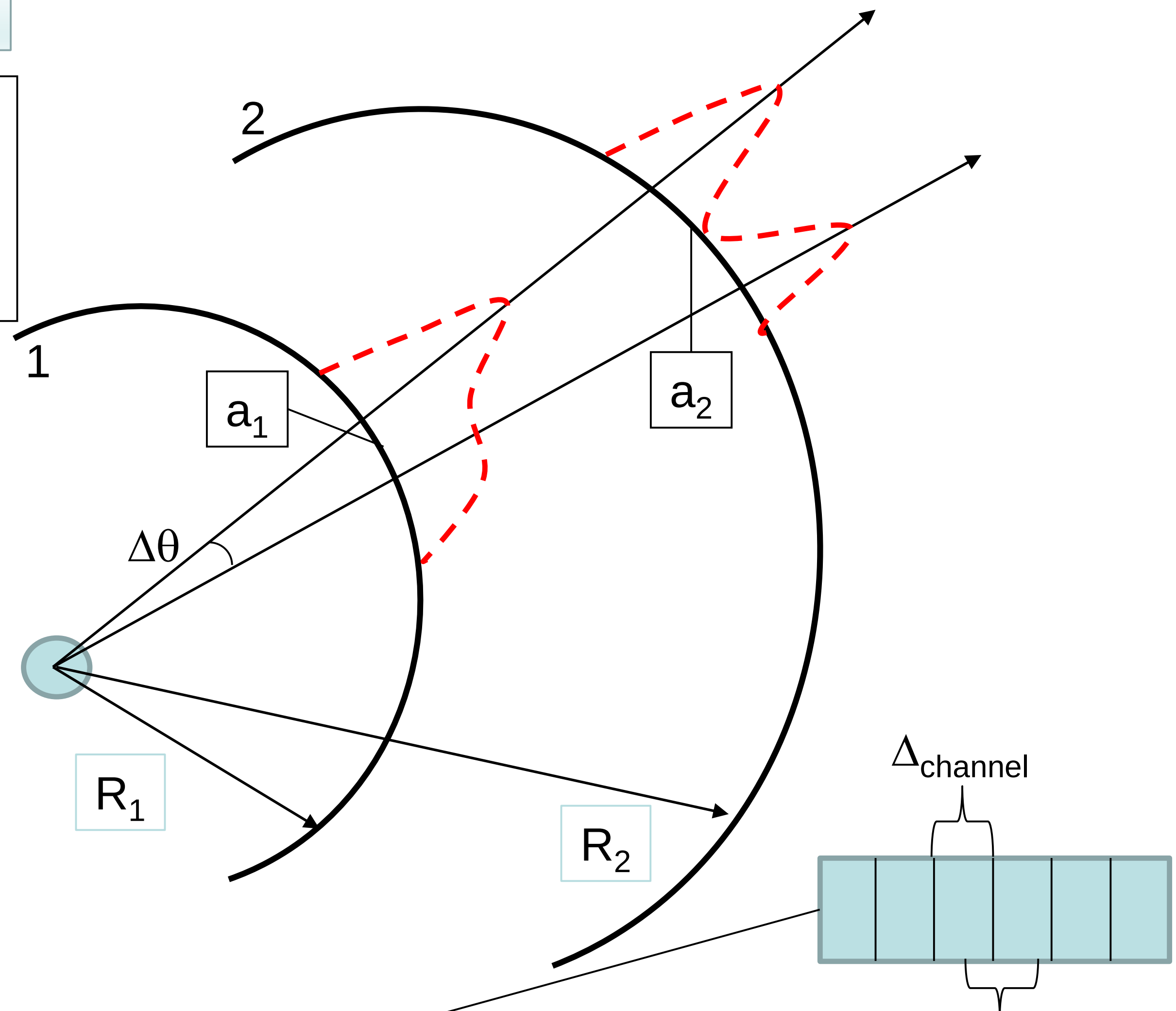

$a_1 = R_1 \times \Delta\theta$

$a_2 = R_2 \times \Delta\theta$

For multi-strip

$\Delta\theta_{min} = \Delta_{channel}/R$

$\Delta\theta_{min}$ =The smallest angular discrimination

$\Delta_{channel}$=Multi-strip channel’s width

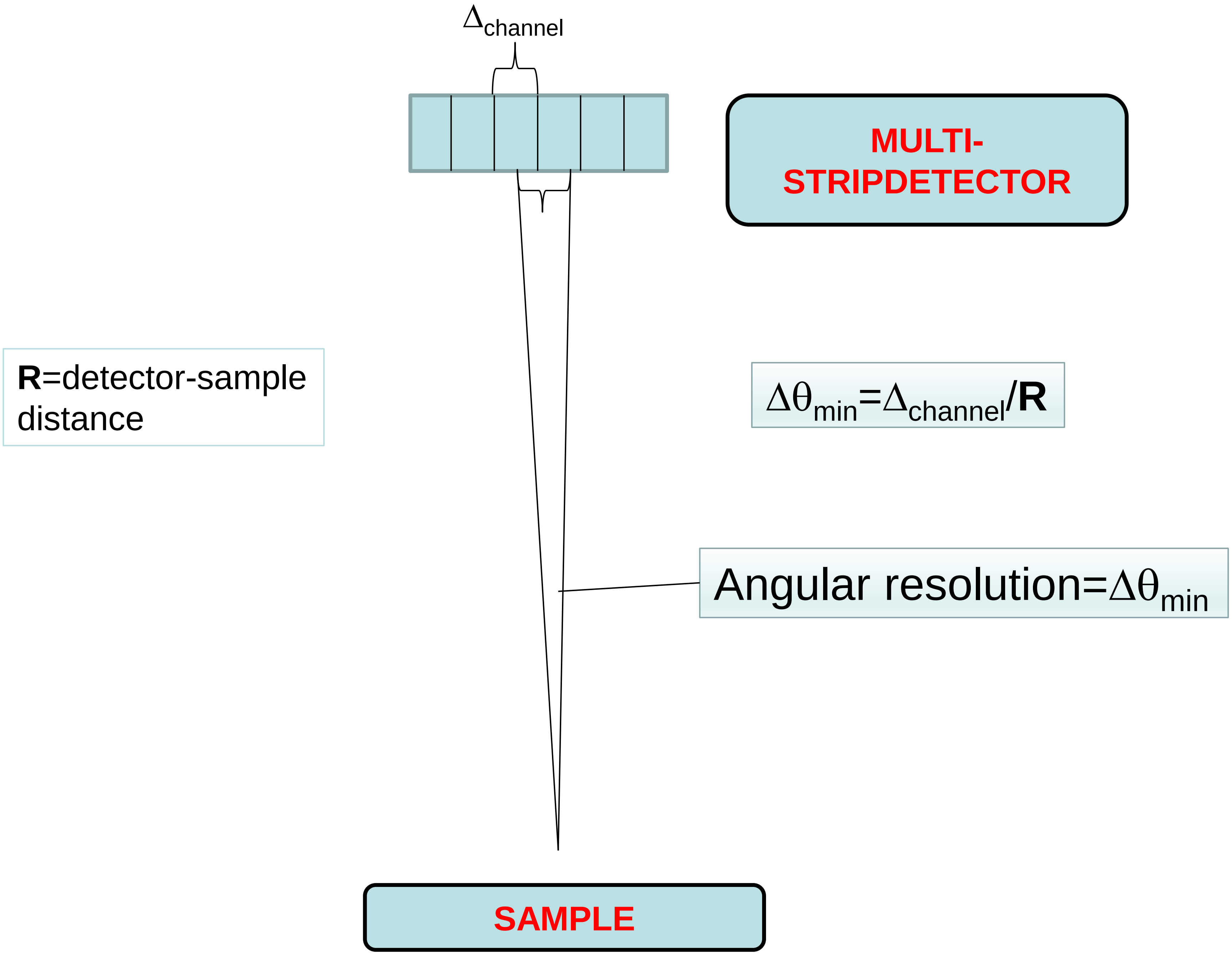
$\Delta_{channel}$
MULTI-STRIPDETECTOR
R=detector-sample distance
$\Delta\theta_{min}=\Delta_{channel}/\mathbf{R}$
Angular resolution=$\Delta\theta_{min}$
SAMPLE

YOU NEED A COMPROMISE!

- THE LARGER THE SAMPLE-DETECTOR DISTANCE, THE BETTER THE ANGULAR RESOLUTION

- THE LARGER THE SAMPLE-DETECTOR DISTANCE, THE WORSE THE TOTAL EFFICIENCY BECAUSE OF A REDUCTION OF PHOTON IRRADIANCE

TRY TO COMPENSATE THROUGH AN ENHANCEMENT OF INTRINSIC EFFICIENCY

COUNTING UNCERTAINTY

$$\sigma(N) \sim \sqrt{N}$$

$$\Downarrow$$

$$\boxed{\frac{\sigma}{N} \sim \frac{1}{\sqrt{N}}}$$

END OF THE GENERAL PART

NEUTRON RADIATION

NEUTRONS

Mass=1.67492729(28)×10$^{−27}$ kg

De Broglie relationship

$$h = p \times \lambda$$

h = Planck constant = 6.62606896(33)×10$^{−34}$ J·s

p

Particle-like

λ

Wave-like

NEUTRON PRODUCTION

FISSION

^{235}U

^{239}Pu

$^{235}U + 1\ n >> \underline{2\ n} + {}^{89}Kr + {}^{144}Ba + ENERGY$

$^{235}U + 1\ n >> \underline{2\ n} + {}^{92}Sr + {}^{140}Xe + ENERGY$

n(energy)~0.025 eV
(*thermal* neutrons=
<u>slow neutrons</u>)

SPALLATION

COMPLEX NUCLEAR REACTION PROCESS

EMBEDDING of
<u>FAST NEUTRONS</u>

EVAPORATION

Fast neutrons: energy greater than 1 eV, up to 0.1 MeV or approximately 1 MeV, depending on the definition.

Slow neutrons: energy less than or equal to 0.4 eV.

Epithermal neutrons: energy from 1 eV to 10 keV.

Hot neutrons: energy of about 0.2 eV.

Thermal neutrons: energy of about 0.025 eV

Cold neutrons: energy from 5×10^{-5} eV to 0.025 eV.

Very cold neutrons: energy from 3×10^{-7} eV to 5×10^{-5} eV.

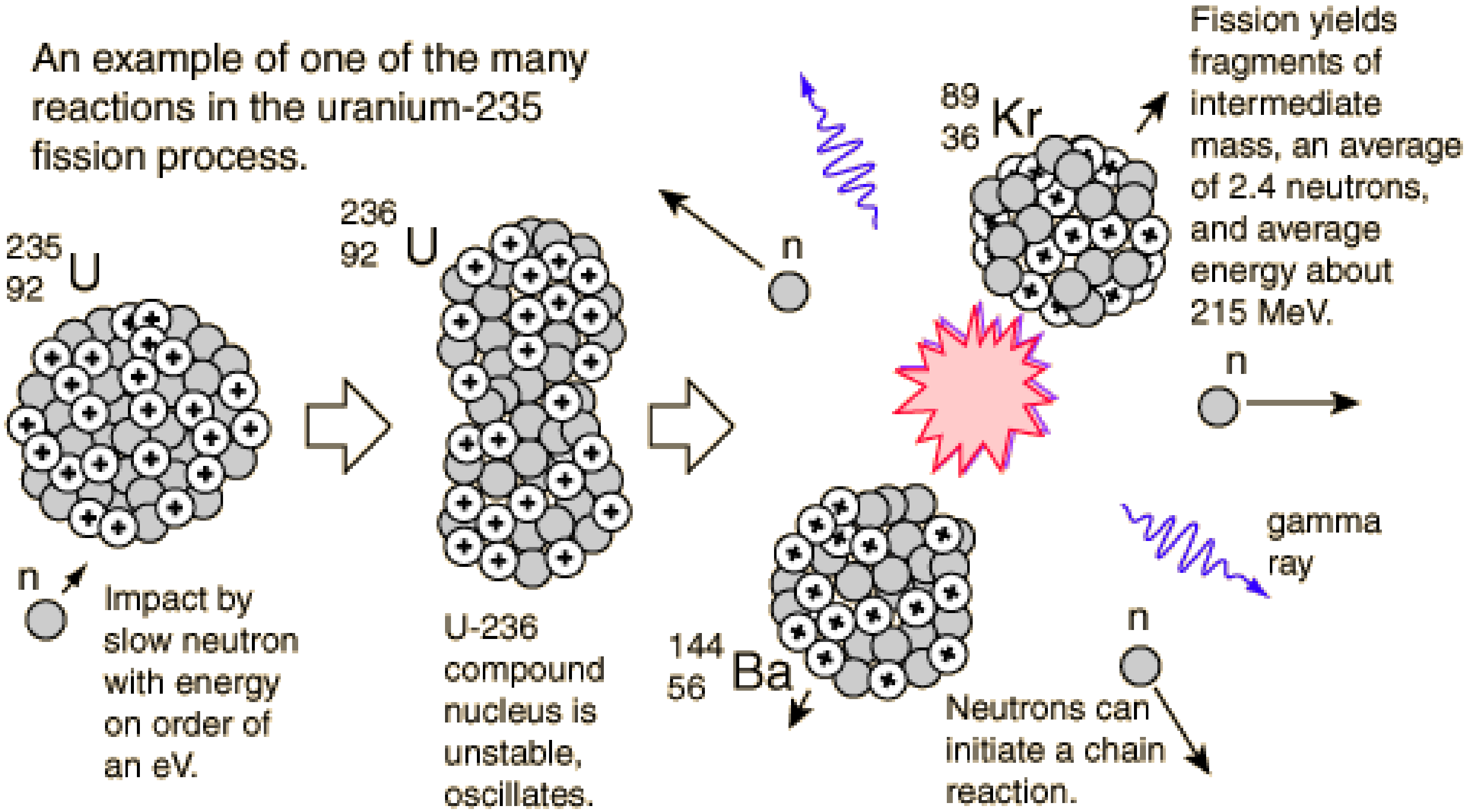

NUCLEAR FISSION

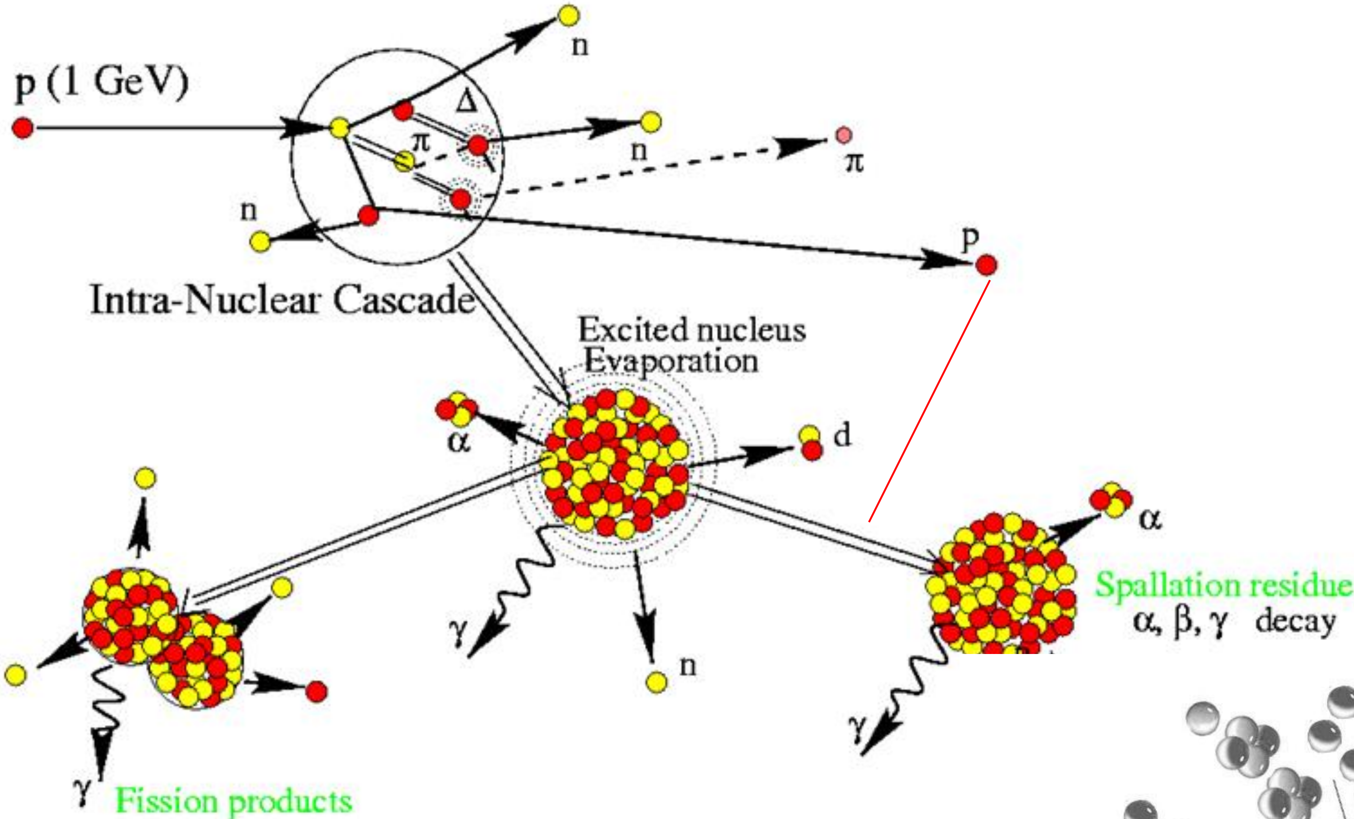
p (1 GeV)
n
Δ
π
n
π
n
p
Intra-Nuclear Cascade
Excited nucleus
Evaporation
α
d
α
Spallation residue
α, β, γ decay
γ
n
γ
γ
Fission products

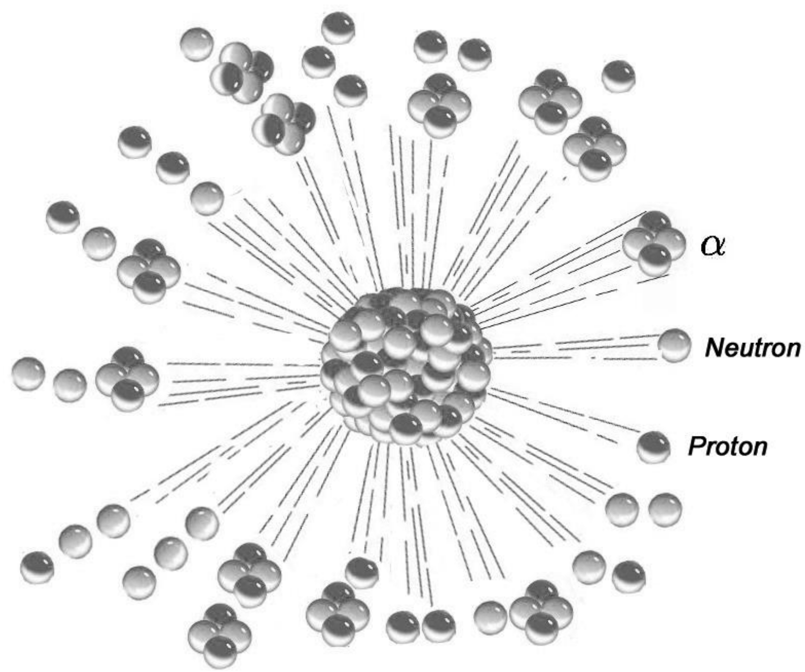
α
Neutron
Proton

SPALLATION

SPALLATION

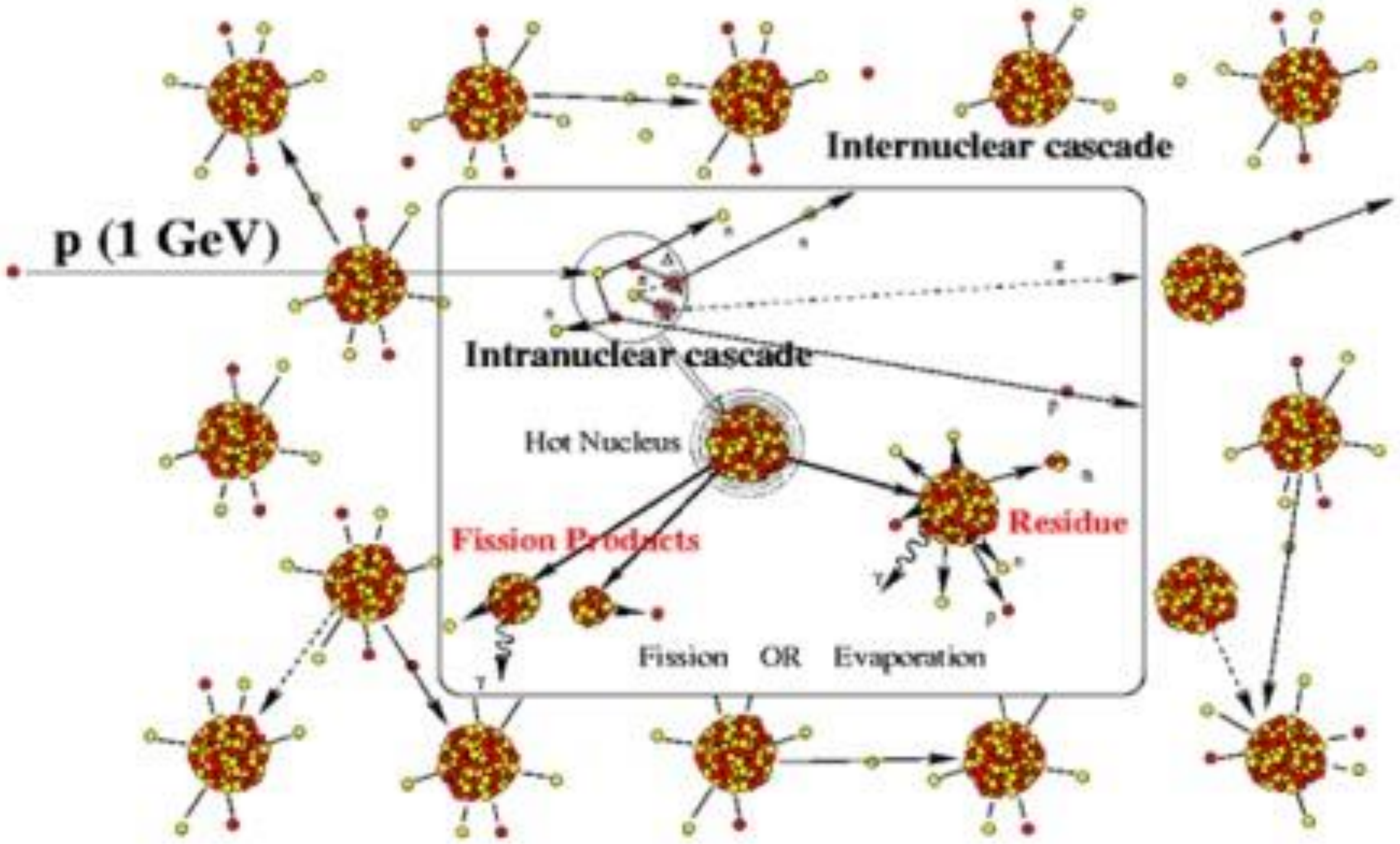

A spallation reaction consists of sending a high energy particle, often a proton, into a nucleus which then ejects different sorts of particles. Among these are many neutrons. These are then fired at the nuclei which we wish to transform and transmute. During transmutation, the excited nucleus effectively captures neutrons and then either it fissions or is evaporated by losing the most energetic particles.

SPALLATION YIELD versus TARGET

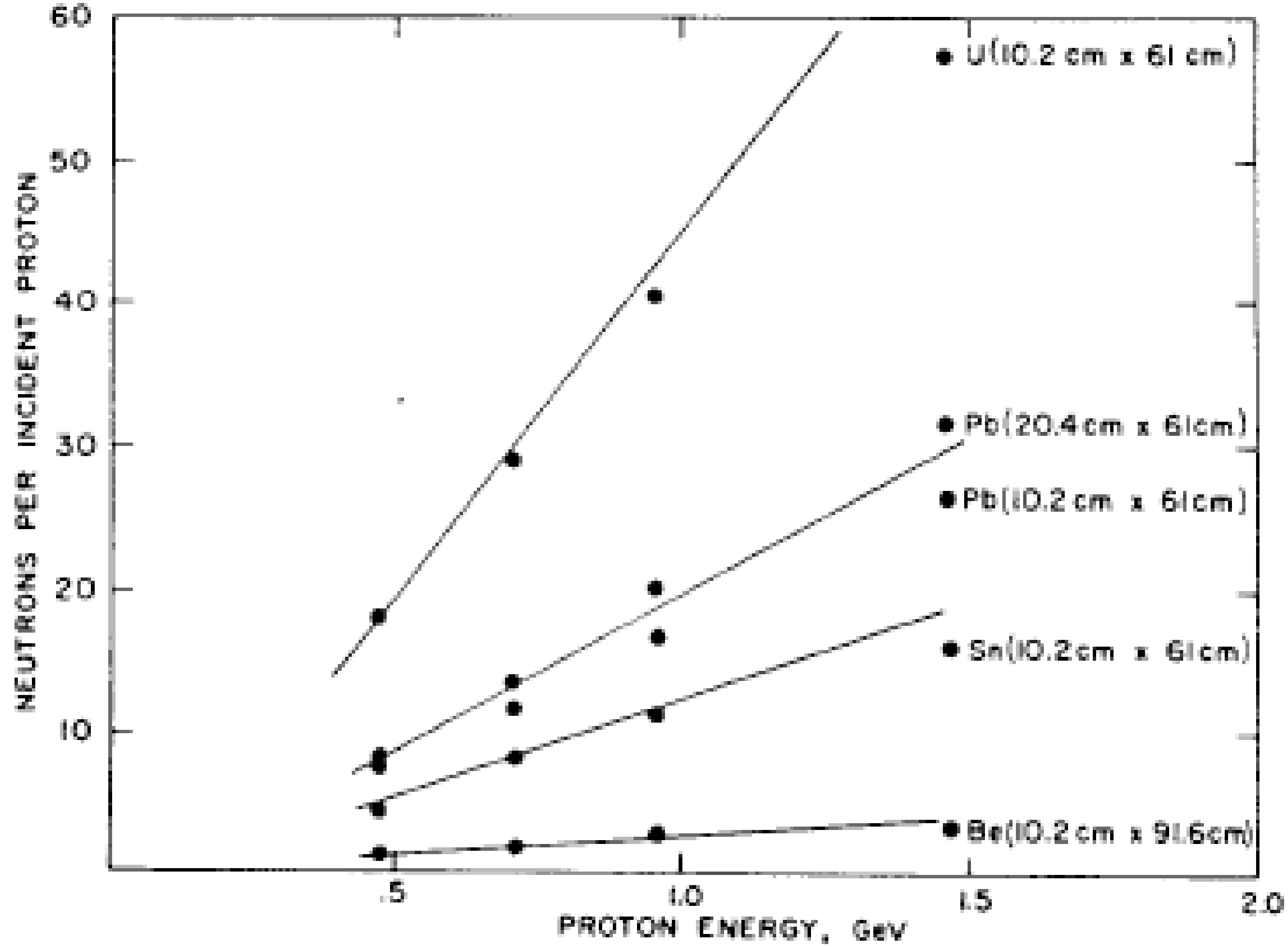

PROTON ENERGY AND ENUTRON PRODUCTION BY SPALLATION: SATURATION

(50-cm-diam × 200-cm-long targets bombarded on axis by ~1-GeV protons)

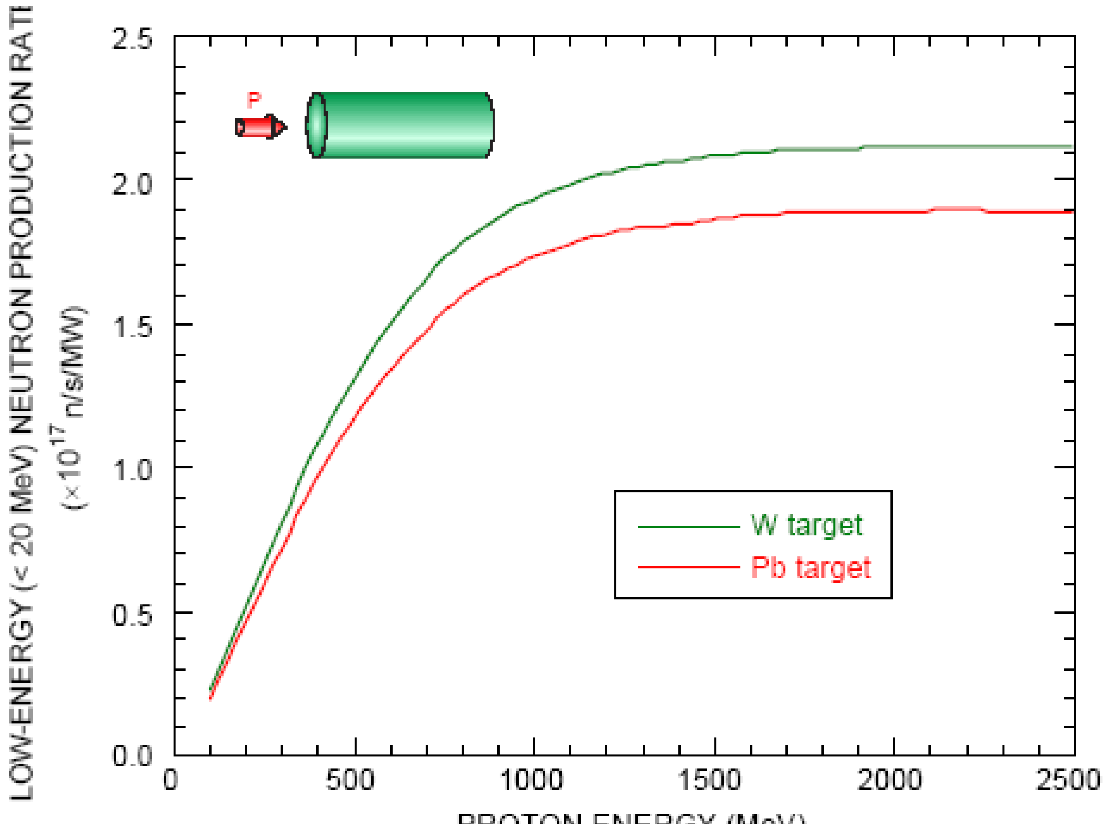

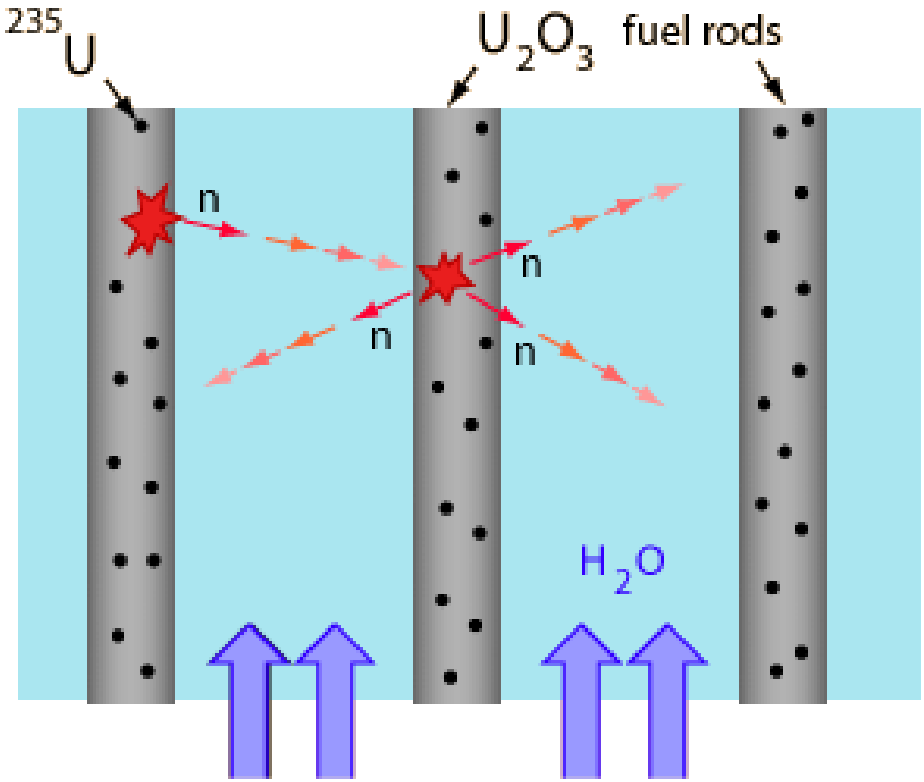

Water as coolant and moderator flows between fuel rods.

NEUTRONS MUST BE SLOWED DOWN BY MEANS OF A **MODERATOR**

TO FEED FISSION

TO HAVE LOW ENERGY NEUTRONS

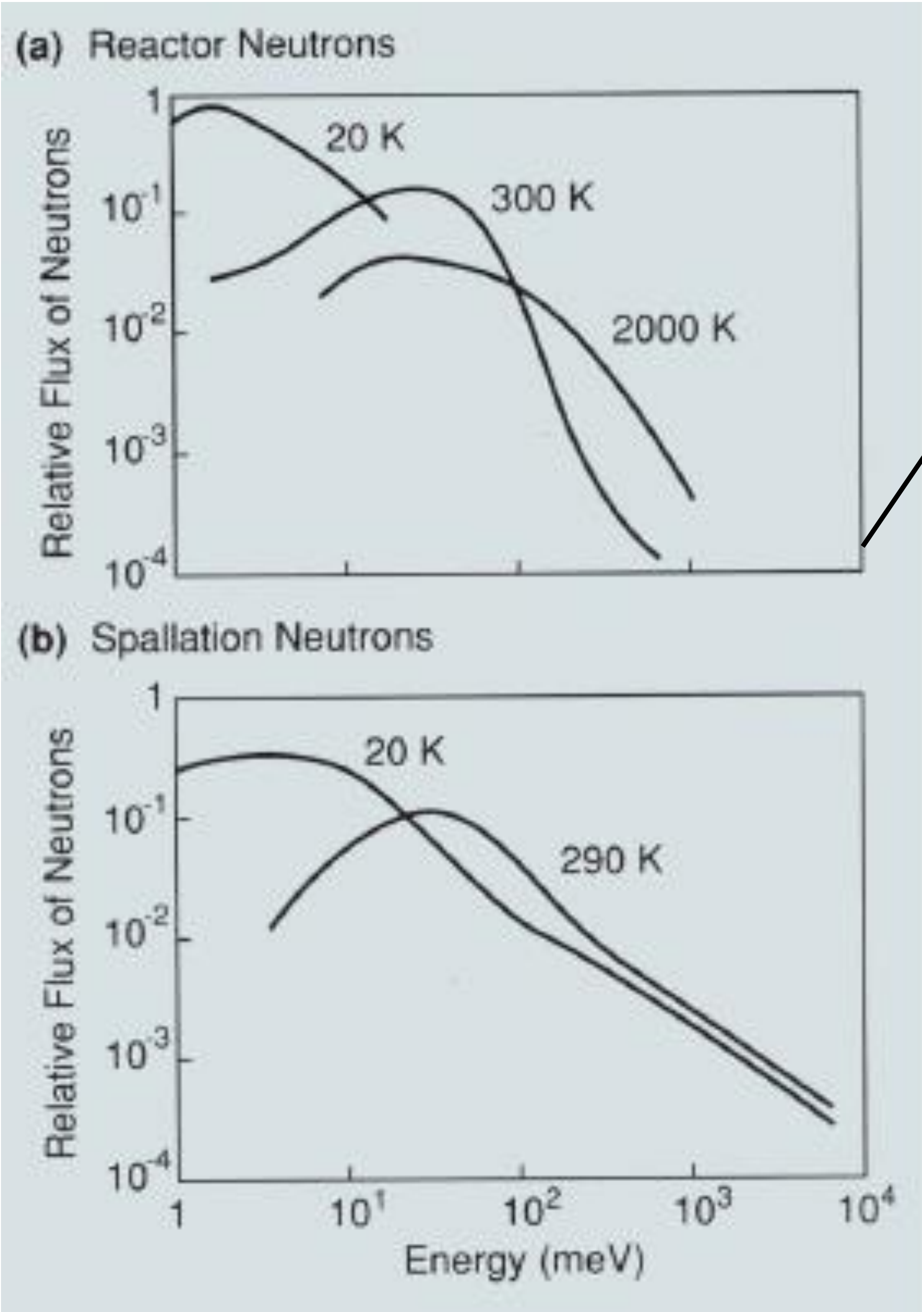

FLUX AS A FUNCTION OF MODERATOR

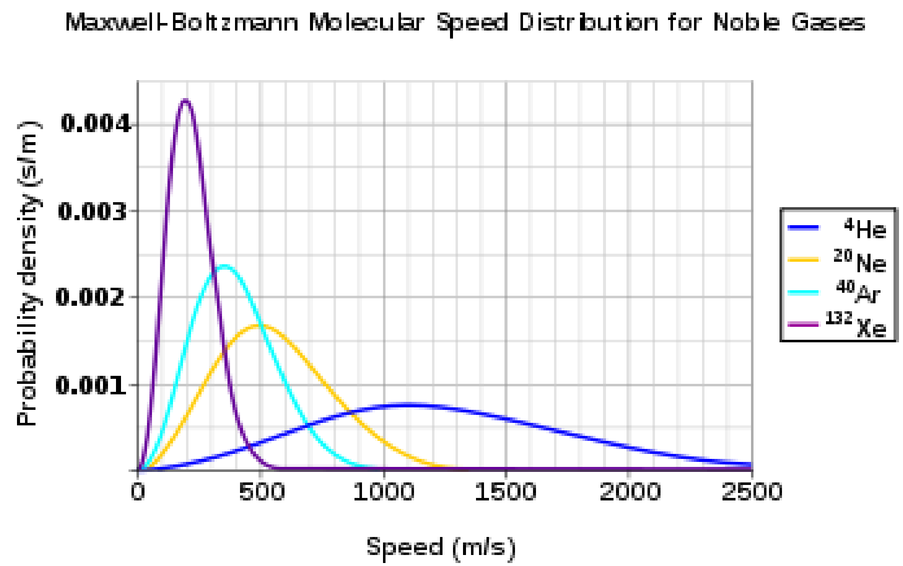

MAXWELL VELOCITY DISTRIBUTION

LAYOUT OF A SPALLATION SOURCE

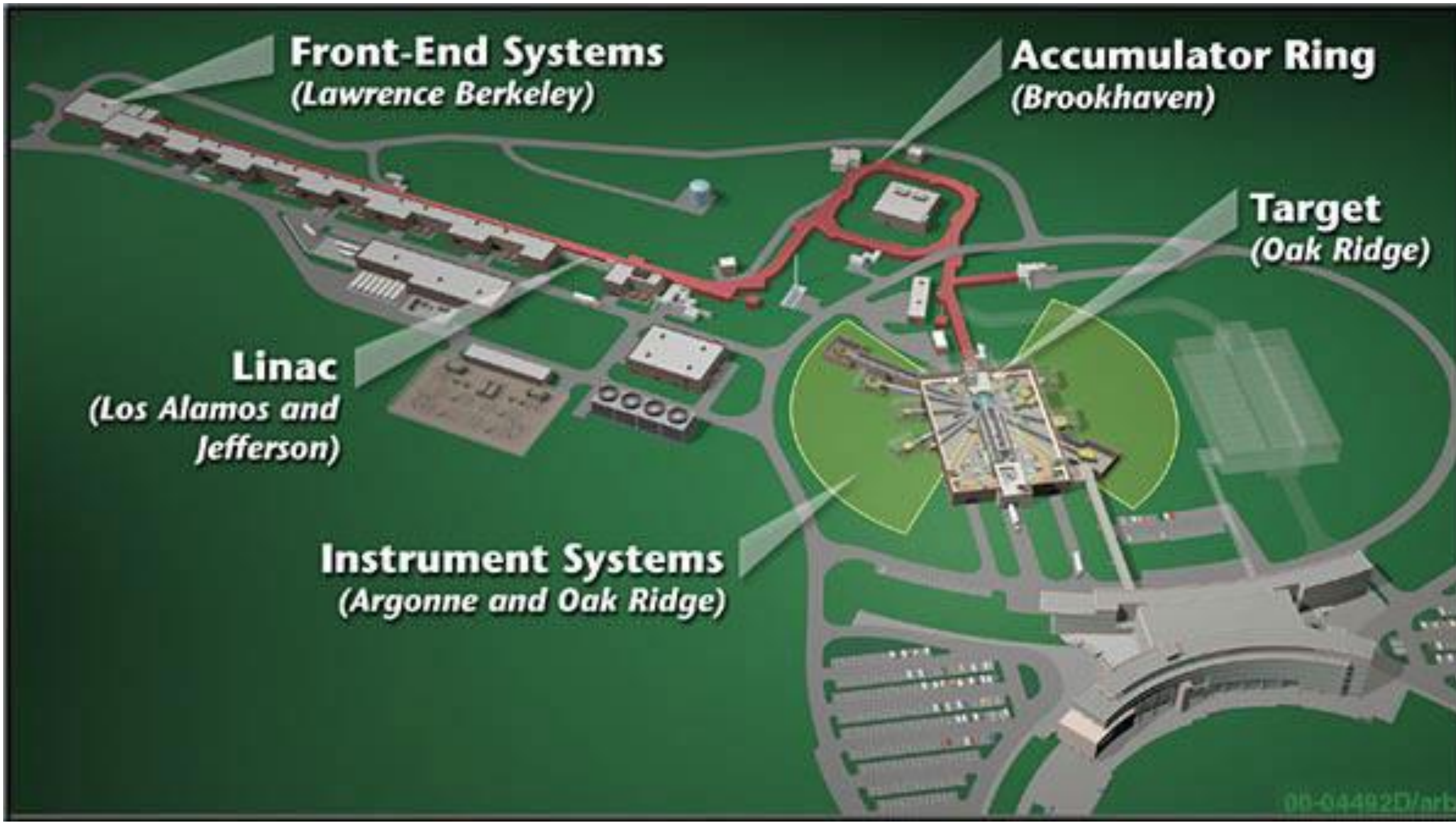

REACTOR CORE OF SPALLATION

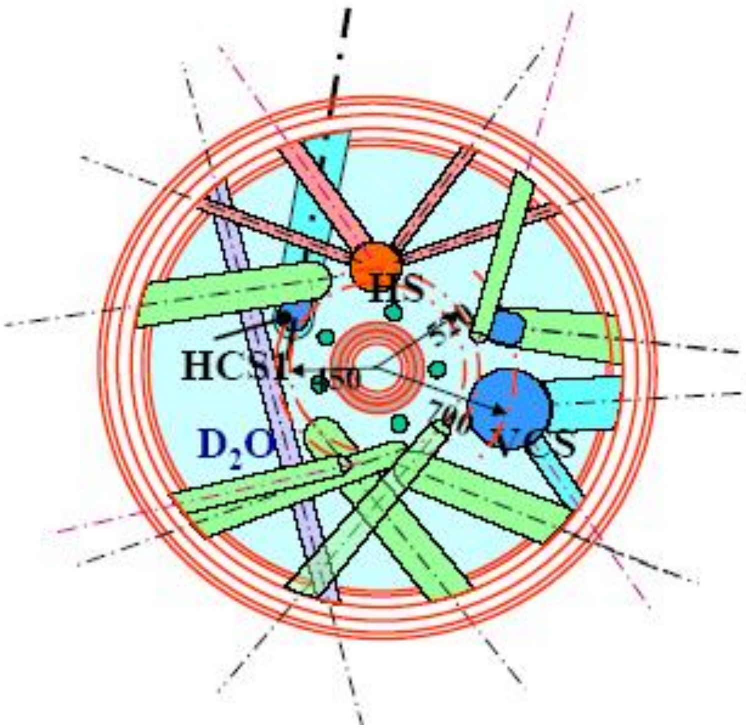

LAYOUT OF ILL: STEADY SOURCE

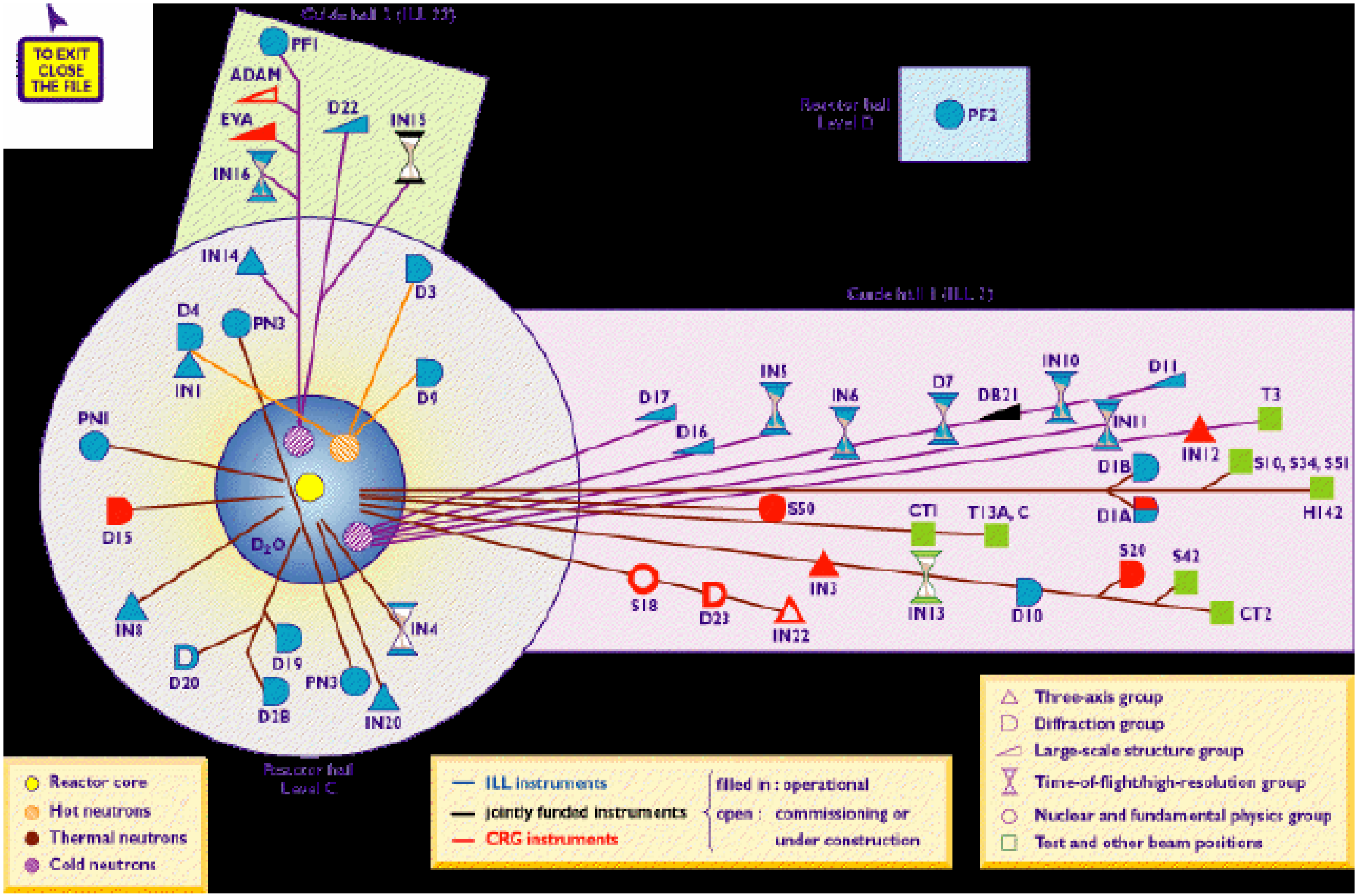

NEUTRON DETECTION

RECOIL MECHANISM

NUCLEAR REACTIONS

- IONIZATION BY COLLISION

- CAUSING NUCLEAR REACTIOS WHICH PRODUCE DETECTABLE ENERGY

THE COMMONEST NUCLEAR REACTIONS FOR NEUTRON DETECTION

$$n + {}^{3}He \rightarrow p + {}^{3}H + 765\ keV$$

$$n + {}^{10}_{5}B \rightarrow \begin{cases} \alpha + {}^{7}_{3}Li + 2.310\ MeV\ (94\%) \\ \alpha + {}^{7}_{3}Li + 2.792\ MeV\ (6\%) \end{cases}$$

DETECTORS

- **GAS FILLED (GAS)**
- **SCINTILLATORS (SOLID STATE)**
- **SEMI-CONDUCTORS (SOLID STATE)**

GAS-FILLED DETECTORS

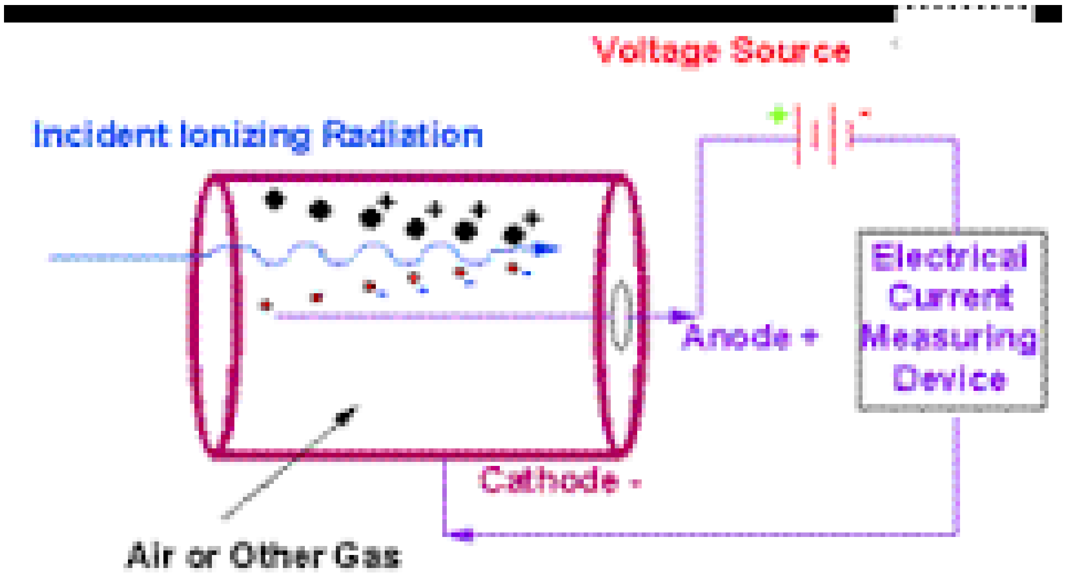

GAS-FILLED DETECTORS LAYOUT

^{3}He – BF_3 – NEUTRON REACTIONS (THERMAL NEUTRONS)
^{4}He – CH_4 – RECOIL MECHANISM (FAST NEUTRONS)

!

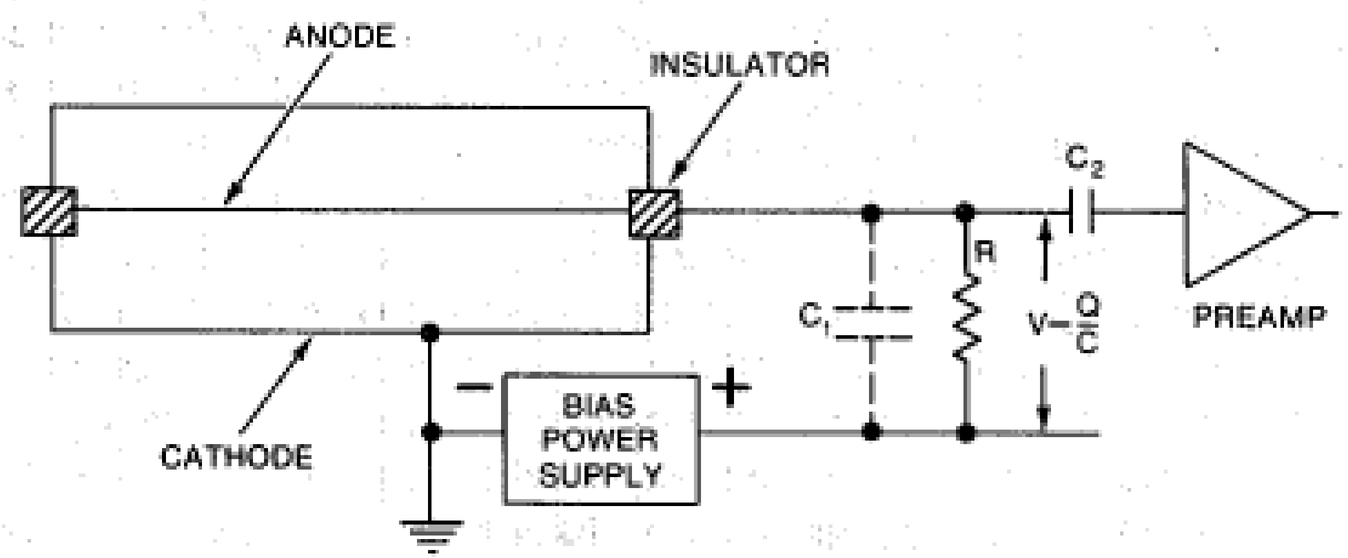

***Fig. 13.1** Typical setup for gas-filled neutron detectors.*

CROSS-SECTIONS OF SOME ELEMENTS AS A FUNCTION OF NEUTRON ENERGY

!

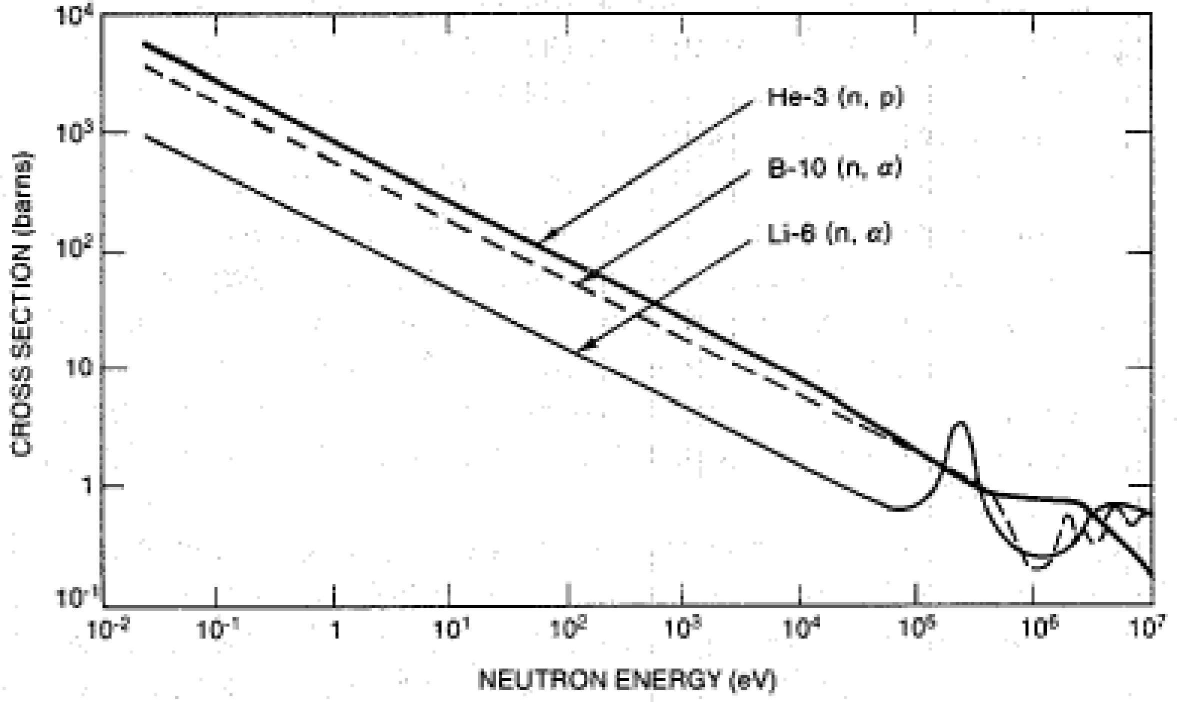

Fig. 13.4 *$^{3}He(n,p)$, $^{10}B(n,\alpha)$, and $^{6}Li(n,\alpha)$ cross sections as a function of incident neutron energy (Ref. 7).*

II

SCINTILLATOR DETECTOR LAYOUT

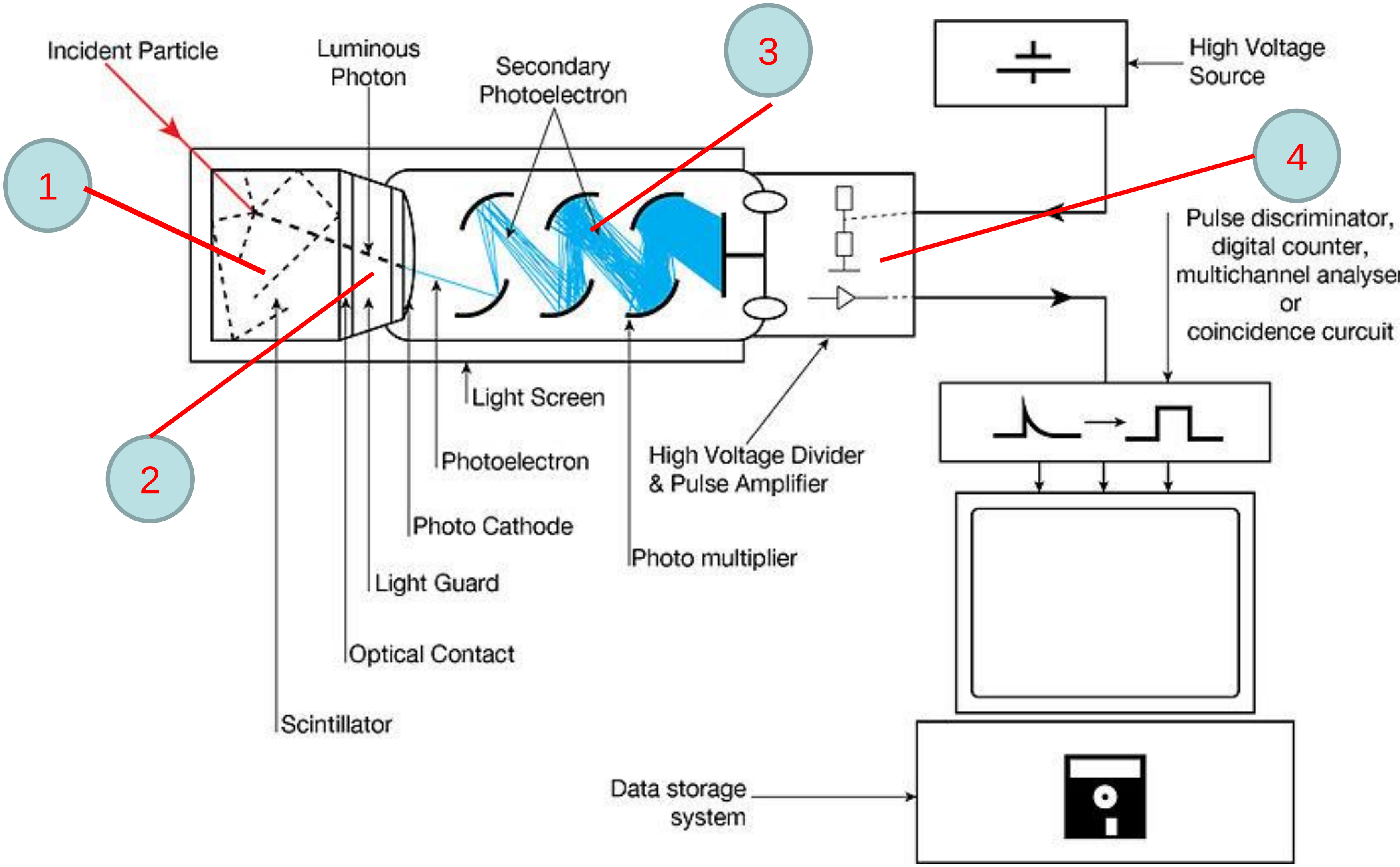

II

ORGANIC SCINTILLATORS

CRYSTALS:
ANTHRACENE, STILBENE, NAPHTHALENE (C_nH_m)
LIQUIDS:
P-TERPHENYL
PLASTIC:
ORGANIC SCINTILLATOR IS EMBEDDED INTO A POLYMER MATRIX

And more…….

INORGANIC SCINTILLATORS

CRYSTALS:
ZnS(Ag), BaF_2, CaF_2(Eu)……..
GLASSES:
Boron silicates

III

SEMICONDUCTOR-BASED NEUTRON DETECTORS

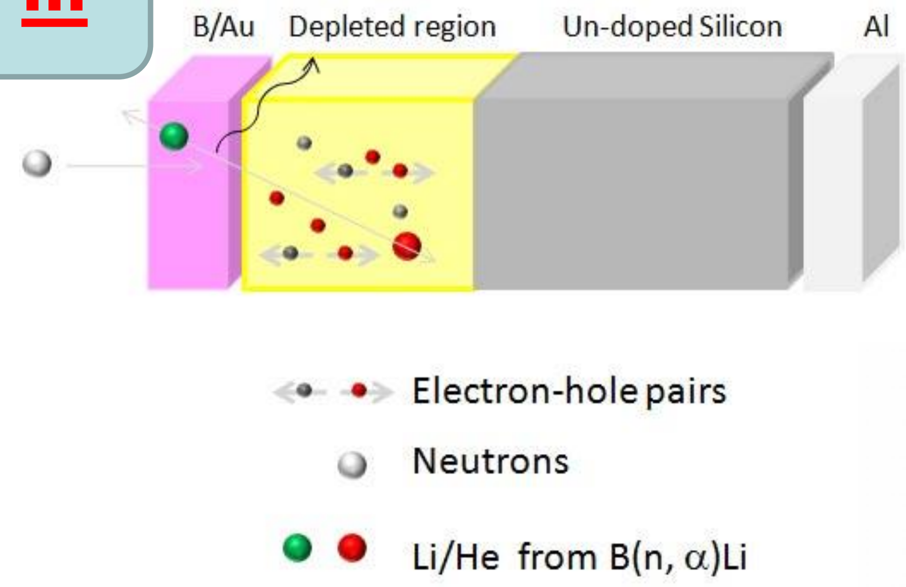

p-n junction

1

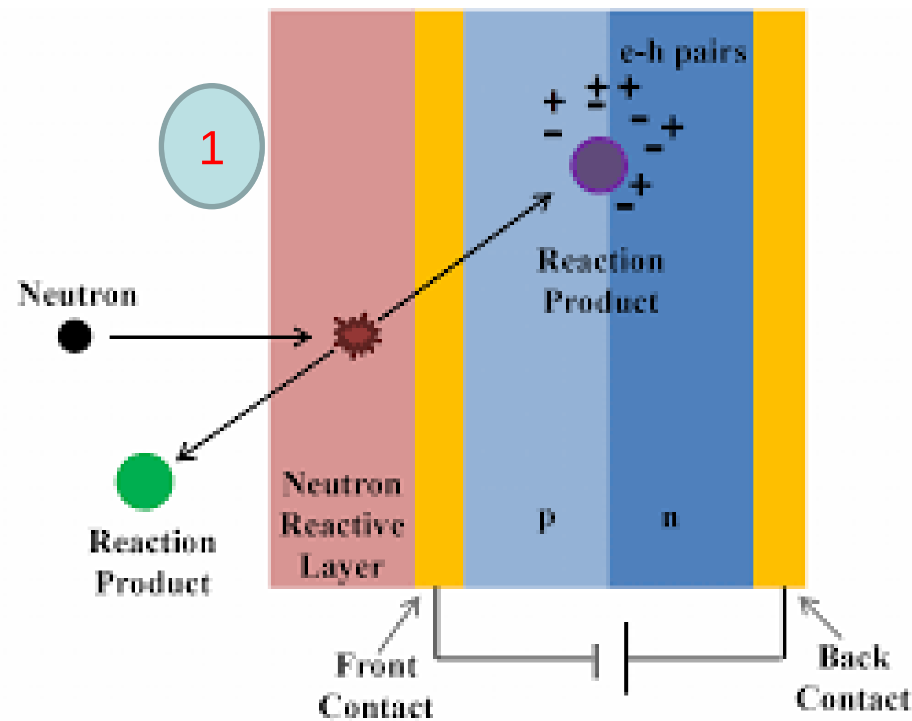

2

p-i-n junction

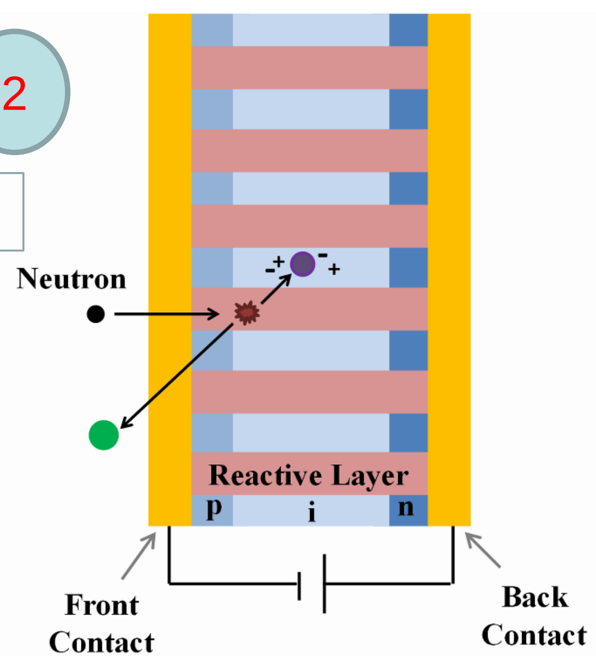

EXPERIMENTAL NEUTRON SCATTERING ARCHITECTURES

TIME OF FLIGHT (TOF)

SPALLATION

- PULSED NEUTRONS PRODUCTION;
- WHITE BEAM

STEADY SOURCES

FISSION

- STEADY FLUX
- CONVENTIONAL

TIME OF FLIGHT (TOF) GEOMETRY

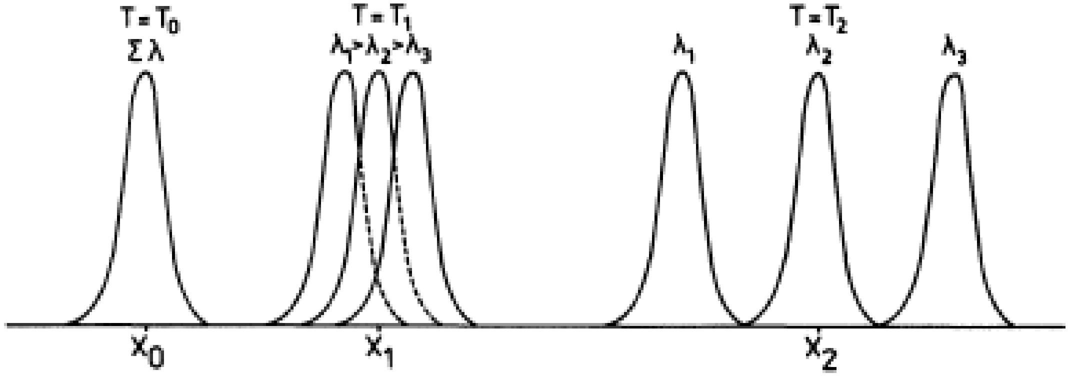

Figure 2 Behaviour of the polycromatic neutron pulse. At time T_0 the pulse leaves the moderator surface. It contains all wavelengths. After a short time T_1 the λ_2-neutrons arrive at the point x_1. The λ_3-neutrons have passed it already, the λ_1 neutrons are slower. Passing a long flight path x_2 (long time T_2) the three different wavelength pulses are separated completely.

- NEUTRONS WITH DIFFERENT WAVELENGTHS HAVE DIFFERENT ARRIVAL TIMES AS A FUNCTION OF THEIR DIVERSE VELOCITIES!
- DETECTORS DISCRIMINATE ON THE BASIS OF A CLOCK REGISTERING NEUTRONS ARRIVAL AND SYNCHRONIZED WITH THE PULSE FROM THE SOURCE

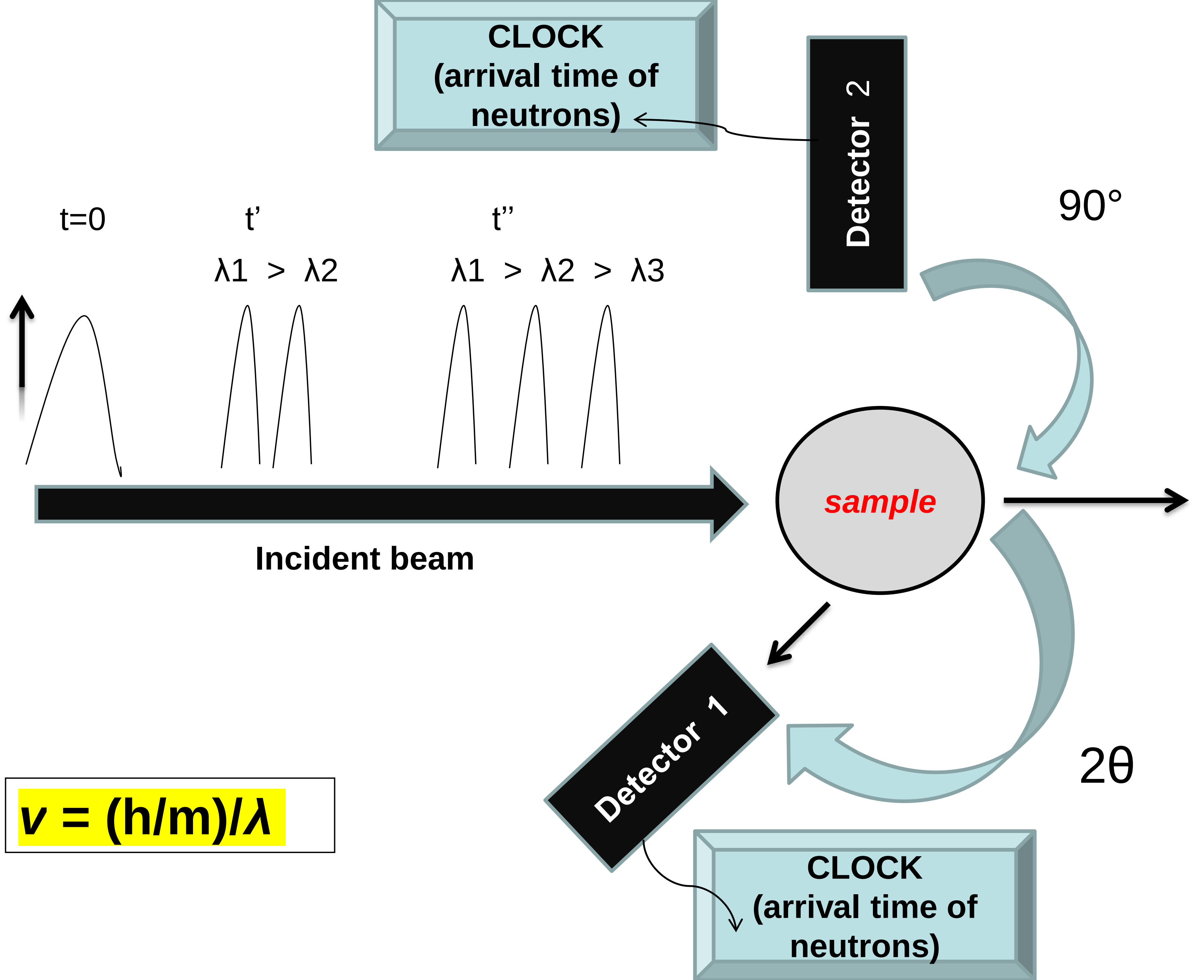
CLOCK
(arrival time of
neutrons)
Detector 2
90°
t=0
t'
t''
λ1 > λ2
λ1 > λ2 > λ3
sample
Incident beam
Detector 1
2θ
CLOCK
(arrival time of
neutrons)
v = (h/m)/λ

time= Time required by neutrons from thier source to the detector, passing through the sample

$v = (L_1+L_0)/time$

$\lambda = h/(m\, v)$

$2\, d\, \sin(\theta) = \lambda = (h/m)*time/(L_0+L_1)$

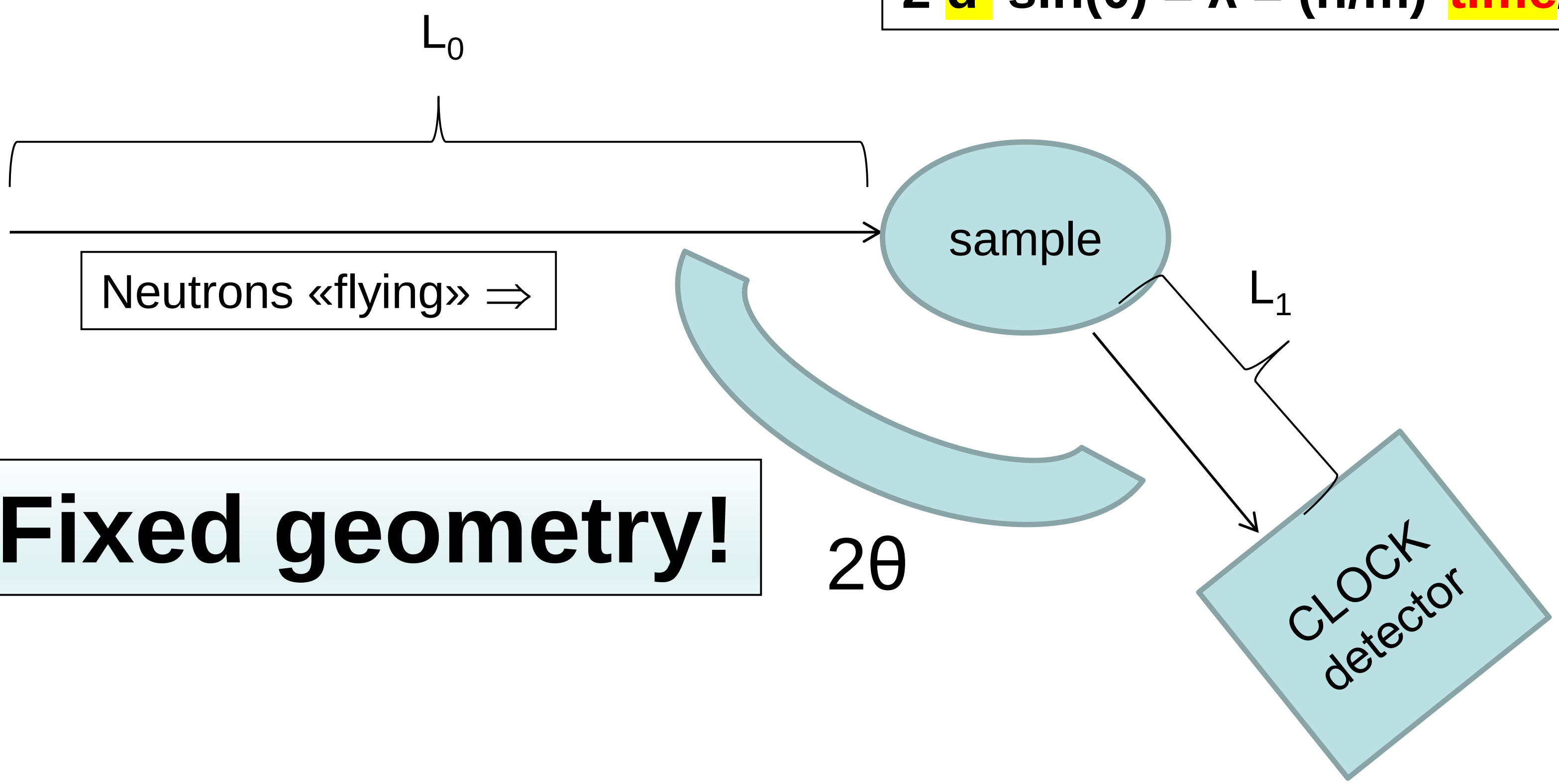

Fixed geometry!

$$d = \frac{h}{2\sin(\theta_0)\, m_N}\frac{t}{(L_0 + L_1)}$$

Bragg-Law with TOF

RESOLUTION

$$R = \frac{\Delta d}{d}$$

Where Δd is obtained by differentiating the Bragg Law:

$$2 \times d \times sin(\theta) = \lambda \text{ (standard)}$$

$$d = \frac{h}{2\sin(\theta_0)m_N}\frac{t}{(L_0+L_1)} \quad \text{(TOF)}$$

RESOLUTION WITH TIME OF FLIGHT

$$\boxed{R = \frac{\Delta d}{d} \approx \frac{\Delta L(flight)}{L(flight)}}$$

RESOLUTION WITH STEADY SOURCES

$$\boxed{R = \frac{\Delta d}{d} \approx ctg(\vartheta)\Delta\vartheta}$$

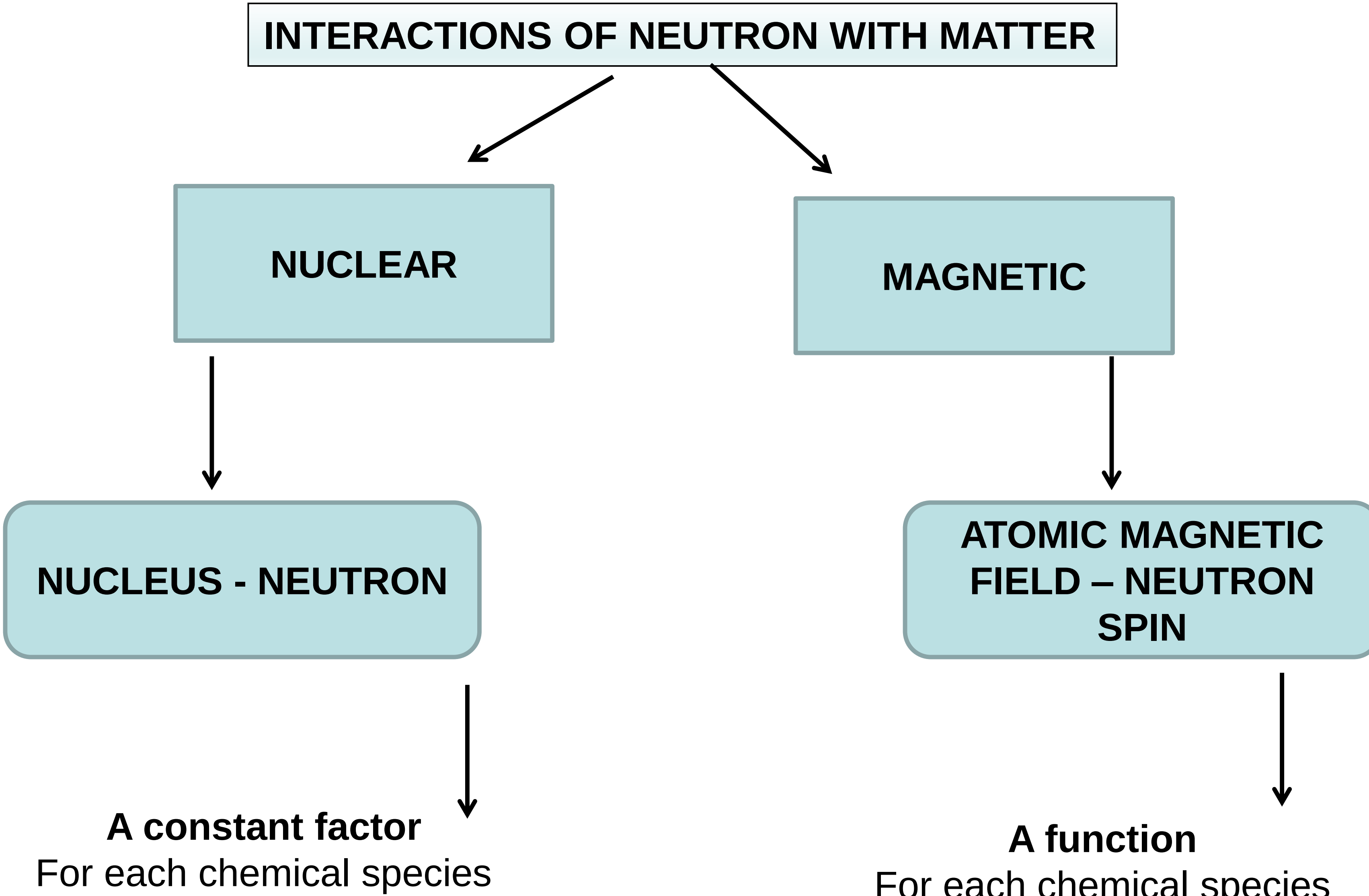
INTERACTIONS OF NEUTRON WITH MATTER
NUCLEAR
MAGNETIC
NUCLEUS - NEUTRON
ATOMIC MAGNETIC FIELD – NEUTRON SPIN
A constant factor
For each chemical species
A function
For each chemical species

NUCLEAR SCATTERING

STRUCTURE FACTOR (DIFFRACTION of CRYSTALS)
X-RAY VERSUS NEUTRONS

$$F_{hkl} = \sum f\left(\frac{\sin\vartheta}{\lambda}\right)_j \times \exp\left(-B_j \times \left(\frac{\sin\vartheta}{\lambda}\right)^2\right) \times \exp\left[2\pi \times \left(h \cdot x_j + k \cdot y_j + l \cdot z_j\right)\right]$$

X-ray structure factor

X-ra scattering power is a function of sin(ϑ)/λ, whereas
Neutron scattering length is a constant
Dependent on the chemical species only

$$F_{hkl} = \sum b_j \times \exp\left(-B_j \times \left(\frac{\sin\vartheta}{\lambda}\right)^2\right) \times \exp\left[2\pi \times \left(h \cdot x_j + k \cdot y_j + l \cdot z_j\right)\right]$$

neutron structure factor
(nuclear contribution)

NEUTRON SCATTERING LENGTH

$$b = b_{\text{coherent}} \;\&\; b_{\text{incoherent}}$$

CONTRIBUTES TO THE BRAGG PEAKS

CONTRIBUTES TO THE BACKGROUND

ORIGIN OF COEHERENT SCATTERING AND INCOHERENT SCATTERING

$$I(Q) \propto \sum_{j=1}^{Natoms\ in\ Cry} b_j e^{-B_j Q^2} e^{2\pi i \vec{Q}\cdot\vec{X}_j} \times \sum_{k=1}^{Natoms\ in\ Cry} b_k e^{-B_k Q^2} e^{-2\pi i \vec{Q}\cdot\vec{X}_k}$$

$$\sum_{j,k=1}^{Natoms\ in\ Cry} b_j b_k e^{-B_j Q^2} e^{-B_k Q^2} e^{2\pi i \vec{Q}\cdot\left(\vec{X}_j - \vec{X}_k\right)}$$

$$b_j = < b_{species\ in\ j} > + \varphi_j \sigma_{species\ in\ j} \qquad < \varphi_j > = 0$$

$$\sum_{j,k=1}^{Natoms\ in\ Cry} b_{j,coe} b_{k,coe} e^{-B_j Q^2} e^{-B_k Q^2} e^{2\pi i \vec{Q}\cdot\left(\vec{X}_j - \vec{X}_k\right)} + \sum_{k=1}^{Natoms\ in\ Cry} \varphi_k^2 \sigma_k^2 e^{-2B_k Q^2}$$

$$\underbrace{\sum_{j,k=1}^{Natoms\ in\ EC} b_{j,coe} b_{k,coe} e^{-B_j Q^2} e^{-B_k Q^2} e^{2\pi i \vec{Q}\cdot\left(\vec{X}_j - \vec{X}_k\right)}}_{\text{BRAGG COHERENT CONTRIBUTION}} + \underbrace{\sum_{k=1}^{Natoms\ in\ EC} b_{k,inc}^2 e^{-2B_k Q^2}}_{\text{INCOHERENT CONTRIBUTION}}$$

MAGNETIC SCATTERING

MAGNETIC SCATTERING ALLOWS US TO INVESTIGATE MAGNETIC PROPERTIES OF MATTER, WHICH ARE RELATED TO THE MAGNETIC MOMENTS OF THE ATOMS

MAGNETIC SCATTERING IS DUE TO INTERACTIONS BETWEEN

- NEUTRON MAGNETIC MOMENT

and

- MAGNETIC FIELD GENERATED BY ATOMIC ELECTRONS

ARRAYS OF MAGNETIC MOMENTS OF ATOMS

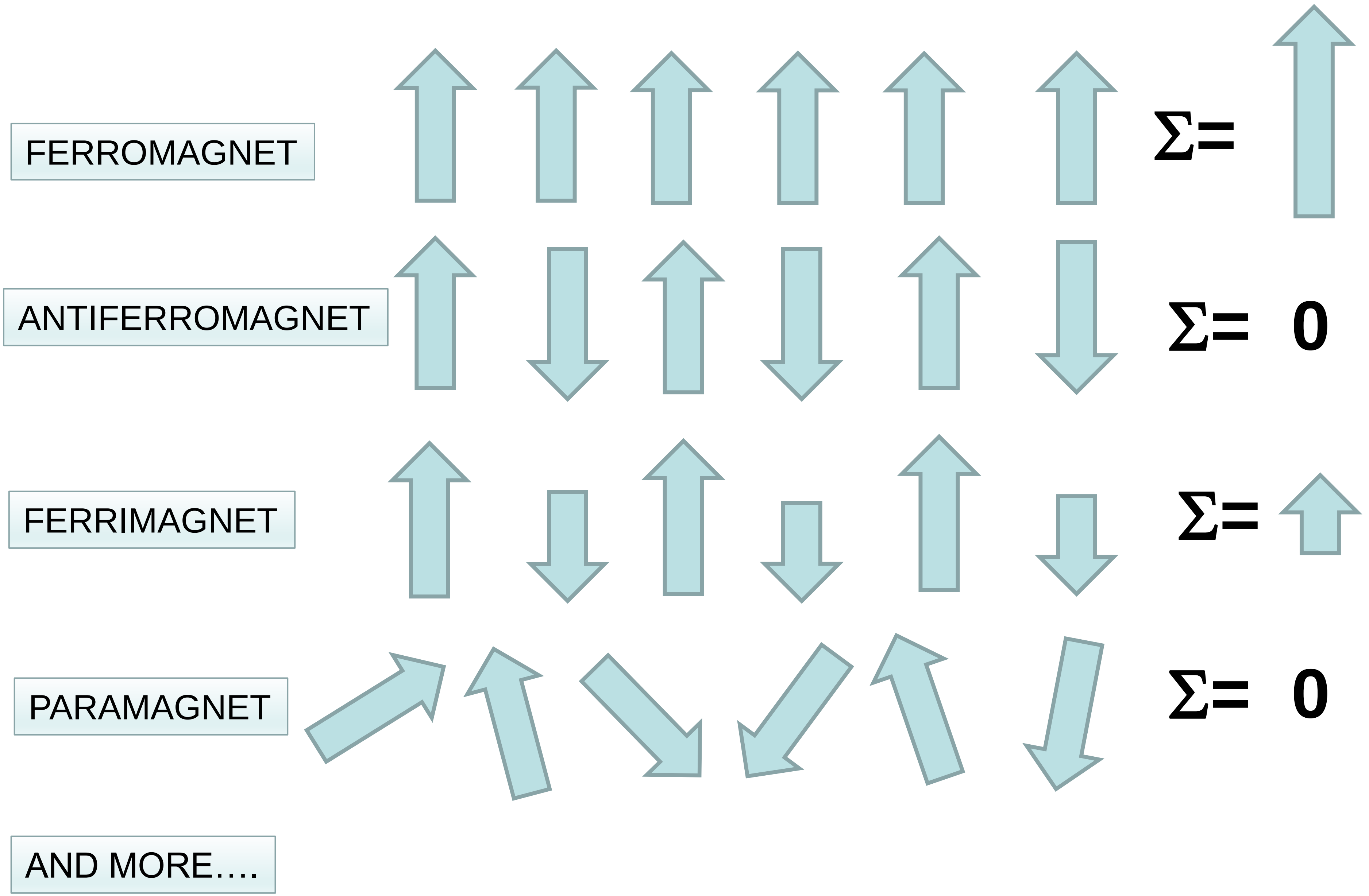

MAGNETIC
VERSUS
CHEMICAL
STRUCTURE

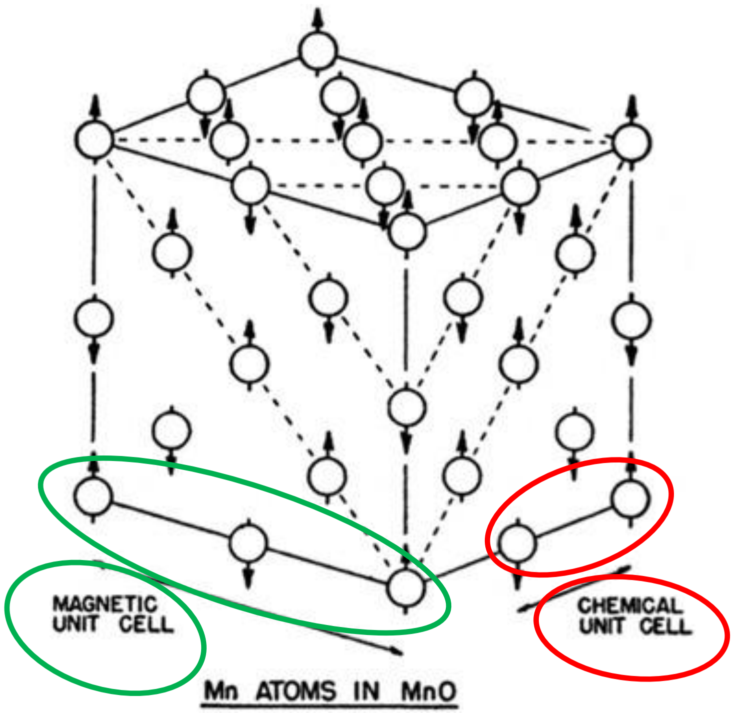

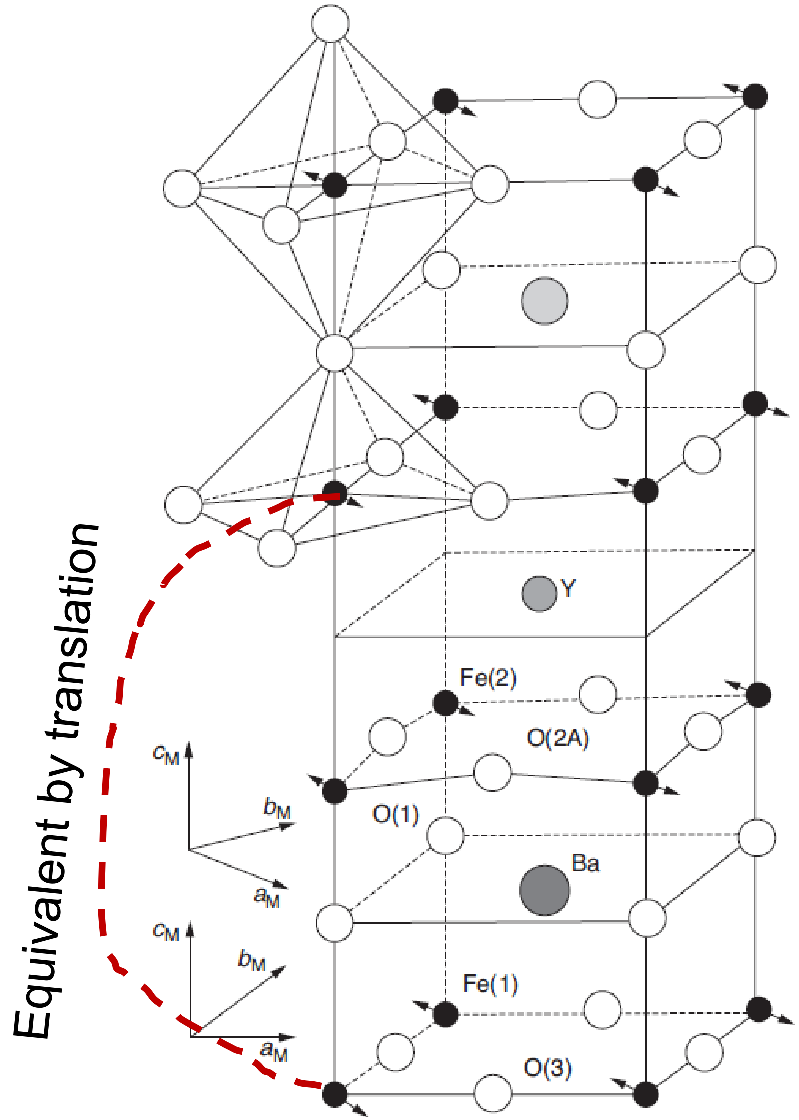

Figure 2. Crystal and magnetic structure for $YBa_2Fe_3O_8$ deduced from the data of Figure 1 (Huang et al., 1992).

ATOMS ARE EQUIVALENT AS A FUNCTION OF THEIR CHEMICAL SPECIES AND MAGNETIC MOMENTS

MAGNETIC STRUCTURES

FERROMAGNETIC **FERRIMAGNETIC**

If $T_{Curie} < T$

PARAMAGNETIC

Fe_2O_3 948 K
Fe_3O_4 858 K
Fe 1043 K

ANTIFERROMAGNETIC

If $T_{Neel} < T$

PARAMAGNETIC

MnO 116 K
FeO 198 K
CoO 291 K

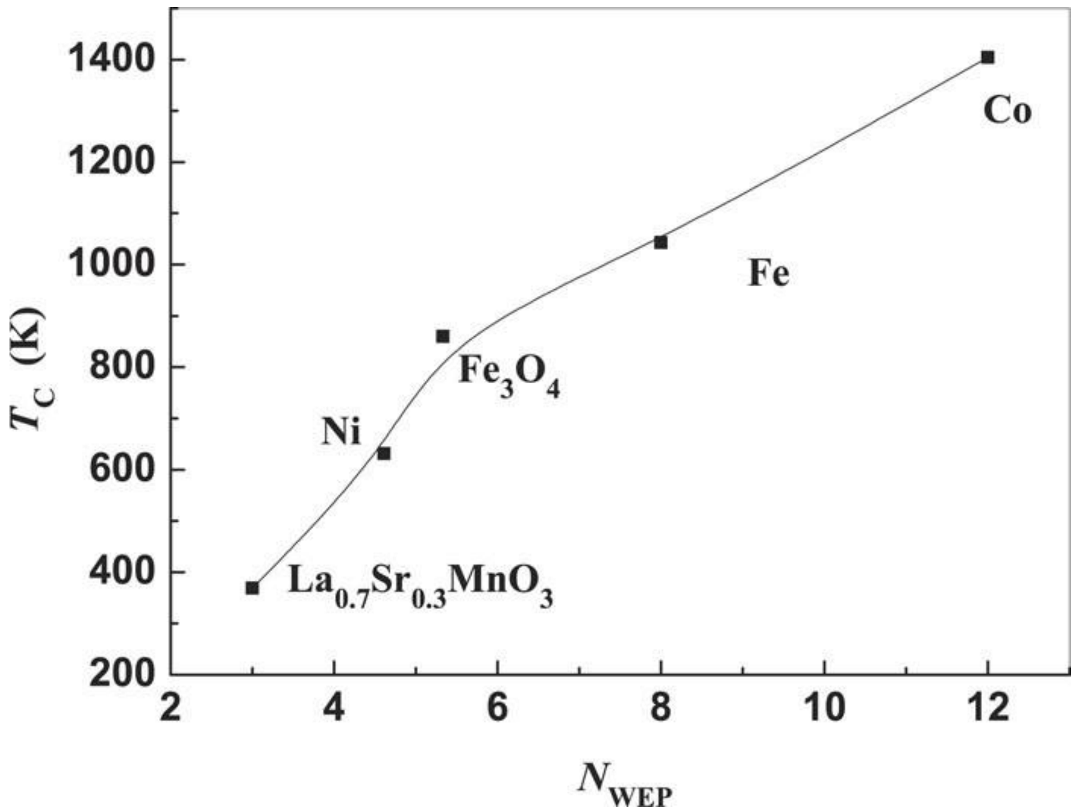

FIG. 2. Dependence of Curie temperature, T_C, on the average number, N_{WEP}, of the bonds near one magnetic cation, at which WEPs can be found.

Weiss electron pair (WEP)

Published in: W. H. Qi; Z. Z. Li; L. Ma; G. D. Tang; G. H. Wu; *AIP Advances* **8,** 065105 (2018)
DOI: 10.1063/1.5035142

MAGNETIC STRUCTURE FACTOR

Magnetic **E**lementary **C**ell = *MEC*

$$F(\vec{Q})_{Magnetic} \propto \sum_{j=1}^{Natoms\ in\ MEC} \vec{\tau} \times \left[\vec{M}(\vec{\tau})_j \times \vec{\tau}\right] e^{-B_j Q^2}\, e^{2\pi i \vec{Q}\cdot\vec{X}_j}$$

$\vec{\tau}$ Versor parallel to ***Q***

$\vec{M}(\vec{\tau})_j$ Vector form factor of the j^{th}-atom

$$I(\vec{Q})_{Magnetic} \propto \left|F(\vec{Q})_{Magnetic}\right|^2$$

MAGNETIC STRUCTURE FACTOR

$$\vec{F}(\vec{Q})_{Magnetic} = \sum_{j=1}^{atoms\ in\ magnetic\ cell} \vec{\tau} \times \left[\vec{M}(\vec{Q})_j \times \vec{\tau}\right] e^{2\pi i \vec{Q}\vec{X}_j}\, e^{-Q^2 B_j}$$

$\vec{\tau}$ Versor parallel to ***Q***

$\vec{M}(\vec{Q})_j \overrightarrow{\times \tau}$ Vector form factor of the j[th]-atom

$$I(\vec{Q})_{Magnetic} \propto \left|\vec{F}(\vec{Q})_{Magnetic}\right|^2$$

Magnetic **E**lementary **C**ell = *MEC*

- General scattering equation and its origin
- Lattice translation invariance: implications on scattering

(metric-component and physical-chemical component – full derivation not required)

- Reciprocal lattrice: what is it?
- Structure factor (thermal vibrations; anomalous scattering; atomic scattering power);
- Occupancy factors; «practical expression» for F_{hkl})
- Relations between structure factor and experiments: i) structure refinements;

ii) structure solving (direct methods; charge flipping; MEM)

- X-ray Powder diffraction: experimental geometries (Debye-Scherre/Bragg-Brentano)
- Rietveld method: what is it? How does it work? What information can we obtain from XRPD using the Rietveld method?
- Neutron scattering: nuclear contribution